

AperTO - Archivio Istituzionale Open Access dell'Università di Torino

Sonochemical processes for the degradation of antibiotics in aqueous solutions: A review

This is the author's manuscript

Original Citation:

Availability:

This version is available <http://hdl.handle.net/2318/1789166> since 2021-05-27T10:55:38Z

Published version:

DOI:10.1016/j.ultsonch.2021.105566

Terms of use:

Open Access

Anyone can freely access the full text of works made available as "Open Access". Works made available under a Creative Commons license can be used according to the terms and conditions of said license. Use of all other works requires consent of the right holder (author or publisher) if not exempted from copyright protection by the applicable law.

(Article begins on next page)

Sonochemical processes for the degradation of antibiotics in aqueous solutions: a review

Pengyun Liu¹, Zhilin Wu¹, Anna V. Abramova², Giancarlo Cravotto^{1,3*}

¹ Department of Drug Science and Technology, University of Turin, via P. Giuria 9, Turin, 10125, Italy.

² Federal State Budgetary Institution of Science N.S. Kurnakov Institute of General Inorganic Chemistry of the Russian Academy of Sciences, GSP-1, V-71, Leninsky Prospekt 31, 119991, Moscow, Russia.

³ World-Class Research Center "Digital biodesign and personalized healthcare", Sechenov First Moscow State Medical University, 8 Trubetskaya ul, Moscow, Russia.

*Correspondence: giancarlo.cravotto@unito.it (G. Cravotto), Tel: +39.011.670.7183, Fax: +39.011.670.7162.

Abstract

Antibiotic residues in water are general health and environmental risks due to the antibiotic-resistance phenomenon. Sonication has been included among the advanced oxidation processes (AOPs) used to remove recalcitrant contaminants in aquatic environments. Sonochemical processes have shown substantial advantages, including cleanliness, safety, energy savings and either negligible or no secondary pollution. This review provides a wide overview of the different protocols and degradation mechanisms for antibiotics that either use sonication alone or in hybrid processes, such as sonication with catalysts, Fenton and Fenton-like processes, photolysis, ozonation, etc.

Keywords: Antibiotic degradation, Sonication, Sonocatalysis, Sono/Fenton, Sonophotocatalysis, Sonozonation.

29 **Abbreviations of antibiotics:**

30 AMP, ampicillin; AMX, amoxicillin; AZI, azithromycin;

31 CAP, chloramphenicol; CDX, cefadroxil; CEF, ceftriaxone; CEFX, cefalexin; CFX,

32 Cefixime); CFZ, cefazolin; CIP, ciprofloxacin; CLA, clarithromycin; CLM, clindamycin;

33 CLX, cloxacillin; CPD, cephadroxyl; CPX, cephalixin; CTC, chlortetracycline; CTX,

34 cefotaxime;

35 DOXO, doxorubicin; DTC, deoxytetracycline; DXC, dicloxacillin;

36 EF, enrofloxacin;

37 FLU, flumequine;

38 GMF, gemifloxacin;

39 LEV, levofloxacin;

40 MNZ, metronidazole; MOX, moxifloxacin;

41 NAF, nafcillin; NOR, norfloxacin;

42 OFX, ofloxacin; OTC, oxytetracycline; OXA, oxacillin;

43 PG, penicillin G;

44 RIF, rifampin; RXM, Roxithromycin;

45 SA, sulfanilamide; SDZ, sulfadiazine; SMR, sulfamerazine; SMX, sulfamethoxazole; SMZ,

46 sulfamethazine; SSZ, sulfasalazine;

47 TC, tetracycline; TNZ, tinidazole; TYL, tylosin.

48

1 Introduction

Antibiotics were first discovered in 1928 by Alexander Fleming and the term was first used in 1942 by Waksman and his collaborators [1, 2]. Initially, the classical definition of antibiotics was: chemotherapeutic agents that can eradicate or restrain the growth of microorganisms, including bacteria, fungi or protozoa [3, 4, 5]. Antibiotics have been widely used for the treatment of infectious diseases in humans and animals to the present day [4]. Macrolides, β -lactams, quinolones, tetracyclines, and sulfonamides are the most consumed antibiotics [6]. Since the 1990s, however, antibiotic residues have been broadly observed in aqueous matrices and soil as well as in microorganism, animal and human bodies over the world thanks to the appearance of the advance analytical technologies [5, 6].

The presence of antibiotic residues in the environment can either be caused by their continuous discharge or inherent high persistence [7]. For example, CEFX and CTX have attained levels surpassing 1000 $\mu\text{g/L}$ in urban wastewater samples in Hong Kong and Shenzhen, South China [8]. 11 antibiotics in hospital wastewater and sewage treatment plants (STPs) have been identified in Beijing, China. Fluoroquinolones, in particular, were found to be the most abundant, with a highest concentration of 16.8 $\mu\text{g/L}$ in the hospital samples. The maximum concentrations of antibiotics in STPs and hospital wastewater were 1-3 orders of magnitude higher than those in the surface water from the Wenyu River and groundwater [9].

Antibiotic concentrations in wastewater and environmental water bodies are obviously correlated with variations in annual consumption data [10]. Some antibiotics, such as penicillins, are easily degraded, whereas others, such as fluoroquinolones (e.g. CIP), macrolides (e.g. TYL) and tetracyclines, are considerably more persistent, resulting in their residues being found in the environment, spreading and accumulating in organisms [10]. Antibiotic occurrence in water is generally in the range of a few to hundreds ng/L [3, 5, 6, 10]. For examples, 77 antibiotics have been reported in Danjiangkou Reservoir in China, but most were present at lower than 5.0 ng/L and

SMX was the most abundant one [11]. 22 antibiotics, including eight quinolones, nine sulfonamides and five macrolides, have been detected in the Huangpu River in Shanghai, China, where the concentration of sulfonamides was in the range of 34–859 ng/L [12]. Sulfonamides (0.86–1563 ng/L) were also found to be the dominant antibiotics in Baiyangdian Lake, China [13]. 9 antibiotics, including sulfonamides, tetracyclines, quinolones and macrolides, have been investigated in 6 urban rivers in Guangzhou, South China. NOR was the most abundant followed by CIP, and the highest concentration was 2702 ng/L [14]. The concentrations of 4 quinolone antibiotics, OFX, NOR, CIP and EF, ranged from 3.49-660.13 ng/L in the Qingshitan reservoir, South China [15]. In addition, according to Ghernaout, *et al.* [8], an elevated number of antibiotics, made up of sulfonamides, trimethoprim and macrolides, was found in Japanese urban rivers.

As a side effect of antibiotic use, antibiotic-resistance genes and antibiotic-resistant bacteria may be formed in microorganisms, causing a significant threat to human health and ecological safety [5, 10, 16]. For example, OXA-resistant bacteria are currently a serious problem in Latin American hospitals [17]. Meanwhile, other adverse effects, such as endocrine disruption and aquatic toxicity, can also destroy ecosystems [16].

Biological degradation [5], adsorption [18], reverse osmosis [18], ion exchange [18] and advanced oxidation processes (AOPs), including ozonation [5], photocatalysis [19-24], electrochemical degradation [23, 24], non-thermal plasma [25], Fenton/photo-Fenton reaction [5], sonochemical degradation, and combination [26, 27], have been extensively studied as means to remove antibiotics from aqueous matrices. Biological processes are widely used in industrial effluent treatments with large effluent flow rates, but the high concentration of pollutants in effluents with high toxicity are recalcitrant to the microorganisms, resulting in limited antibiotic removal efficiency (RE) [5]. High-concentration antibiotics can be transported from water matrices onto solid adsorbents via adsorption, but the loaded adsorbents must be subsequently treated, causing higher

treatment costs [28, 29]. Reverse osmosis has been used to remove antibiotics with larger molecules, it can efficient to reduce levels of dissolved salts. However, with this process, the contaminants are slowly concentrated rather than removed. Besides, the deterioration/fouling of the membrane structure caused by high-concentration compounds is another drawback. Therefore, frequent back-washing and regeneration is required [30].

Due to the limitations of physical and biological processes, AOPs have gradually emerged as means for the degradation/mineralization of organic pollutants over recent decades [31]. As non-selective oxidation technologies, AOPs have attained the total removal of antibiotics, efficient reductions in toxicity and antimicrobial activity, and have also increased biodegradability [17, 31-38]. The generation of reactive oxygen species (ROS), such as $\cdot\text{O}$, $\cdot\text{O}^{2-}$, $\cdot\text{OH}$, $\cdot\text{OOH}$, H_2O_2 , etc., via various methods was the origin of AOPs [4, 10, 21, 22, 31, 33, 39-48].

Hydroxyl radicals ($\cdot\text{OH}$) and other ROS are released by ozone (O_3) decomposition in water during the ozonation process. Meanwhile, O_3 often selectively reacts with nucleophilic molecules. However, the high costs of equipment, maintenance and operation, the high quantities of energy required, lower mass transfer, extreme pH-dependence and potential effluent ecotoxicity limit the application of ozonation [49, 50]. Photocatalysis has often been applied under ambient conditions and may gain energy from sunlight with the advantages of simple operation and scale-up applicability, but it also suffers from mass-transfer limitations, and is affected by catalyst amount, light wavelength, radiation intensity, pH and water quality. Additionally, the catalysts consumed need to be specially treated or recycled, causing high overall costs [19-22, 26, 27, 30]. Electrochemical degradation is an effective, versatile, cost-effective, easy and clean technology, and is suitable for the treatment of toxic wastewater that contains high-concentration antibiotics and COD. However, the RE depends on the nature and structure of the electrode material, electrolyte composition, the applied current and the diffusion rates of substrates to the active sites of the anode. The low flow rates and high

operating costs limit the application of electrochemical methods [23, 24]. Non-thermal plasma generated in electrical discharges in liquid or at the gas-liquid interface leads to the formation of ROS and the power introduced into the plasma is very high, leading to low energy yields [25]. The Fenton reaction is usually used in homogeneous and heterogeneous systems and in conjugation with UV radiation to enhance the oxidation process. However, the narrow acidic pH range of the operation and dissolved catalysts limits this process [5].

Sonochemical degradation (sonolysis), namely, degradation that is driven or enhanced by sonication, emerged in the 1990s. Ultrasound (US) is sound that exceeds the human hearing range, and has a wide frequency range of 18 kHz to 500 MHz [37, 45, 51-54]. Ultrasonic propagation, with cycles of compression and rarefaction, causes acoustic cavitation phenomena, which is defined as the sonochemical origin [52, 55-61]. Such numerous cavitation bubbles are also referred to as microreactors, since they act as the centre of chemical reactions [45, 62]. Gas-filled cavitation bubbles grow and extensively implode under the positive pressure that occurs during the compression cycle of US in water bulk [37, 45, 51, 52, 54]. Meanwhile, enormous local temperatures (ca. 5000 K) and high pressures (ca. 500 atm), microjets and shockwaves are produced [10, 27, 63, 64]. Subsequently, ROS are produced through the pyrolysis of water molecules at the collapsing bubbles (hotspots), and oxidize the substrates in water [45, 51]. Among these formed ROS, $\cdot\text{OH}$ is a significantly important, very strong and nonspecific oxidizing species [45, 51, 54]. Besides, hydrophobic volatile compounds also suffer thermal decomposition at hotspots, and both the above actions contribute to the degradation of organic contaminants [65-67].

In theory, a large variety of organic pollutants are capable of being degraded by sonication without additional chemicals. Thus, sonication is usually seen as a green and safe technique to perform wastewater treatment. However, the sonolysis of organic contaminants has limited efficiency and consumes considerable amounts of energy [23, 45, 68]. To improve the RE and reduce energy consumption, sonication-based

combinations, such as sonocatalysis [69-73], Sono/Fenton [19, 21, 35, 43, 44, 74-77], sonication-ozonation (Sonozonation) [78-81], sonication-persulfate (Sono/PS) [82], sonophotocatalysis (Sono/Photo) [31, 39, 83-85], sonoelectrochemical degradation [86-88], sonication-microwaves [89], sonication-hydrodynamic cavitation [90], and ultrasound-assisted biological processes [91-93], have attracted great attention.

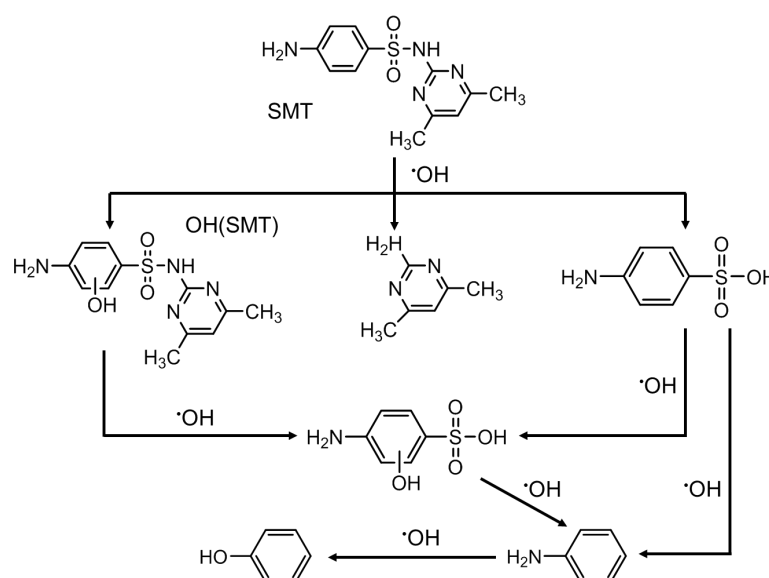
This review aims to provide an overview, and evaluate the REs, of the degradation of antibiotics in aqueous matrices by various sonochemical processes, including sonication alone [31, 36, 41, 46, 69, 71, 94-100], sonocatalysis [35, 40, 52, 72, 75, 101-110], Sono/Fenton [21, 22, 32, 33, 34, 35, 43, 44, 111, 112, 113], Sono/PS, Sono/Photo [20, 31, 39, 83, 84, 85, 114-119], sonozonation [78, 79, 80, 120-123], etc., and will focus on the degradation mechanisms and influence of operating conditions indicated in appropriate studies that have been published in the last few years.

2 Antibiotic degradation by sonication alone

2.1 Mechanisms of sonolysis

In general, sonochemical degradation occurs in three reaction zones relative to the collapsing cavitation bubbles: inside the cavitation bubbles; in the interfacial region between cavitation bubbles and the bulk solution; and in the bulk solution [5, 10, 45]. Inside and around the collapsing cavitation bubbles, the thermal dissociation of water molecules and oxygen occurs to release ROS [45]. Moreover, hydrophobic volatile compounds around the hotspots are also thermally decomposed [10, 45, 62, 63, 64]. Hydrophilic and non-volatile compounds, such as LEV [42], that remain in the bulk solutions are oxidized by ROS. The sonochemical reaction with $\cdot\text{OH}$ has been speculated to occur at the cavitation interface, where the maximum $\cdot\text{OH}$ concentration is present [42]. Only ca. 10% of the radicals created in the interfacial region diffuse or escape to the bulk liquid [10, 41]. Therefore, antibiotic degradation is strongly dependent on the distance between non-volatile antibiotic molecules and the cavitation bubbles, and this distance is determined by hydrophobicity [4, 41, 42, 45].

Figure S1 clearly shows the HPLCs of SMT degradation and the appearance of intermediates with sonication time. In addition, LC/MS/MS analyses have indicated that the sonolytic degradation of SMT is mainly ascribed to OH oxidation. The sonolytic degradation pathway of SMT is shown in Scheme 1. As can be seen, SMT is first oxidized by $\cdot\text{OH}$ radicals, resulting in the formation of (OH)SMT and the cleavage of the N–S bond [41]. 4,6-dimethylpyrimidin-2-amine, sulfanilic acid and the mono-hydroxyl derivative of sulfanilic acid are probably produced by the cleavage of the N–S bond of SMT or (OH)SMT. The mono-hydroxyl derivative of sulfanilic acid may also be formed by the $\cdot\text{OH}$ radical that directly attacks the sulfanilic acid. Aniline is an intermediate product in SMT degradation via the breakage of the C–S bond in SMT or sulfanilic acid, and can be oxidized to phenol [41].



Scheme 1 Pathway of intermediate formation in the sonolytic degradation of SMT [41].

However, the sonochemical degradation products were rarely mineralized. About 100% of 180 μM SMT was decomposed, but only 8.31% TOC was reduced by sonication for 2 h at 800 kHz and 100 W. Fortunately, the effluent became much more biodegradable (BOD_5/COD was increased from 0.04 to 0.45), indicating that the toxicity of the effluent to microorganisms was obviously reduced [41].

Extensive investigation with the addition of a radical scavenger, such as isopropyl

alcohol, ethanol, methanol [41], *n*-butanol [97], terephthalate (TA) and Suwannee River Fulvic Acid (SRFA) [124], has revealed that reaction with $\cdot\text{OH}$ is the main degradation route for antibiotics during sonication [41, 97, 124, 125]. For example, with a hydrophobic character in the whole pH range, *n*-butanol diffuses to the gas/liquid interface of the microbubbles where it is able to scavenge $\cdot\text{OH}$ and quench the antibiotic degradation as a consequence [97]. In the presence of TA, CIP (a hydrophilic compound) degradation was inhibited by a factor of 40–1500 depending on the frequency and initial concentration, while degradation was slightly affected by SRFA [124]. TA reacts with $\cdot\text{OH}$ in bulk solution and accumulates around cavitation bubbles, greatly quenching $\cdot\text{OH}$, while SRFA stays in bulk solution and catches $\cdot\text{OH}$ and competes with CIP [124].

In addition, the inhibition of DXC degradation via the addition of a radical scavenger (2-propanol or glucose) was observed [96]. DXC degradation was not affected significantly when low- or high-concentration glucose (high hydrophilicity) and low-concentration 2-propanol (miscible with water) were individually added. It was speculated that both glucose and low-concentration 2-propanol are dissolved in the bulk liquid far away from the bubbles, while DXC is relatively closer to the cavitation bubbles. As a result, no competing reactions between glucose or 2-propanol with $\cdot\text{OH}$ occurred around the hotspots. However, a significant decrease in the DXC degradation rate was observed in the presence of a high concentration of 2-propanol due to its relatively high volatility [126]. Therefore, the addition of the radical scavengers confirmed that $\cdot\text{OH}$ -mediated reactions either occur at the interface of the cavitation bubbles, or in the bulk liquid depending on the properties of the antibiotics [65, 97]. Unreacted $\cdot\text{OH}$ will be recombined into H_2O_2 , for example, 77.6 and 57.3 μM of H_2O_2 have been observed as being generated after 30 min sonication in the presence of AMP and NAF, respectively [69].

Overall, two reaction mechanisms are presumably responsible for the sonolysis of antibiotics: pyrolysis and oxidation by the $\cdot\text{OH}$ generated in the system [27, 43, 52, 53].

2.2 Application of sonication for antibiotic degradation

Sonication systems used for the degradation of antibiotics mainly include ultrasonic horn-type and bath-type apparatus, as shown in Figure 1.

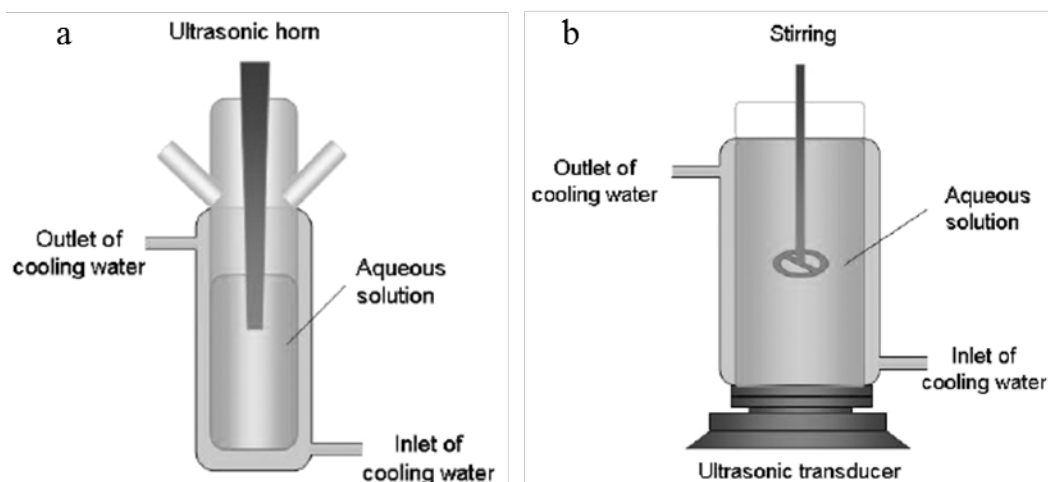


Figure 1 Schematic diagram of ultrasonic horn-type (a) and bath-type (b) setups for degradation. Reprinted from ref. [68] Copyright (2006), with permission from Elsevier.

Hapeshi, *et al.* have investigated the degradation of OFX using a 20 kHz horn-type ultrasonic reactor. The results showed that the RE of OFX increases with increasing US power density and decreasing initial OFX concentration. Under the optimal conditions, 27.7 μM OFX and 640 W/L of US power density, the RE of OFX in a 350 mL solution reached 31% after 240 min sonication [36]. As a result, 12.5 nmol of OFX was removed per minute by 20 kHz sonication, and the radical reactions are responsible for OFX degradation.

Villegas-Guzman, *et al.* have studied the degradation of DXC using a 600 kHz bath reactor [96]. 210 μM DXC was fully removed in 100 mL aqueous solution for 180 min under acid and neutral conditions. Thus, 117 nmol of DXC was removed per minute by 600 kHz sonication with 0.6 W/L of power density. However, no significant change in TOC concentration and a 30% reduction in COD were observed during 480 min of sonication, indicating that either no or less mineralization occurred under sonication alone.

To date, sonication has been extensively used to probe the RE of a large number of antibiotics, which are summarized in Table 1.

Table 1 Summary of the degradation of antibiotics in water by sonication alone.

Antibiotics	F _{US} /P _E (kHz/W)	P _{US} (W)	t (min)	C ₀ /V (mg/L)/mL	pH	RE (%)	Other results	Refs.
OFX	20/224	-	240	10/350	-	31	Mainly radical reactions.	[36]
LEV	20/400	-	20	20/50	5.9	9.4	BOD ₅ /COD increased.	[42]
CIP	20/-	20	-	~50	8.5	-	CIP is far away from cavitation bubbles.	[124]
CPX	24/200	17.3	60	20/50	6.5	~52	BOD ₅ /COD ratio was raised.	[127]
PG	35/860	-	70	200/50	3.0	66.7	RE is pH dependent.	[95]
PG	40/100	-	60	50/1000	-	-	24.8% COD was removed.	[114]
CIP	205/-	13.5	35/70	10 µM/300	3.5	~65	Molar volume is critical.	[70]
PG	205/-	13.5	35/70	10 µM/300	3.5	<10	Molar volume is critical.	[70]
OXA	275/60	20.7	120	20/250	5.6	100	Mineralization is difficult	[128]
CIP/NOR/ CPX/CDX/ OXA/CLX	354/-	26.4	75- 120	40 µM/300	6.5	-	Hydrophobicity was critical.	[129]
CIP	520/-	13.8	120	15/150	3.0- 10.0	57	RE is pH-dependent.	[38]
CIP	544/200	-	150	15/<1000	7.0	~60	544 kHz>801/1081 kHz	[125]
SDZ	580/-	22	120	25/250	5.5	90	H ₂ O ₂ affects negatively	[97]
DXC	600/60	34.8	300	0.21 mM/300	3.0	100	~ 0 mineralization was obtained.	[130]
DXC	600/60	34.8	480	98.8/100	5.5	100	30% of COD was eliminated.	[96]
SMZ	800/100	-	120	180 µM/-	-	100	8.31% TOC was reduced.	[41]

Note: F_{US}: ultrasonic frequency; P_E: electrical power input; P_{US}: the power dissipated by the reactor (calculated using the calorimetric method); t: sonication time; C₀: initial antibiotic concentration; V: volume of solution; RE: removal

efficiency; Refs.: references.

As listed in Table 1, the sonolysis of CIP, CPX, LEV, PG and OFX, etc., have been conducted at low US frequency (20-40 kHz) and high electrical power (200-860 W); their REs are lower, lying in the range of 9.4%-66.7% after 20-240 min sonication. In addition, COD was slightly removed, leading to an increasing BOD₅/COD ratio. By contrast, the sonolysis of CDX, CIP, CLX, CPX, DXC, NOR, OXA, PG, SDZ and SMZ, etc., was performed at medium US frequency (205-600 kHz) and lower electrical power (60-200 W), and their REs are relatively higher, lying in the range of 10%-100% after 35-300 min sonication. However, the mineralization of antibiotics is difficult under sonication alone.

2.3 Role of effective factors

Under sonication, the degradation of antibiotics mostly occurs via radical reactions in the bulk liquid and generally follows pseudo-first order (PFO) kinetics [38, 69, 96, 99]. The degradation rate and RE of antibiotics are dependent on many factors, such as US frequency [36, 42, 97, 129], power [36, 96, 97], and sonication mode (continuous or pulse) [70], chemical structure and physicochemical properties [129, 131], initial concentration [36, 129, 131], solution volume [36, 69, 132], pH value [38, 97], temperature [33, 40, 111, 125], and sonication time [36, 129, 131, 132], etc. The influence of the critical parameters on the sonochemical degradation of antibiotics is discussed below.

2.3.1 Effect of US frequency and power

As summarized in Table 1, the radical reactions that take place in the bulk liquid dominate antibiotic degradation, while more reactive radicals are formed at higher ultrasonic frequencies, e.g., 300-1000 kHz, than at lower frequencies, e.g. 20-45 kHz [54, 68]. Therefore, higher REs for SDZ at 580 kHz and 22 W [97], and for AMP at 375 kHz and 24.4 W (actual ultrasonic powers, determined by calorimetric method) [46] have been observed. Al-Hamadani, *et al.* have investigated the degradation of SMX by

sonication in the absence of catalysts [71]. The removal of 10 μ M SMX was higher at 1000 kHz sonication for 60 min (72%, 160 nmol/min of removal rate) than at 28 kHz sonication (33%, 55 nmol/min of removal rate), while all other experimental conditions remained the same (0.18 W/mL of US power density at pH 7 and 15 °C in 1000 mL solutions), because more \cdot OH were generated at 1000 kHz than at 28 kHz [71]. In addition, 187.29 nmol (90%) SDZ was removed per minute in 250 mL of 0.1 mM aqueous SDZ solutions for 120 min under 580 kHz sonication at 30 °C and pH 5.5, whereas 41.7 nmol (82%) AMP was removed per minute in 250 mL of 0.03 mM aqueous AMP solutions after 180 min under 375 kHz sonication at 20 °C and pH 6.5.

Higher RE of antibiotics can be generally achieved at higher US energies and higher dissipated powers [31, 36, 41, 69, 94-100]. At higher input powers (400-600 W), however, a large number of gas bubbles exist in solution, which has been seen to scatter the US to the walls of the vessel or back to the transducer. Thus, less energy is dissipated into the liquid, as a result of cavitational activity, although the vessel was exposed to higher power [42]. In addition, changing the solution volume inside the reactor also changes the power density, which also significantly affects the degradation rate; increasing the solution volume will decrease the degradation rate [132].

2.3.2 Effect of Physicochemical properties of antibiotics

The physicochemical properties of antibiotics greatly affect their sonochemical degradation, with sonochemical eliminating showing significant selectivity for certain antibiotics in aqueous matrices [129]. Serna-Galvis, *et al.*, have studied the degradation of various antibiotics, including fluoroquinolones (CIP and NOR), penicillins (OXA and CLX) and cephalosporins (CPX and CPD) using 354 kHz sonication [129]. Different degradation rates, $CLX > OXA > CPX > NOR > CIP > CDX$, were observed under identical sonication conditions: 200 W; 375kHz; 300 mL of 40 μ M of antibiotics, pH 6.5 [129]. Similarly, NAF was degraded faster than AMP by 375 kHz and 24.4 W sonication at pH 6.5 and 20 °C for 250 mL in 30 μ M aqueous AMP solutions, and the rate constants of PFO (k_I) of NAF and AMP were calculated to be 0.5 min⁻¹ and 0.4

min⁻¹, respectively [69].

It has been demonstrated that the initial degradation rate of pollutants exhibited good correlation with LogP (Octanol-water partition coefficient, i.e., the hydrophobicity). Thus, the fast elimination of penicillins is attributed to their high hydrophobicity, leading to the accumulation of penicillins near cavitation bubbles, compared to fluoroquinolones or cephalosporins [129]. In addition, Lastre-Acosta, *et al.* have indicated that the sonochemical degradation mechanism of SDZ is directly related to the *pKa*-dependent speciation of SDZ molecules [97]. Moreover, small-sized molecules (molar volumes less than 130 mL/mol) more quickly diffuse to bubble interfaces and are impacted most by pulsing US, resulting in a higher portion of the antibiotic in and around cavitation bubbles. Large-sized molecules slowly diffuse to the bubble surface, resulting in a higher portion of these personal care products (PPCPs) degrading in bulk solution [70].

2.3.3 Effect of pH value

The effect of pH value on antibiotic degradation is also related to the properties of antibiotics (i.e., ionic species or molecule states). Some antibiotics are more sophisticated, being zwitterions (a molecule containing both a basic and an acidic group). For example, LEV has two different acid-dissociation constant values (*pKa* 5.7 and 7.9) [124]. De Bel, *et al.* have explored the effect of pH on CIP sonolysis at 520 kHz [38]. The *k_l* value (0.021 min⁻¹) at pH 3 is almost 4-fold higher than those at pH 7 (0.0058 min⁻¹) and pH 10 (0.0069 min⁻¹). The solution can even be considered readily biodegradable after sonication at pH 3 (BOD₅/COD > 0.4) [38]. Degradation is clearly faster when the main part of the CIP molecules carries an overall positive charge. These positively charged molecules will accumulate at the negatively charged liquid–bubble interface, where the concentration of ROS and the reaction temperature are higher. Hence, degradation is faster [38]. Similarly, Villegas-Guzman, *et al.* have found that the highest sonolysis of DXC was achieved under 600 kHz sonication at pH=3 [96]. Acidic media also favour the sonochemical degradation of DXC (pH=3.0) [30], LEV

(pH =5.9) [42], SDZ (pH=5.5) [97], and TNZ (pH=3.0) [100], etc.

By contrast, Wang, *et al.* have reported that the TC degradation rate is highly pH-dependent, and that higher pH values favour TC degradation under sonication, due to the transformation of TC molecules at different pH values [99].

2.3.4 Effect of temperature

Generally, the degradation rate of antibiotics increases with increasing temperature [33, 40, 125]. The influence of temperature on the sonodegradation of antibiotics is complicated. As far as we know, high temperature usually results in a high solvent vapour pressure, followed by the formation of more water-vapour-containing cavitation bubbles, causing the cavitation bubbles to collapse less violently, which leads to reduced $\cdot\text{OH}$ production. However, the reduction of the viscosity and surface tension at high temperatures leads to a low threshold intensity for cavitation, which can increase the number of cavitation bubbles, and then promote the generation of $\cdot\text{OH}$ and $\text{HOO}\cdot$. Moreover, the strengthened reactions of the hydroxyl radicals and mass transfer at high temperatures are favourable to the removal of antibiotics [33, 40, 111, 125]. According to De Bel *et al.*, increased temperature (15-45 °C) leads to faster CIP degradation (k_I was increased from 0.0055 to 0.0105 min^{-1}). The low apparent activation energy (17.5 kJ/mol) suggests that the degradation of CIP is diffusion controlled (usually in the range of 12-15 kJ/mol) [125]. Higher temperature (in the range of 30-60 °C) facilitates the removal of FLU by the Sono/ H_2O_2 process [111]. 3% of FLU was removed from 200 mL of 1 mM aqueous FLU solutions for 120 min under 40 kHz and 120W sonication at 60 °C and pH 4 in the presence of 20 mM H_2O_2 . The activation energy for the degradation of FLU was 6.510 kJ/mol [111].

2.3.5 Effect of initial concentration of antibiotics

In general, low concentrations of antibiotics favour their sonochemical degradation; RE decreases with increasing initial concentration [30, 31, 36, 41, 69, 94-100]. The degradation of antibiotics is limited by the available surface at the bubble–

liquid interface. According to the Arrhenius law, for example, the apparent activation energy for the sonochemical degradation of CIP has been determined to be 17.5 kJ/mol, which suggests that the degradation of CIP is diffusion controlled. A Langmuir-type heterogeneous-reaction-kinetics model could be used to explain why the k_l value increases with decreasing initial CIP concentration from 0.0204 min⁻¹ (C_0 : 0.15 mg/L) to 0.0009 min⁻¹ (C_0 : 150 mg/L). According to the model, the molecules at the interface region of the cavitation bubbles can be readily oxidized by the formed $\cdot\text{OH}$ [125].

2.3.6 Effect of additives

Antibiotics can be degraded to a certain degree by sonication alone, but the REs of non-volatile compounds are somewhat lower and degradation is really time consuming. For example, it has been observed that only 30% DXC was degraded after 8 h [96], and most antibiotics were converted into hydrophilic organics rather than CO₂ [17]. Although the BOD₅/COD ratio (biodegradability) noticeably increased, e.g., from 0 to 0.36, after the sonochemical degradation of CPX [127], the mineralization of antibiotics is challenging even after a long period of sonication [30, 98, 127, 128]. For example, 180 μM SMZ was almost fully removed, but only 8.31% TOC was reduced by sonication at 800 kHz and 100 W in 2 h [41]. Therefore, a great deal of effort has been devoted to enhancing sonolysis to increase the RE, with an eye on practical applications, using simple additives, such as noble gas Argon (Ar), anions, CCl₄, H₂O₂, etc. in the sonication system.

Due to Ar's physical properties (e.g. solubility, thermal conductivity and specific heat ratio), an Ar atmosphere favours sonolytic activity compared to diatomic gases [36, 109]. Gao, *et al.* have reported that the sonolytic degradation of SMZ is accelerated in the presence of Ar or O₂, but inhibited by N₂ [41]. Meanwhile, the SMZ degradation rate was slightly inhibited by NO₃⁻, Cl⁻ and SO₄²⁻, which is consistent with the sonochemical degradation of TC [99], but significantly improved by HCO₃⁻ and Br⁻ [41]. The enhancement of TC degradation by adding HCO₃⁻ has also been demonstrated [99], while a negligible influence was observed when adding mannitol or

calcium carbonate during the sonochemical degradation of OXA at a high frequency in wastewater (from a municipal wastewater treatment plant) [128]. In another sonication system, KI and H₂O₂ were used as an iodine source to enhance the RE of SMZ, and the RE value increased from 3.4 to 85.1 under 60 min sonication with 0.04 mM SMZ, 2.4 mM KI and 120 mM H₂O₂ at 195 W US under acidic conditions. I[•] and I^{2•+} radicals were the most predominant active species. The activation energy of SMZ degradation was calculated to be 7.75 ± 0.61 kJ/mol (15–55 °C), which indicates that the reaction is potentially a diffusion-controlled process [98]. Furthermore, the addition of CCl₄ can also enhance sonochemical degradation, which is attributed mainly to the formation of chlorine-containing oxidizing species, such as HClO, Cl₂, [•]Cl, [•]CCl₃ and [•]CCl₂, from the sonolysis of CCl₄ [42, 133].

Zhang, *et al.* have investigated the degradation of sulfa antibiotics by potassium ferrate in combination with sonication (Sono/Fe(VI)) [75]. SDZ, SMR and SMX were all well degraded by sonication, and the reaction process was in accordance with pseudo-second order reaction kinetics; the REs of SDZ, SMR and SMX were 77.5, 82.5 and 82.5% for 30 min sonication, respectively. H₂O₂ was often added to the sonication system to enhance antibiotic degradation [36, 99, 100, 132]. Matouq, *et al.* have investigated AMX degradation at 2.4 MHz sonication, with the addition of H₂O₂ providing a great increase to the RE of AMX [132]. The effect of adding H₂O₂ to the sonochemical degradation of antibiotics has been summarized in Table 2.

As seen in Table 2, the sonolysis of TC, LEV, NOR, MTZ, OFX and FLU, etc., has been conducted in a US-frequency range of (20-2400 kHz) and a US-power range of (100-750 W). Their REs are located in the range of 1.88%-81.00%, under sonication alone, and 0-30%, under oxidation alone with 0.29-333.00 mM H₂O₂ for 30-240 min. In some cases, significantly higher REs (5.9-93%) were given by sono/H₂O₂ processes than in those performed with sonication alone, or oxidation with H₂O₂ alone. In addition, COD was slightly removed, leading to increasing ratio of BOD₅/COD.

Table 2 Summary of sonochemical degradation of antibiotics in the presence of H₂O₂.

Antibiotics	C _{H2O2} (mM)	F _{US} /P _E (kHz/W)	t (min)	C ₀ /V (mg/L)/mL	pH	RE _{H2O2} (%)	RE _{Sono} (%)	RE _{Sono/H2O2} (%)	Refs.
TC	0.29	20/400	60	10/100	5.5	~0	81.0	93.0	[99]
LEV	5.0	20/195	150	20/100	7.1	6.7	1.9	65.0	[43]
NOR	20.0	20/240	30	5/200	7.0	~0	<5.0	5.9	[20]
MTZ	60.0	20/-	180	500/200	3.0	-	42.0	68.0	[41]
OFX	100.0	20/224	240	10/350	-	-	31.0	50.0	[36]
TNZ	333.0	120/750	150	80/100	3.0	-	5.0	75.0	[100]
CLM	1.0	130/500	150	45/-	3.0	~25.0	~30.0	~45.0	[21]
CIP	1.0	580/-	60	100/250	3.0	5.9	35.8	36.5	[32]
AMX	5.0 mL	2400/9.5	90	50/50	3.5- 5.5	~30.0	-	70.0	[132]

Note: C_{H2O2}: H₂O₂ concentration; F_{US}: ultrasonic frequency; P_E: electrical power input; t: sonication time; C₀: initial antibiotic concentration; V: volume of solution; RE: removal efficiency; Refs.: references.

However, the addition of H₂O₂, used as a radical promoter, does not always promote sonication processes [20, 32]. When sonication was applied without H₂O₂, degradation and mineralization (35.8 and 22.6%, respectively) were similar to the results obtained in sono/H₂O₂ processes (36.5 and 24.4%, respectively) [32]. Therefore, excess H₂O₂ can act as a [•]OH scavenger and decrease the RE of antibiotics, resulting in the presence of an optimal amount of H₂O₂ for the sonochemical degradation of the target compounds.

In addition, Serna-Galvis, *et al.* have reported the role of mechanical agitation in the removal of OXA (or AMP) via sonication [129], photo-Fenton, TiO₂ photo-electro [17, 69, 128], and sono-Fenton processes [46]. These results suggest that mechanical agitation is not required in the processes that involve sonication on the lab-scale [17, 46, 69, 128, 129]. The exception is the degradation of CIP in the US-assisted *Laccase* catalytic process, in which degradation increased from 8% to 50%, due to improved mass transfer, when the agitation speed was increased from 0 rpm to 200 rpm. However, no further enhancement in degradation efficiency was observed when the agitation speed was increased to 300 rpm [91].

Moreover, although the application of sonication has been shown to be feasible on small scales, its use in large-scale treatment process is still a challenge because of high

energy requirements [105]. Therefore, sonication has been combined with other additives (catalysts and persulfate) and other AOPs (Fenton reaction, photocatalysis, ozonation, etc.) to increase the RE, reduce reaction times and enhance mineralization [36, 38]. These hybrid methods are discussed below.

3 Degradation of antibiotics by sonocatalysis

The ability of sonication to enhance the heterogeneous catalytic degradation of antibiotics is discussed in this section, while the role of sonication in the homogeneous catalytic degradation of antibiotics, mainly Fenton reactions, will be discussed in the following section. In most cases, higher REs are obtained by sonocatalysis than the sum of those obtained under catalysis and sonication alone [40, 44, 71, 102, 103, 106, 109, 134, 135]. More importantly, antibiotics, such as TC, OTC, CTC and DTC, can be decomposed into a suite of non-toxic intermediates by sonocatalytic processes [136]. For example, GMF was first decomposed to aromatic and aliphatic intermediates in the early stage of reactions, and then mineralized to CO₂, H₂O and inorganic ions, leading to significant reductions in solution toxicity after the sonocatalytic degradation of GMF [103]. Similarly, a substantial reduction in the toxicity of an AMP solution has been observed after the sonocatalytic degradation of AMP with Zn(OH)F [101].

A bio-toxicity examination, using an inhibition test conducted on activated sludge, revealed diminishing oxygen-consumption-inhibition percentage [IOUR (%)], from 33.6 to 22.1%, during the sono/ZnO/nano-cellulose process. The utilization of the sono/ZnO/nano-cellulose process can convert TC molecules to less toxic compounds. However, longer reaction times are required for complete conversion into non-toxic substances [104].

3.1 Mechanisms of sonocatalysis

In sonocatalytic systems, [•]OH radicals are the dominant reactive species that contribute to antibiotic degradation. The pronounced degradation effectiveness with the catalysts under sonication can be assigned to their synergetic ability to produce ROS

and subsequent radical reactions [109]. Sonocatalysis includes two reaction pathways (Figure 2): (1) catalytic degradation enhanced by sonication; (2) sonolysis enhanced by the catalyst.

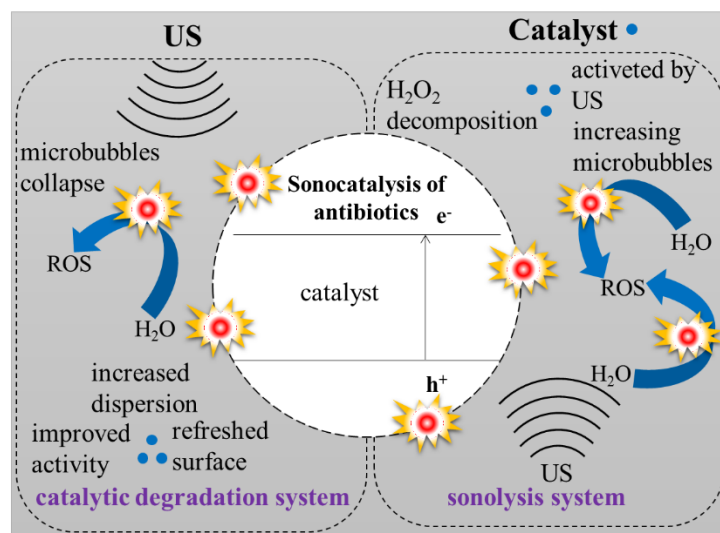


Figure 2 The mechanisms of antibiotic removal by sonocatalysis.

In an attempt to clarify the effects of sonication on heterogeneous catalysis, increased dispersion has been considered as a reason for the increased reaction rate. The removal of the passivating layer, the reduction of the catalyst particle size and enhanced interparticle collisions, all induced by cavitation shock waves and local turbulent microjets, may increase the number of active reaction sites on catalysts as well as increasing the contact area, improving mass transfer and minimizing fouling, which all result in increased catalytic activity [52].

In homogeneous systems, it is also critical to activate the catalyst and to keep it active during antibiotic degradation. Sonication can improve mass transfer, catalyst activation and the production of higher ROS concentrations, e.g., in Fenton reactions [77, 137]. Organometallic compounds are often used for the homogeneous catalysis of various reactions. The starting organometallic compound, however, is often catalytically inactive until it loses the metal-bonded ligands (such as carbon monoxide) from the metal. Sonication can induce ligand dissociation, making the initiation of homogeneous catalysis by sonication practical. The transient, coordinatively

unsaturated species produced from the sonolysis of metal carbonyls are likely candidates [37, 52].

On the other hand, solid catalyst particles may increase the density of microbubbles, meaning that more ROS will be produced during bubbles collapse. H₂O₂ formation is significantly increased due to the dispersion of catalysts under sonication, indicating that the dispersed catalyst particles can act as additional nuclei for the pyrolysis of water molecules and the formation of $\cdot\text{OH}$ [40]. As a result, increased radical transfer from cavitation bubbles to the interface and bulk solution is promoted, and with it the RE of antibiotics [37, 52, 126]. In homogeneous systems, catalysts, such as Fe²⁺, promote radical formation via the decomposition of H₂O₂, formed under sonication, to enhance and accelerate the degradation of antibiotics [137, 138]. For example, the sonolysis of SMZ was accelerated in the presence of ferrous ion. The synergetic effect was mainly attributed to the production of additional $\cdot\text{OH}$ via Fenton chemistry [41].

3.2 Application of sonocatalysis in antibiotic degradation

To date, a great many catalysts, including single walled carbon nanotubes (SWNTs) [40, 71], novel Fe-Cu layered double hydroxide/biochar nanocomposites (Fe-Cu-LDH/biochar) [102], biochar-supported ZnO nanorods (ZnO-biochar) [103], ZnO nanostructures loaded on nano-cellulose (ZnO/NC) [104], cerium-substituted magnetite (CeO₂/Fe₃O₄) [106], and novel Z-scheme composites (mMBIP-MWCNT-In₂O₃) [107], etc., have been synthesized for the sonocatalytic degradation of antibiotics. Moreover, semiconductors, such as Ni powder, Raney Ni, Pd or Pt and metal oxides have recently been added to carbon to accelerate the degradation of antibiotics by sonication [52, 103].

Al-Hamadani, *et al.* have investigated the degradation of SMX via sonication at 1000 kHz in the presence of SWNTs [40]. The REs of SMX reached 92% and 70% at pH 7 for 60 min of treatment by sonocatalysis and sonication alone, respectively, with

the other conditions being constant (0.18 W/L of power density, 1 L of 2.5 mg/L SMX solution), and 48% of RE was achieved by the SWNT alone [40]. Hoseini, *et al.* have investigated the degradation of TC by sonocatalysis using TiO₂ nano-particles under 35 kHz US [105]. The efficacy of sonication alone in the removal of TC was negligible, but the RE increased upon the addition of TiO₂.

The REs of various antibiotics under catalysis alone, sonication alone and sonocatalysis have been compared and summarized in Table 3.

Table 3 Summary of sonocatalytic degradation of antibiotics in water.

Antibiotics	Catalyst	F_{US}/P_E (kHz/W)	t (min)	C_0/V (mg/L)/mL	pH	RE _{Catal.} (%)	RE _{Sono} (%)	RE _{Sono/Catal} (%)	SF	Refs.
AMX	0.8 g/L ZnO@Fe ₃ O ₄	20/60	120	10/100	3.0	47.0	9.6	90.0	1.6	[134]
CIP	0.2 g/L TiO ₂ /Montmorillonite	35/65	120	10/100	6.0	<25.0	8.1	65.0	~2.0	[135]
MOX	1 g/L NiFeLDH/rGO	36/150	60	20/100	8.0	33.8	8.2	72.4	1.7	[118]
TC	0.5 g/L ZnO/nano-cellulose	37/256	15	50/50	7.0	28.2	12.8	87.6	2.1	[104]
TC	0.5 g/L ZnO;	37/256	15	50/50	7.0	4.4	12.8	70.0	4.1	[104]
RIF	1.5 g/L ZrO ₂ -pumice	40/300	90	20/100	5.0	~10.0	7.2	~95.3	15.5	[109]
RIF	1.5 g/L ZrO ₂ -tuff	40/300	90	20/100	5.0	~10.0	7.2	83.1	9.1	[109]
CFZ	1 g/L Fe-Cu layered double hydroxide	40/300	80	47.6/100	6.5	32.6	6.8	97.6	2.5	[102]
NOR	0.3 g/L multilayer ZnO nanoflowers	40/200	80	2.0/50	7.5	19.2	6.4	47.5	1.9	[140]
OTC	0.75 g/L Fe _{2.8} Ce _{0.2} O ₄	40/300	120	50/150	4.7	37.0	17.0	64.0	1.2	[106]
GMF	1.5 g/L Nano-ZnO- biochar	40/300	45	20/100	5.5	15.1	10.4	96.1	3.8	[103]
SDZ	0.05 mM K ₂ FeO ₄	100/800	30	5.1/100	7.0	~68.0	~52.0	~80.0	~0.7	[75]
SMR	0.05 mM K ₂ FeO ₄	100/800	30	5.1/100	7.0	~70.0	~55.0	~82.0	~0.7	[75]
SMX	0.05 mM K ₂ FeO ₄	100/800	30	5.1/100	7.0	~70.0	~56.0	~75.0	~0.6	[75]
SMX	45 mg/L SWCNs	1000/180	60	2.5/1000	7.0	48.0	70.0	92.0	1.1	[40]

Note: F_{US}: ultrasonic frequency; P_E: electrical power input; t: sonication time; C₀: initial antibiotic concentration; V: volume of solution; RE: removal efficiency; SF: synergy factors = $RE_{Sono/Catal}/(RE_{Sono}+RE_{Catal})$ [71, 81, 109]; Refs.: references.

As summarized in Table 3, the sonolysis of AMX, CIP, MOX, TC, TC and CIP, etc., has been conducted by sonocatalysis. At low US frequency ranges (20-40 kHz)

and US power ranges (60-350 W), REs are located in the range of 2.5%-17.0% under sonication alone for 15-120 min. At high US frequency (100-1000 kHz) and power (180-800 W), high REs (52-70%) were observed for the removal of SDZ, SMR and SMX via sonication alone after 30-60 min. The adsorption by catalysts of these antibiotics was also performed at a dosage of 0.2-1.5 g/L, and the REs were observed to be in the range of 3.3-70%. The degradation of antibiotics by sonication was enhanced greatly by the addition of catalysts, due to the synergistic effect, and the REs reached a range of 47.5-95.3%.

In addition, most of the catalysts can be considered composite catalysts, in which both the effective component and support play important role. Khataee, *et al.* have investigated the sonocatalytic degradation of RIF using ZrO₂ nanoparticles on pumice (ZrO₂-pumice) and tuff (ZrO₂-tuff), which were synthesized using a modified sol-gel method [109]. About 95% and 83% of 20 mg/L RIF was removed by sonication at 40 kHz and 300 W using 1.5 g/L of ZrO₂-pumice or ZrO₂-tuff, respectively, under natural pH conditions [109].

A ZnO-biochar nanocomposite has exhibited better sonocatalytic performance than biochar and ZnO nanorods because of its huge surface area, narrow band gap and enhanced cavitation phenomenon [103]. The enhancement in the adsorption capacity of sonocatalyst is caused by reducing electron and hole recombination using fluorine and enhancing the oxidation potential of the valence band of ZF1 (ZnO with F/Zn molar ratio of 1:1) compared to ZnO. The prepared Z-scheme KTaO₃/FeVO₄/Bi₂O₃ sonocatalyst displayed much higher sonocatalytic activity in the sonocatalytic degradation of CEF sodium than Z-scheme KTaO₃/Bi₂O₃ [110]. This excellent sonocatalytic performance is attributed to the introduction of the FeVO₄ conductive channel in which the valence state changes of Fe and V provides driving force for e⁻ transfer, which obviously enhances the sonocatalytic activity of KTaO₃/Bi₂O₃ [110].

3.3 Role of effective factors

Similar to degradation by sonication alone, sonocatalytic efficiency is also affected by various factors, including initial substrate concentration [101, 105, 140], pH value [40, 141], temperature [40, 142], catalyst amount [139], US power/frequency [40, 71] and the presence of additives (IO_4^- [134], H_2O_2 [71, 102, 104, 134, 135, 139], and gases [103, 106]).

3.3.1 Effect of US frequency

Al-Hamadani, *et al.* have investigated the effect of US frequency on the degradation of SMX via sonocatalysis with glass beads (GBs) and SWCNs [71]. The removal of SMX was enhanced significantly in the presence of GBs at 28 kHz, whereas it was significantly reduced at 1000 kHz as the GB particle size was similar to or larger than that of the cavitation bubbles at high frequency, leading to interference between the US and GB particles that resulted in a reduction in H_2O_2 production [71]. Additionally, the presence of SWNTs was effective under low and high frequencies in both the sonochemical degradation mechanism and adsorption mechanism because the dispersed SWNT particles acted as additional nuclei for the pyrolysis of water molecules and the formation of more $\cdot\text{OH}$. Moreover, the dispersion of SWNTs, due to sonication, enhanced the adsorption process by providing more adsorption sites, leading to increased adsorption capacity. However, maximum SMX removal was achieved at both frequencies when GBs and SWNTs were combined, as a result of enhanced sonochemical degradation via $\cdot\text{OH}$ formation and the adsorption process resulting from SWNT dispersion [71].

3.3.2 Effect of pH value

Hoseini, *et al.* have investigated the effect of pH on TC degradation using sonocatalysis with TiO_2 nanoparticles, and it was found that an increase in pH attenuated TC degradation [105]. The relatively high *RE* values of sonocatalytic degradation for PG using MgO and SMX, with SWCNs nanoparticles, were also

obtained under acidic conditions at pH 3.0 and pH 3.5, respectively [40, 141]. Seid-Mohammadi, *et al.* have found that pH value clearly affects the removal of CPX in sono/H₂O₂/NiO hybrid process, and that process efficiency was reduced at pH 9, with pH 3 giving the highest RE (93.8%) [74].

3.3.3 Effect of temperature

The influence of increased temperature on the degradation of antibiotics is exerted via: i) the cavitation intensity; ii) changes in the physicochemical properties of the antibiotics; and iii) the type of cavities formed [40]. An increased k_1 was observed for SMX with increased temperature (15-55 °C) in a sono/SWNT system. The low apparent activation energy values (7.28 kJ/mol) for SMX indicate that the degradation of SMX is influenced by diffusion. This is presumably because the degradation rate reflects the fact that the SMX molecule in the bulk solution moves to the gas-liquid interface region, where temperatures and $\cdot\text{OH}$ concentrations are high [40]. The removal rate for AZI increased with increasing temperature (20-40°C) in the sono/ZnO system, especially from 20 to 40 °C. However, a steady decrease in removal rate was observed at 40 to 60°C [142]. The removal of TYL was enhanced by increased temperature (10-40 °C). The k_1 values of the degradation of TYL were 0.0107, 0.0126, 0.0148 and 0.0165 min⁻¹ at 10, 20, 30 and 40 °C, respectively [142].

3.3.4 Effect of initial concentration

Hoseini, *et al.* have investigated the effect of initial TC concentration on its degradation by sonocatalysis using TiO₂ nanoparticles, and it was found that an increase in initial TC concentration attenuated TC degradation [105]. Similarly, the *RE* values of NOR and AMP also decreased with increased initial concentrations [101, 107].

3.3.5 Effect of catalyst amount

Gao, *et al.* have found that increases in both the MnSO₄ concentration of the wet impregnation solution and the catalyst dosage enhanced the sonocatalytic degradation of TC with Mn-modified diatomite [139]. NOR degradation rate also increased with an

increase in ZnO dosage [140].

3.3.6 Effect of additives

Adding noble gas Ar, CCl₄, or H₂O₂ to the sonocatalytic system can often enhance RE, while the presence of inorganic and organic scavengers suppresses the performance of the sonocatalytic removal of antibiotics [71, 102, 135]. Furthermore, the degradation mechanisms, namely the interactions between $\cdot\text{OH}$ and the antibiotics, can be demonstrated [71]. For example, the presence of ethanol suppressed SSZ degradation due to the quenching of $\cdot\text{OH}$, while the addition of K₂S₂O₈ and H₂O₂ increased the RE due to the formation of $\text{SO}_4^{\cdot-}$ and extra $\cdot\text{OH}$, respectively [52, 54, 73, 74, 97, 111, 126, 128].

Seid-Mohammadi, *et al.* have investigated the removal of CFX from aqueous solutions using sono/H₂O₂/NiO process at 40 kHz. Under optimum conditions (pH 3, reaction time 90 min, 40 mg/L CEX, 7.5 mg/L NiO and 30 mL/L (30%, w/w) H₂O₂), the REs of CEX, COD and TOC were 93.9, 72.5 and 54.6%, respectively. The pH value is the most critical factor [74]. Yazdani, *et al.* have investigated the sonocatalytic degradation of AZI with ZnO, finding that H₂O₂ addition significantly increased the RE of AZI from 90.6% to 98.4% [142]. H₂O₂ addition also improved the sonocatalytic REs of RIF [109]. However, Hoseini, *et al.* have reported that the addition of H₂O₂ attenuated the sonocatalytic degradation of TC with TiO₂ nano-particles [105].

In addition, Dehghan, *et al.* have investigated the effect of adding IO_4^- on the sonocatalytic degradation of AMX with a ZnO@Fe₃O₄ magnetic nanocomposite. It was observed that the degradation rate was accelerated in the presence of IO_4^- , showing the greater oxidation potential compared to the other oxidant agents [134]. Moreover, peroxydisulfate ($\text{S}_2\text{O}_8^{2-}$) has been extensively investigated as a means to enhance the sonocatalytic degradation of antibiotics [109, 140], which is discussed particularly in chapter 5.

Besides, Khataee, *et al.* have investigated the sonocatalytic degradation of OTC

with CeO₂/Fe₃O₄, and it was found that the addition of O₂ and Ar improved the RE of OTC by up to 78 % and 76 %, respectively [106]. The enhancement of adding gases on RE is attributed to an increase in the number of nucleation sites in aqueous media, and enhancements in the pressure and temperature of collapsing cavitation bubbles [103].

On the other hand, inorganic and organic scavenging additives reduced the REs of antibiotics in sonocatalytic systems, indicating that [•]OH-mediation oxidation is responsible for the degradation of antibiotics, including SMX [71], CFZ [102], AMX [134], CIP [135], and TC [104, 139]. For example, the RE of TC decreased by over 25% in the presence of tert-butanol [104]. The presence of isopropanol, KBr and NaN₃ sharply quenched a series of reactive oxygen species [139]. Of these water matrix components, chloride and sulfate anions had the highest and lowest inhibiting effects on the RE of AMX, respectively [134].

3.3.7 Reusability of catalysts

From the perspective of cost reduction and environmental protection, the recyclability of catalysts is essential to promoting sonocatalytic processes. In many cases, catalysts exhibited higher stability for the sonocatalytic degradation of antibiotics due to the strong ultrasonic surface cleaning [108]. Under sonication, catalysts can maintain their catalytic activity for antibiotic removal for 4-5 consecutive runs [73]. For example, the RE of AMP was reduced by only 5% even after Zn(OH)F was reused for four experiments [101]. Similarly, the REs of AMX with ZnO@Fe₃O₄ and CFZ with Fe-Cu-LDH/biochar nanocomposite dropped by only 5-9 % after five successive runs [102, 134]. Er³⁺: Y₃Al₅O₁₂@Ni (Fe_{0.05}Ga_{0.95})₂O₄-Au-BiVO₄ coated composite also exhibited excellent recyclability and sustainability for the sonocatalytic degradation of SA for five repetitive cycles without any apparent deactivation [72].

Overall, sonocatalysis can significantly increase the RE of antibiotics compared with catalysis or sonication alone, but this process is still highly energy demanding and limited to laboratory-scale investigation at present. Thus, additional chemicals are

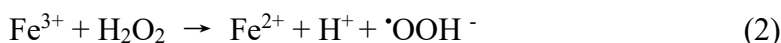
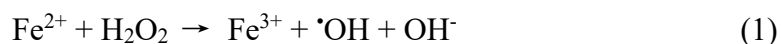
required in many cases to improve the RE. To overcome the drawbacks and reduce the operating costs, a combination of sonication and other AOPs has been proposed to exploit the benefits of the synergistic effects of the AOPs [37].

4 Degradation of antibiotics by sono/Fenton and sono/Fenton-like processes

4.1 Mechanisms of sono/Fenton processes

Fenton oxidation is one of the AOP techniques that has been most widely applied for antibiotic removal [17, 32-35]. So far, the Fenton processes that have been applied to the degradation of antibiotics can be divided into: classic homogeneous Fenton processes; and heterogeneous Fenton processes or Fenton-like processes. The classic Fenton reaction usually occurs in acidic homogeneous systems where Fe^{2+} , or other metal ions (Cu^{2+} , Zn^{2+} , etc.), and H_2O_2 exist simultaneously. By contrast, Fenton-like reactions generally occur in acidic heterogeneous systems where solid catalysts (Fe^0 , Fe_3O_4 , etc.) and H_2O_2 exist simultaneously.

As a green oxidant, H_2O_2 is frequently used to form ROS for organic removal [43]. In classic Fenton processes, Fenton's reagent is a mixture of H_2O_2 and ferrous iron [48], where the dissociation of the oxidant and the formation of highly reactive $\cdot\text{OH}$ are included, as shown in Eq. (1) - (3) [47, 48].



In sono/Fenton processes, the radical reactions near the hotspots and/or in the bulk liquid dominate the degradation of antibiotics [96]. On the one hand, sonication can improve mass transfer, thus enhancing the generation of $\cdot\text{OH}$ and reducing the consumption of chemicals [47, 48]. On the other, adding the right amount of Fe^{2+} (e.g.,

1.0 mM) can also enhance $\cdot\text{OH}$ production via the reactions between $\text{Fe}^{2+}/\text{Fe}^{3+}$ and H_2O_2 , including H_2O_2 that is formed *in situ* [17, 30, 34, 41, 43, 46, 69, 95, 96, 97, 139].

Unfortunately, excessive H_2O_2 and Fe^{2+} negatively influence the degradation of antibiotics [30, 34, 96], since large doses of Fe^{2+} and H_2O_2 can act as scavengers for $\cdot\text{OH}$ in aqueous matrices [34, 41, 95, 96]. In addition, the pH value of solutions significantly affects the degradation of antibiotics [111]. For $\text{pH} > 4$, the total concentration of Fe^{2+} and Fe^{3+} decreases considerably as their complexes and hydroxides are formed in solution. At $\text{pH} < 2$, Fe^{2+} and Fe^{3+} exists as $[\text{Fe}(\text{H}_2\text{O})_6]^{2+}$ and $[\text{Fe}(\text{H}_2\text{O})_6]^{3+}$ respectively, and the regeneration of Fe^{2+} in the form of $[\text{Fe}(\text{H}_2\text{O})_6]^{2+}$ from $[\text{Fe}(\text{H}_2\text{O})_6]^{3+}$ is slow. Meanwhile, H_2O_2 forms oxonium ions (H_3O_2^+). These are more stable than H_2O_2 and their reactivity with ferrous ions decreases. In addition, the scavenging effect of $\cdot\text{OH}$ by H^+ is enhanced at $\text{pH} < 2$ [111]. Therefore, the optimal pH range for classic Fenton reactions is 2-4 [21, 22, 41, 111]. Also, the pH value affects the chemical structures of the antibiotics, thus influencing REs in sono-Fenton process [96, 99].

4.2 Application of sono/Fenton processes on antibiotic degradation

Wang, *et al.* have reported the degradation of 50 mg/L TC via sonication at 20 kHz and 100 W US in 1 L solution at pH 6, in the presence of 0.2 mM Fe^{2+} and 2.0 mM H_2O_2 [34]. Consequently, an RE of 91.3% was achieved in 60 min using this sono/Fenton process, which is higher than the sum of those obtained under Fenton (70.2%) and sonication alone (6.7%). Meanwhile, mineralization reached 45.8% in the sono/Fenton process, resulting in the toxicity of the TC solution being significantly decreased [34].

Labrada, *et al.* have studied CIP degradation in wastewater using a homogeneous sono/Fenton process at high frequency [32]. 100 mg/L CIP was sonicated with 580 kHz and 30.6 W US in a 250 mL solution at pH 3, in the presence of 2.4 mM Fe^{2+} and 14.2 mM H_2O_2 . An RE of about 98.4% was achieved using this sono/Fenton process in 15

min. However, the RE obtained by sono/Fenton is lower than the sum of those obtained under Fenton and sonication alone (96.4% and 9.3%). However, the mineralization reached 60% using the sono/Fenton process after 60 min [32]. Ammar *et al.* have investigated the degradation of 500 mg/L MTZ by sonication at 20 kHz US in a 200 mL solution at pH 3.0 in the presence of 3 mM Fe^{2+} and 60 mM H_2O_2 [113]. The results indicate that 98% of MTZ was removed using the sono/Fenton process in 180 min at 30 °C, which is higher than those obtained by sonication alone (42%) and Fenton process alone (90.0%), but is lower than sum of REs of the two individual processes [113]. At 40 kHz, 261.2 mg/L FLU was sonicated with 120 W US in a 200 mL solution at pH 4.0 in the presence of 4 mM Fe^{2+} and 20 mM H_2O_2 [111]. As a result, an RE of 93% was achieved using the sono/Fenton process in 120 min at 60 °C, which is obviously higher than that (73%) obtained by the Fenton process alone [111].

Overall, this suggests that the synergistic effects of sonication and the Fenton reaction for antibiotic degradation is dependent on the physicochemical properties of the antibiotics and Fenton reagents rather than the character of the US used.

4.3 Mechanisms of sono/Fenton-like processes

The Fenton process requires a large amount of Fe^{2+} and acidic conditions, which requires neutralization with alkaline, resulting in large-scale sedimentation and high costs. With the development of Fenton-like technologies, the drawbacks of the conventional Fenton process have been overcome to some extent [44]. Fe^0 , Fe_3O_4 particles and their nanoparticles are important catalysts to promote the decomposition of H_2O_2 for the formation of $\cdot\text{OH}$ [21, 22, 33, 43, 44]. Unfortunately, the solid catalysts may be poisoned during Fenton reactions, nano-catalysts particles can aggregate and solid-catalyst passivation can occur, thus decreasing the degradation rate and limiting potential applications [21, 22, 33, 119]. Therefore, sonication has been applied in the Fenton-like process to maintain the activity of catalysts and improve antibiotic removal. The mechanism of sono/Fenton-like processes is shown in Figure 3.

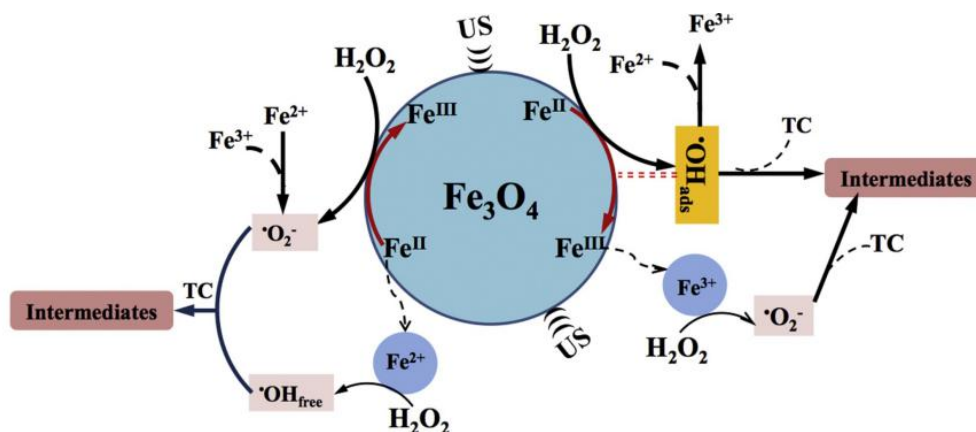
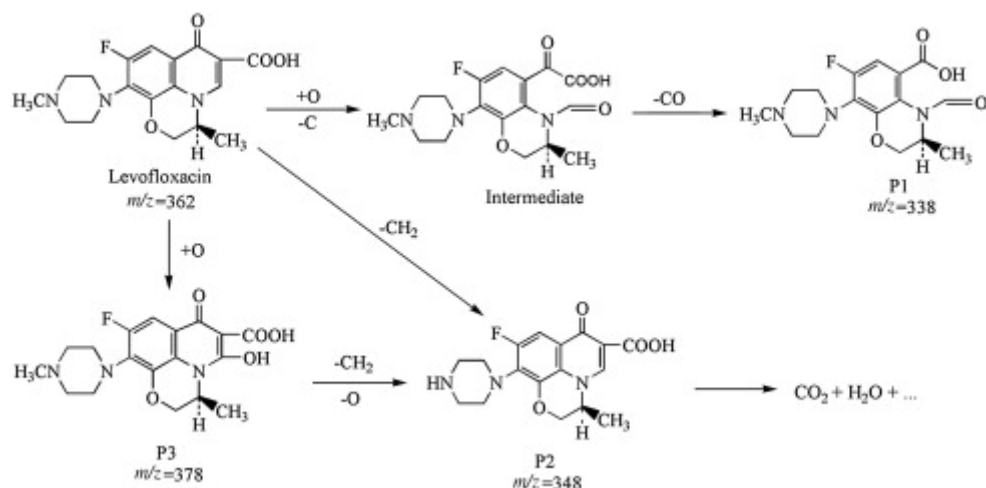


Figure 3 Mechanism schematic of sono/Fenton-like processes. Reprinted from ref. [33] Copyright (2016), with permission from Elsevier.

As shown in Figure 3, solid-liquid interfacial iron corrosion, bulk homogenous oxygen activation and Fenton reactions are the main reaction pathways in sono/Fenton processes, during which sonication plays both mechanical and chemical roles [35]. The antibiotics and intermediates adsorbed onto the Fe_3O_4 surface are oxidized preferentially [33]. $\cdot\text{OH}$, $\cdot\text{O}_2^-$ and H_2O_2 , formed *in-situ* on the catalyst surface, have been identified as the dominant reactive species in Fenton-like processes [21, 22, 33, 35, 44].

Figure S2 exhibits the LC/MS analysis of the intermediate formation during the degradation of LEV in a sono/ H_2O_2 / Fe_3O_4 (magnetic nanoparticles) process [43]. The degradation pathway of LEV is shown in Scheme 2. The formation of isatin and anthranilic acid analogues is attributed to the oxidation of LEV by $\cdot\text{OH}$. The demethylation of the piperazinyl ring and the degradation at the oxazinyl group result in the generation of the other two intermediates [43]. Unfortunately, this study does not provide the mineralization data of LEV and toxicity variation of LEV solutions by the treatment.



Scheme 2 A tentative partial degradation pathway of LEV in a sono/ H_2O_2 / Fe_3O_4 (magnetic nanoparticles) system. Reprinted from ref. [43] Copyright (2015), with permission from Elsevier.

4.4 Application of sono/Fenton-like processes on antibiotic degradation

So far, sono/Fenton-like processes have been used to remove some antibiotics, such as LEV, TC, NOR, CLA, RXM, TNZ, CLM, etc., and Fe_3O_4 , nano- Fe^0 , ZnS quantum dots/ SnO_2 , nano- Cu^0 and micro- Cu^0 , etc. have been used as catalysts. The concentrations of H_2O_2 addition cover a wide range, 5-1000 mM, and degradations have been performed in the pH range of 3.0-7.1. In sono/Fenton-like systems, the three factors, sonication, Fenton catalyst and H_2O_2 , act together to cause a strong synergistic effect for the degradation of antibiotics (such as MNZ [44]). The application of sono/Fenton-like processes on the degradation of antibiotics has been summarized in Table 4.

Table 4 Summary of antibiotic degradation by sono/Fenton-like processes.

Antibiotics	Fenton reagents	$F_{\text{US}}/P_{\text{E}}$ (kHz/W)	t (min)	C_0/V (mg/L)/mL	pH	RE Fenton-like (%)	RE Sono (%)	RE Sono/Fenton-like (%)	SF	Refs.
LEV	1 g/L Fe_3O_4 , 5 mM H_2O_2	20/195	150	20/100	7.1	71.5	1.9	99.0	1.35	[43]
TC	1 g/L Fe_3O_4 , 150 mM H_2O_2	20/80	60	100/200	3.7	72.2	-	93.6	-	[33]

CLA	0.3 g/L ZnS quantum dots/SnO ₂ , 6 mM H ₂ O ₂	20/75	60	10/100	3.0	31.4	~8.0	61.2	~1.56	[119]
RXM	0.3 g/L ZnS quantum dots/SnO ₂ , 6 mM H ₂ O ₂	20/75	60	10/100	3.0	36.4	~12.0	65.5	~1.35	[119]
NOR	0.25 g/L nano-Cu ⁰ or micro-Cu ⁰ , 20 mM H ₂ O ₂	20/240	30	5/200	7.0	46.7	<5.0	91.5	>1.77	[20]
CEX	7.5 mg/L NiO, 30 mL/L H ₂ O ₂	40/-	90	40/<500	3.0	-	-	93.0	-	[74]
CLM	0.2 g /L Fe ⁰ , 1 M H ₂ O ₂	130/500	150	45/-	3.0	~40.0	~30.0	95.0	~1.36	[21]
TNZ	0.2 g /L Fe ⁰ , 1 M H ₂ O ₂	130/500	150	45/-	3.0	~20.0	-	93.0	-	[22]

Note: FUS: ultrasonic frequency; P_E: electrical power input; t: sonication time; C₀: initial antibiotic concentration; V: volume of solution; RE: removal efficiency; SF: synergy factors = $RE_{sono/Fenton-like}/(RE_{sono}+RE_{Fenton-like})$ [71, 81, 109]; Refs.: references.

As shown in Table 4, the REs of most antibiotics are over 91.5% in 30-150 min, except for the degradation of CLA and RXM in the system with 0.3 g/L ZnS/quantum dots/SnO₂ and 6 mM H₂O₂, and the REs are obviously higher than the sum of those obtained using Fenton-like processes and sonication alone in most cases. In addition, the synergistic degradation of NOR in a heterogeneous sono/Fenton-like system with Fe⁰/tetrphosphate has been reported [35]. 400 mL of a 10 mg/L NOR solution was sonicated at pH 7 with 1 g/L Fe⁰ and 0.3 mM tetrphosphate. As a result, an RE of 90% was achieved in 60 min using this sono/Fenton-like process, which is obviously higher than the sum of those obtained using the Fenton-like process and sonication alone (50% and <5%) [35].

Ma, *et al.* have investigated the degradation of NOR via the ultrasound-enhanced nanosized zero-valent copper (Cu⁰) activation of hydrogen [20]. Compared with the silent degradation system, significantly enhanced NOR removal was obtained in the sono/Fenton-like process. The Cu⁺ released during Cu⁰ dissolution was the predominant

copper species that activated H_2O_2 , yielding $\cdot\text{OH}$ in the sono/ $\text{Cu}^0/\text{H}_2\text{O}_2$ system. According to radical quenching experiments and electron paramagnetic resonance technique, free $\cdot\text{OH}$ in solution was verified as the primary reactive species, and superoxide anion radicals ($\cdot\text{O}_2^-$) were regarded as the mediator for copper cycling, via the reduction of Cu^{2+} to Cu^+ [20].

Importantly, the toxicity of the solution increased during the first 60 min and then decreased with treatment time for the degradation of TC in a sono/Fenton-like process with a Fe_3O_4 catalyst [33]. In general, an increase in the biodegradability of wastewater has been demonstrated after antibiotic degradation by sono/Fenton and sono/Fenton-like processes [32], indicating that these processes are suitable for the treatment of wastewater that contains highly toxic and bio-recalcitrant compounds [113].

4.5 Role of effective factors

The factors influencing the RE of antibiotics using sono/Fenton-like processes includes the initial concentration of antibiotics, US power density, reaction temperature [33], etc. In general, lower antibiotic concentrations, higher temperature (up to 60°C), higher US frequency and power are favourable for RE [21, 22]. The effects of the critical factors, dose of catalysts, the concentration of H_2O_2 , and the pH value of the solution [21, 35, 43, 44, 74], are discussed below.

4.5.1 Effect of Fenton-Reagent dose

In general, a larger amount of catalyst increases the sites for H_2O_2 decomposition and the production of more ROS, resulting in higher antibiotic RE [21]. Gholami, *et al.* and Rahmani, *et al.* have investigated the effects of catalyst amount on the degradation of CLM and TNZ using sono/Fenton-like processes with nanoscale Fe^0 , respectively [21, 22]. The REs increased with increasing Fe^0 nanoparticle dosage, and the highest REs (93%-95%) were observed in a 130 kHz sonochemical system with 0.2 g/L Fe^0 nanoparticles and 1 mM H_2O_2 [21, 22]. It was speculated that the increasing nano- Fe^0 dosage results in an increase in total surface area and therefore increased adsorption

onto active sites. Over 0.2 g/L Fe⁰ nanoparticles, the RE values reached a plateau due to the agglomeration of Fe⁰ nanoparticles and the scavenging of •OH in undesirable reactions [21, 22].

Wei, *et al.* have reported the effect of Fe₃O₄ magnetic-nanoparticle amount on the removal of LEV in a sono/Fenton-like process [43]. As the amount of Fe₃O₄ magnetic nanoparticles increased from 0 to 1.0 g/L, the k_I value increased from 4.69×10^{-3} to $21.3 \times 10^{-3} \text{ min}^{-1}$ in the 20 kHz sonication system. The higher catalyst dose favoured LEV removal due to higher number of nucleation sites for the generation of •OH [43].

4.5.2 Effect of H₂O₂ concentration

Without H₂O₂ present initially, the RE of LEV was approximately 30%, which is mostly attributed to the adsorption of LEV onto the catalyst. As H₂O₂ concentration increased from 1.5 to 15.0 mM, the RE of LEV increased until it reached a peak. The results are mainly related to the adsorption amount of H₂O₂ onto the catalyst [43]. During the degradation of CLM and TNZ in a sono/Fenton-like process with nanoscale Fe⁰, the RE increased with increasing H₂O₂ concentration due to the increase of •OH formed. The system had the highest efficiency with 1 mM H₂O₂ [21, 22].

However, excessive amounts of H₂O₂ adversely affected the REs [82], as the excess H₂O₂ consumes the •OH formed *in situ* and inhibits iron corrosion. In the chemical reaction of •OH with the nanoparticle, hydroxyl ions are produced, which are less active than •OH and reduced system efficiency [21, 22].

4.5.3 Effect of pH value

In general, the pH value can affect the surface-charge properties, adsorption behaviour and electron-transfer ability of the catalyst, which all affect catalytic degradation. Thus, it is necessary to study the effect of the pH value on RE and degradation kinetics in a wide range of pH conditions [44]. The acidic condition (pH 2-4) has been demonstrated to be suitable for the Fenton reaction. Gholami, *et al.* and Rahmani, *et al.* have investigated the effect of pH on the degradation of CLM and TNZ,

using a sono/Fenton-like process with nanoscale Fe^0 [21, 22]. Over the pH range of 3-9, the system had the highest efficiency under acidic conditions (pH 3), as Fe^0 corrosion and the reactivity of $\cdot\text{OH}$ were greatly influenced by H^+ concentration [21, 22].

Guo, *et al.* have reported the effect of pH value on the degradation of LEV in a sono/Fenton-like process with Fe_3O_4 magnetic nanoparticles [43]. Over the pH range of 4-9, the k_1 values of LEV degradation were calculated to be 2.13×10^{-2} , 2.85×10^{-2} and $1.26 \times 10^{-2} \text{ min}^{-1}$ at pH 4, pH 8 and pH 9, respectively. It seems that pH 8 is the optimal condition. LEV exists as different species depending on pH value. At $5.7 \leq \text{pH} \leq 7.9$, LEV mainly exists in its zwitterion form in solution, while at $\text{pH} > 7.9$ and < 5.7 , LEV exists in its cationic or anionic form in solution, respectively. Therefore, the hydrophilicity and solubility of LEV at different pH values play the critical role in its oxidative degradation by $\cdot\text{OH}$. In addition, pH value affects not only LEV adsorption onto the catalyst, but also the heterogeneous Fenton-like reaction on the catalyst surface. The enhanced degradation of LEV over the wide range $4.0 \leq \text{pH} \leq 8.0$ occurred due to nucleation sites on the catalyst for the formation of cavities. At pH 9.0, the decrease of RE was partly due to the decrease in H_2O_2 adsorption onto the catalyst, which was covered with $\text{Fe}(\text{OH})_6^{3-}$, and the self-decomposition of H_2O_2 , resulting in the low availability of H_2O_2 and a low yield of $\cdot\text{OH}$ [43].

20 mg/L MNZ has been degraded with 157.4 mM H_2O_2 and 500 mg/L nano- Fe_3O_4 at 30 °C within a wide pH range, from 3 to 9, and the REs were considerably enhanced by sonication [44]. The RE reached its highest value (98%) after 5 h at pH 3, and the k_1 was $1.4 \times 10^{-2} \text{ min}^{-1}$. k_1 decreased to 1.25×10^{-2} , 7×10^{-3} , 6×10^{-3} and $3.1 \times 10^{-3} \text{ min}^{-1}$ at pH 5.00, 5.79, 7.00 and 9.00, respectively. This dependence on pH is similar to that of the traditional Fenton reaction, and was attribute to a sharp decrease in the concentration of Fe in the oxidation state Fe^{2+} with increasing pH value, thus hindering the activity of the catalyst [44].

4.5.4 Effect of temperature

The k_1 of TC removal ($0.04\text{--}0.12\text{ min}^{-1}$) was enhanced by increased temperature ($22\text{--}50\text{ }^{\circ}\text{C}$) in the sono/ $\text{Fe}_3\text{O}_4/\text{H}_2\text{O}_2$ system. The chemical reaction was the dominant step during the degradation of TC, and the activation energy was 33.8 kJ/mol . The RE of TC was almost the same ($> 90\%$) for all temperatures in 60 min, which indicates that a sufficient amount of $\cdot\text{OH}$ was generated by the sono/ $\text{Fe}_3\text{O}_4/\text{H}_2\text{O}_2$ process [33].

4.5.5 Stability of catalysts

The stability and recyclability of catalysts are important to the promotion of the sono/Fenton-like process [44]. Fortunately, the stability of the catalyst is significantly improved with sonication [33]. The reusability of Fe_3O_4 was evaluated 3 times under identical oxidation conditions, and the RE decreased slightly after 3 cycles. Moreover, these values were still much higher than those obtained in the simple catalytic process [33].

Fe^0 particles can be reused in the relative long-term and not lead to high concentration levels of dissolved iron in the treated effluents ($<0.6\text{ mg/L}$) [35]. A consecutive triplicate-repeated sono/ Fe^0 /tetrapolyphosphate experiment was conducted to examine the reusability of Fe^0 particles for NOR degradation. The k_1 for the three repeated runs were 0.039 , 0.032 and 0.029 min^{-1} , respectively. This indicates that sonication is able to effectively clean and refresh the surface of used Fe^0 particles over a long-term treatment schedule. The Sono/ Fe^0 /tetrapolyphosphate system only led to acceptable levels of dissolved iron in the effluents even after repeated runs.

5 Degradation of antibiotics by sonication with peroxydisulfate (PS) and peroxymonosulfate (PMS)

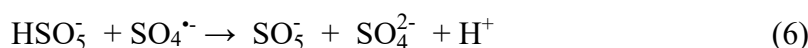
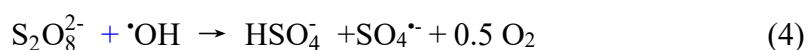
5.1 Mechanisms of sono/PS and sono/PMS processes

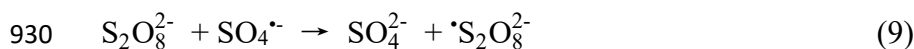
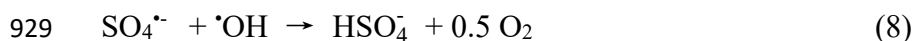
Sulfate radical-based advanced oxidation processes (SR-AOP) are considered to be a promising technology for wastewater treatment [143]. In this technique, sulfate

radicals ($\text{SO}_4^{\bullet-}$, SR) can be formed by the activation of persulfate salts (PS, SO_5^{2-} or $\text{S}_2\text{O}_8^{2-}$) or peroxymonosulfate (PMS, HSO_5^-) via multiple approaches, including heat, UV, sonication, alkaline pH and transition metal ions [21, 119, 144-146]. The triple salt $\text{KHSO}_5 \cdot 0.5 \text{KHSO}_4 \cdot 0.5 \text{K}_2\text{SO}_4$ (Oxone) is a form with higher stability [147]. SR-AOP appears to be more advantageous, efficient and powerful than $\cdot\text{OH}$ -based AOPs [143, 145], as SR appears to be more stable than $\cdot\text{OH}$ in reacting with target antibiotics and is able to oxidize antibiotics efficiently over a wide pH range of 2-8 [148, 149].

In general, $\cdot\text{OH}$ is a powerful oxidant with a redox potential of 1.89-2.8 V [150, 151]. In comparison, SR has an equal or even higher redox potential (1.81–3.1 V), depending on activation method [113, 146, 150, 152]. SR is generated from PS, which has a higher standard redox potential (2.01 V) than PMS (1.81 V) [145, 150]. Therefore, the RE order of acid orange 7 by heat activation is $\text{PS} \gg \text{PMS} > \text{H}_2\text{O}_2$, but by UV activation, the RE order of acid orange 7 becomes $\text{PS} > \text{H}_2\text{O}_2 > \text{PMS}$ [153, 154]. Under sonication activation, the REs of 25 mg/L furfural with PS or PMS reached 95.3% or 58.4%, respectively [155]. However, the REs of SMX by UV activation were observed to follow a different order: $\text{PMS} > \text{PS} > \text{H}_2\text{O}_2$ [156]. Even with a TiO_2 catalyst, k_I by UV activation still shows the same order: $\text{PMS} > \text{PS} > \text{H}_2\text{O}_2$ [157]. A similar order was observed during the degradation of rhodamine B by $\text{Fe}^{2+}/\text{PMS}$ or PS/MoS_2 [158]. Therefore, the oxidation potential of PS and PMS was affected by the whole oxidation system rather than by one factor.

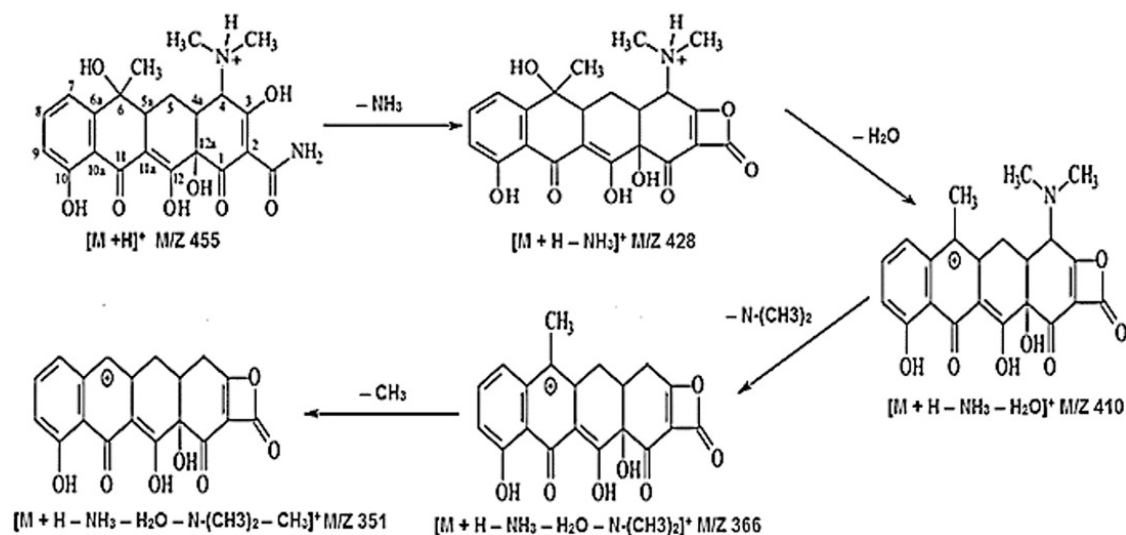
Sonication not only offers a new option for the removal of recalcitrant organic pollutants, but also promotes SR production from the reactions of PS and PMS with $\cdot\text{OH}$ that is formed *in situ* during sonication, as shown in Eqs (4)-(9) [31, 34, 104, 131, 150, 159, 160]:





931 Therefore, the SR and $\bullet\text{OH}$ that are formed from the activation of PS or PMS under
 932 sonication have been considered the origins of antibiotic degradation [82, 131].
 933 Subsequently, the cleavage of chemical bonds of antibiotic molecules, such as the S–N,
 934 S–C and N–C of SMZ [82], or the removal of the N-methyl, hydroxyl and amino groups
 935 of TC occurs via oxidation with SR and $\bullet\text{OH}$ [131].

936 Figure S3 shows the LC-MS of the intermediates during the degradation of TC
 937 using the sono/ $\text{S}_2\text{O}_8^{2-}$ process [160]. Three new peaks, observed after 120 min of
 938 reaction, were related to the formation of polar by-products. The protonated TC
 939 molecular ion $[\text{M}+\text{H}]^+$ and the 4 main by-products generated are shown in the
 940 degradation pathway of TC via the sono/ $\text{S}_2\text{O}_8^{2-}$ process (Scheme 3) [160]. After 120
 941 min sonication of 100 mL of 0.052 mM TC with 4 mM PS at pH 10, 35 kHz and 500
 942 W, nearly 96.5% of TC, 74% of COD and 61.2% of TOC were removed, indicating that
 943 the mineralization of TC was achieved to a certain degree, but incompletely.



945 **Scheme 3.** Proposed degradation pathway for the TC antibiotic in a sono/ $\text{S}_2\text{O}_8^{2-}$ process. Reprinted from ref.
 946 [160] Copyright (2017), with permission from Elsevier.

5.2 Application of Sono/PS or PMS on antibiotic degradation

Safari, *et al.* have reported that 95.0% of 30 mg/L TC was removed by sonication in the presence of PS in 100 mL of a TC solution under 35 kHz and 500 W at pH 10.0 after 120 min. Meanwhile, the REs of COD and TOC reached 72.8% and 59.7%, respectively [131]. Yin, *et al.* have reported that the REs of 50 mg/L SMZ reached 8.6%, 54.3% and 99.6% using sonication alone, PMS alone and Sono/PMS, respectively, under 20 kHz and 600 W at pH 7.5 for 30 min (Figure 4) [82].

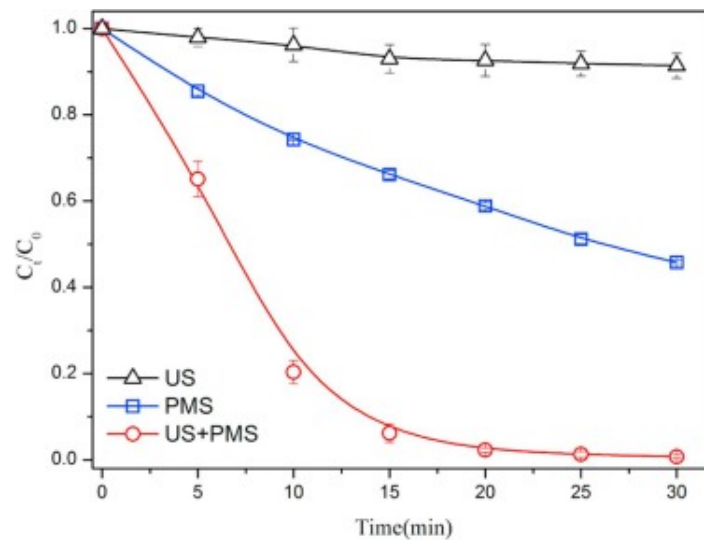


Figure 4 SMT degradation by different processes: US, PMS and US/PMS systems. Reprinted from ref. [82]

Copyright (2018), with permission from Elsevier.

So far, the sonochemical degradation of antibiotics, such as CAP, CIP, TC, SMZ, SDZ, etc., with PS in aqueous solution have been studied. 5-100 mg/L of antibiotics has been sonicated for 30-240 min with 1-200 mM PS or Oxone in 50-1000 mL of aqueous solution. The application of sonication for the degradation of antibiotics with PS or Oxone has been summarized in Table 5.

Table 5 Summary of the degradation of antibiotics by sonication with PS or Oxone.

Antibiotics	C _{PS} (mM)	F _{US} /P _E (kHz/W)	t (min)	C ₀ /V (mg/L)/mL	pH	RE _{PS} (%)	RE _{Sono} (%)	RE _{Sono/PS} (%)	SF	Refs.
TC	2	20/100	60	50/1000	3.0	-	6.7	91.3	-	[34]
TC	200	20/80	90	100/200	3.7	~20.0	~0	51.5	~2.60	[149]
TC	5	35/500	120	23/100	10.0	57.3	26.9	88.5	1.05	[160]

CAP	4	22/200	240	20/50	1.0	<5.0	37.3	62.4	>1.47	[145]
CIP	4.4	40/350	60	50/<1000	4.5	7.5	2.5	18.5	1.85	[19]
SDZ	1.84	20/-	60	-/400	3.0– 7.0	-	9.7	13.7	-	[76]
SMZ	1	40/60	60	5/500	7.0	-	1.6	7.2	-	[161]
SMZ	Oxone 2	20/600	30	50/<100	7.5	54.3	8.6	99.6	1.58	[82]

Note: C_{PS}: PS concentration; F_{US}: ultrasonic frequency; P_E: electrical power input; C₀: initial concentration of antibiotic solution; V: the volume of antibiotic solution; RE: removal efficiency; SF: synergy factors = $RE_{sono/PS}/(RE_{sono}+RE_{PS})$ [71, 81, 109]; Refs.: references.

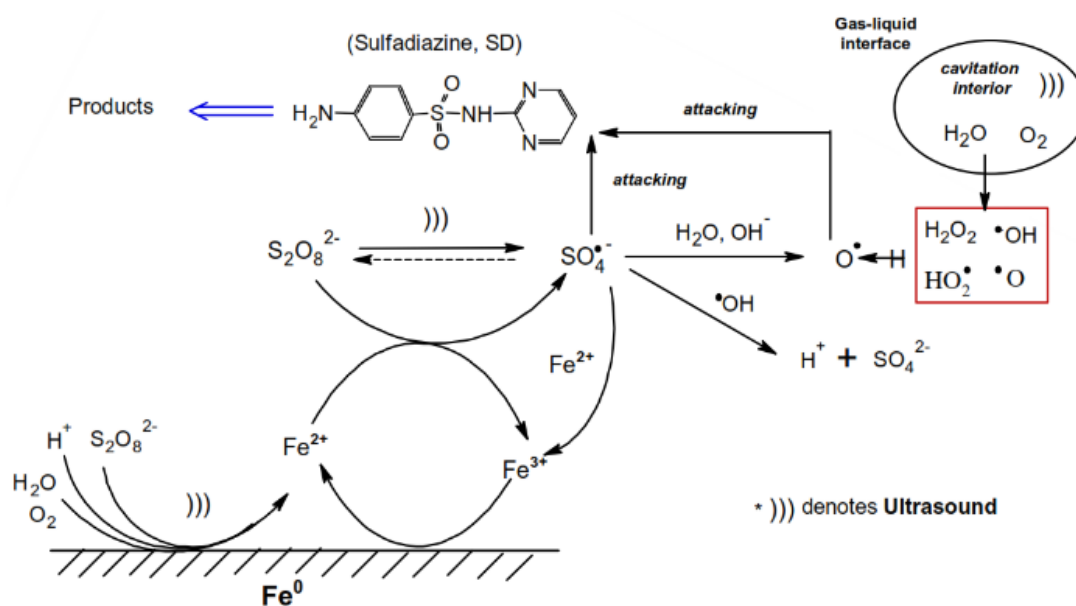
As summarized in Table 5, the dosage of PS or Oxone was in the range of 2-5 mM. Combined sonication with PS or Oxone exhibits higher degradation of antibiotics than sonication alone or oxidation alone under the given conditions. Meanwhile, mineralization can be achieved to a certain degree [34, 162]. For example, the RE of TC reached 96.5% using sono/PS, and 74% of COD removal and 61.2% of TOC removal were achieved [160]. However, some antibiotics, such as CAP, are difficult to degraded using such combined process, even after long treatment times (240 min).

5.3 Mechanism of sono/PS and sono/PMS in the presence of catalysts

To effectively remove antibiotics from aqueous solutions using sono/PS, PMS or Oxone, catalysts have been added to enhance RE [149, 163]. For example, Fe⁰ or PS alone cannot cause significant SDZ degradation, and sonication alone only led to marginal degradation of SDZ after 1 h treatment (9.7% RE). Moreover, the RE of SDZ reached only 9.8% and 13.7% in 1 h using a combination of two factors, such as sono/Fe⁰ and sono/PS, respectively. By contrast, 45.5% of SDZ was removed in 1 h using the Fe⁰/PS combination due to the catalytic decomposition of PS by Fe⁰ and higher SR formation. However, surface passivation prevented the dissolution of Fe⁰ and the release of Fe²⁺, hampering the continuous degradation of SDZ. Therefore, sonication was used to remove the passivation film and improve mass transfer, inducing an SDZ RE of 95.7% in 1 h in the sono/Fe⁰/PS reaction system [76]. Similarly, it is also

difficult to remove TC by sonication alone, or PS alone. Furthermore, little TC was removed with only the Fe_3O_4 catalyst and even the catalyst with sonication due to the insignificant adsorption of TC onto Fe_3O_4 and the inadequate formation of active radicals. However, the RE of TC increased greatly and reached 50.5% and 51.5% in 90 min using the $\text{Fe}_3\text{O}_4/\text{PS}$ and sono/PS combinations, respectively, due to the activation of PS by the catalyst or sonication; the formation of more SR and $\cdot\text{OH}$ on the surface of catalyst. More significantly, the RE of TC reached 89% with sono/ $\text{Fe}_3\text{O}_4/\text{PS}$ since the activity of Fe_3O_4 was maintained by sonication and PS was activated by Fe_3O_4 and sonication simultaneously to produce more SR [149].

Fe^0 [76, 161], ZnO [104], Fe^{2+} [111, 113], Co^{2+} [145, 162], Ag [150], Fe_3O_4 [163], etc. can enhance the activation of PS, PMS or Oxone in sonication systems. Obviously, transition metals or their ions and oxides were the important catalysts for the activation of PS, PMS or Oxone to generate SR [19, 76, 140, 145, 149, 150, 159, 161, 162]. The cavitation effects mean that sonication not only induces the release of SR from PS or PMS, but also enhances mass transfer in the solid-liquid interphases, and removes the passivated films, while continuously keeping the catalyst surface active. The degradation mechanisms of SDZ by sono/ Fe^0/PS are shown in Scheme 4 [76].



Scheme 4 The degradation mechanism of SDZ by sono/ Fe^0/PS . Reprinted from ref. [76] Copyright (2014), with

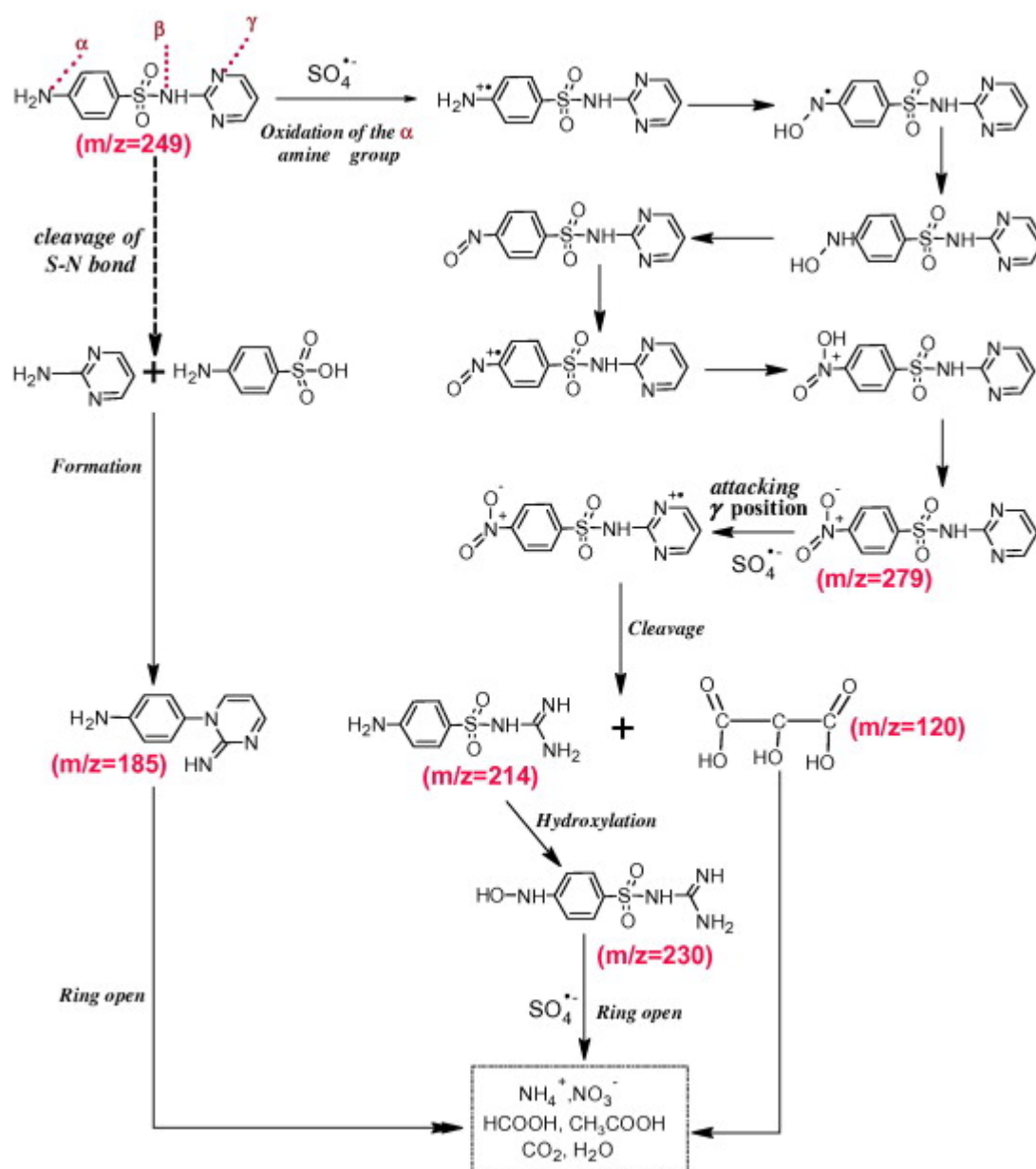
As shown in Scheme 4, sonication played important roles in the Fe⁰/PS system, including producing radicals, enhancing iron-corrosion reactions and accelerating the radical reactions in the bulk liquid [76, 149]. The microstreaming or microjets, shockwaves, and turbulence generated by sonication promoted mixing at the solid-liquid interfaces and the continuous cleaning of the solid catalyst surface, which favour the above reactions [149].

Based on an HPLC-ESI-MS examination, oxidation by SR was the main SDZ degradation pathway, as shown in Scheme 5 [76]. The main degradation step was the oxidation of the amine group (α -position in the benzene ring) by SR to generate the nitro-SD derivatives. SR then further attacks the nitro-SD derivatives (the C–N bonds on the γ -position in the heterocyclic ring), leading to ring opening. Another degradation pathway was the direct oxidative cleavage of the S–N bond, and then the intermediate (4-[2-iminopyr-imidine-1(2H)-yl]aniline), which was formed via reaction between the products, 2-aminopyrimidine and sulfanilic acid. Furthermore, the low molecular weight organic acids (formate and acetate), inorganic ions (nitrate, nitrite and sulfate) were examined using an ion chromatograph, which demonstrated the mineralization of SDZ [76]. Unfortunately, this study does not provide the variation of TOC and toxicity of the SDZ solutions by the treatment.

Pan, *et al.* have investigated SMZ degradation in a pre-magnetized Fe⁰/PS process enhanced by sonication [161]. The stronger signals of the DMPO–SO₄ and DMPO–OH adducts illustrated that more SR and [•]OH radicals were produced in the system and that this occurred more quickly. Similarly, [•]OH played important roles in the degradation of TC by sonication with Fe₃O₄ and PS. The oxidation of TC mainly took place on the surface of Fe₃O₄ and the concentration of leaching iron during the reaction could be neglected [149].

Moreover, Hu, *et al.* have demonstrated that the sonocatalytic degradation of NOR is principally induced by [•]OH and SR in the system with PS and multilayer flower-like

ZnO [140]. Soltani, *et al.* have also demonstrated that $\cdot\text{OH}$ -mediated oxidation was the main mechanism in the decomposition of TC, and that PMS led to the more significant enhancing effect on the removal of TC, compared with percarbonate, PS and periodate [104]. Guo, *et al.* have reported that the reactive radicals were generated through the Co_3O_4 -mediated activation of PMS during the sonocatalytic degradation of AMX using Co_3O_4 -catalyzed PMS [159]. Furthermore, the sonocatalytic degradation of CAP was accelerated remarkably by adding PS and Co^{2+} simultaneously [145].



Scheme 5 Proposed SDZ degradation pathways in the sono/Fe⁰/PS system. Reprinted from ref. [76] Copyright (2014), with permission from Elsevier.

5.4 Application of sono/PS and PMS/catalyst in antibiotic degradation

So far, the sono/PS and PMS/catalyst processes have been extensively applied in antibiotic degradation. For example, the elimination of FLU was significantly accelerated and the RE increased when 1.0 mM PS was added to a sono/Fenton system. As a result, 98% of FLU elimination was achieved in 80 min [111]. Roy, *et al.* have investigated SDZ degradation in a sono/Fenton-like process with PS and yolk-shell $\text{Fe}_3\text{O}_4@\text{hollow}@m\text{SiO}_2$ nanoparticles [164]. The faster leaching of $\text{Fe}^{2+}/\text{Fe}^{3+}$ ions from the metal core of the $\text{Fe}_3\text{O}_4@\text{hollow}@m\text{SiO}_2$ particles, due to micro-convection generated by sonication, enhanced SDZ degradation [164].

Rahmani, *et al.* have reported the sonocatalytic degradation of CIP associated with PS and Zn^0 under 40 kHz and 350 W sonication [19]. With 4.4 mM PS and 1.84 mM Zn^0 at pH 4.5 for 60 min, the RE of CIP reached 55% under sono/ Zn^0 /PS in 1 L of a 50 mg/L CIP solution, which was much higher than those (39.7, 18.5, 9.9, 7.5, 3.3 and 2.5%) obtained by PS/ Zn^0 , sono/PS, sono/ Zn^0 , PS, Zn^0 and sonication alone, respectively [19]. This indicates that the production of $\cdot\text{OH}$, activation of PS and Zn^0 dispersion in solution were enhanced by sonication [19]. In the presence of 10 mM PMS, periodate, PS and percarbonate, the sonocatalytic RE of TC reached 99.6, 94.2, 90.4 and 98.2% in 50 mL of 50 mg/L TC solutions with 0.5 g/L ZnO/nano-cellulose at pH 4.0 for 30 min, respectively, under 37 kHz and 256 W sonication, which are higher than that of the sono/ZnO/nano-cellulose process (87.6%) [104].

Besides the removal of antibiotics, the mineralization of antibiotic solutions can be significantly enhanced by sonication with PS, PMS and catalysts. Su, *et al.* have investigated the sonocatalytic degradation of AMX and the removal of COD with Co^{2+} and Oxone [162]. The REs of COD were in the order of: Oxone < Oxone/ Co^{2+} < Sono/Oxone < Sono/Oxone/ Co^{2+} . More than 98% of COD removal was achieved by sonication with 20 kHz and 200 W at 24 °C for 60 min in the presence of 0.095 mM

AMX and 0.025 mM Co^{2+} [162]. Consequently, sonication reduced the energy barrier of the reaction and enhanced the COD removal of antibiotics [162]. The degradation of antibiotics by sonication with PS or PMS and catalysts has been summarized in Table 6. As shown in Table 6, 20-40 kHz US has usually been used to enhance the degradation of antibiotics via oxidation with a PS/Catalyst. CIP, NOR and CAP are difficult to oxidize, and their REs only reached 55.0%-68.5% under sono/PS/Catal after 60-240 min of treatment. By contrast, the REs of SDZ, TC and SMZ reached higher values (95.7%-98.3%) after 15-60 min of treatment. Importantly, all synergy factors fall over the range from 1.3-1.9. Meanwhile, mineralization can be achieved to a certain degree by sono/PS/Catal. For example, 50 mL of 0.1 mM AMX was sonicated with 20 kHz and 300 W US in the presence of 5 mM Oxone and 0.25 mM Co^{2+} at pH 7 for 60 min, giving a RE of COD of 85%, which is higher than that (51%) of oxidation with 5 mM Oxone and 0.25 mM Co^{2+} without sonication [162]. In addition, 89% of COD was removed as the RE of TC reached 93% under sono/PS/ Fe_3O_4 nanoparticles [163].

Table 6 The degradation of antibiotics by sonication with PS and catalysts.

Antibiotics	PS/Catal. (mM/mM)	$F_{\text{US}}/P_{\text{E}}$ (kHz/W)	t (min)	C_0/V (mg/L)/mL	pH	RE _{PS/Catal.} (%)	RE _{Sono} (%)	RE _{Sono/PS/Catal.} (%)	SF	Refs.
CIP	PS/ Zn^0 4.4/1.84	40/350	60	100/<1000	4.5	39.7	2.5	55.0	1.3	[19]
NOR	PS/ Zn^0 0.42/6.14	40/200	80	2.0/50	7.5	-	6.4	66.8	-	[140]
CAP	PS/ Co^{2+} 5.0/0.1	22/200	240	20/50	1.0	<5.0	37.3	68.5	1.6	[145]
SDZ	PS/ Fe^0 1.84/0.92	20/40	60	20/400	3.0–7.0	45.5	9.7	95.7	1.7	[76]
TC	PMS/ ZnO/NC 10.0/0.5 g/L	37/256	15	50/50	7.0	-	12.8	96.4	-	[104]
SMZ	PS/ Fe^0 1.0/0.1	40/60	60	5/500	7.0	49.3	1.6	98.3	1.9	[161]

Note: F_{US} : ultrasonic frequency; P_{E} : electrical power input; C_0 : initial antibiotic concentration; V: the volume of antibiotic solution; RE: removal efficiency; SF: synergy factors = $\text{RE}_{\text{Sono/PS/Catal}}/(\text{RE}_{\text{Sono}} + \text{RE}_{\text{PS/Catal}})$ [71, 81, 109]; Refs.: references.

5.5 Role of effective factors

As shown in Table 5 and Table 6, the removal of antibiotics is highly pH dependent and acidic conditions favour the degradation of antibiotics by sono/PS and sono/PS/Catal [76, 149, 145]. Other factors, including US frequency, initial concentration of antibiotics, concentration of PS or PMS, contact time and temperature [76, 131, 159, 160, 162], are also important. Additives are also critical for antibiotic degradation under sonication with PS, PMS, Oxone, or/and catalyst [19, 34, 76, 82, 104, 111, 112, 113, 131, 140, 145, 148, 149, 150, 160, 161, 162, 163].

The sonocatalytic degradation of antibiotics, such as TC [31], AMX [159, 162], etc., with PS or PMS generally follows PFO kinetics [131]. For example, a k_I value for 20 mg/L SDZ in a 400 mL solution was measured to be about 0.057 min^{-1} at pH 7 and room temperature under 20 kHz and 40 W sonication with 0.92 mM Fe^0 and 1.84 mM PS [76]. In general, initial antibiotic concentration, catalyst dosage, PS and PMS concentration, and the initial pH value of the solution, temperature and US frequency and power affect the degradation kinetics [112, 131, 149, 160]. At lower US power ranges, the RE increased with increased US power [76, 112, 148, 149, 161], but the benefits of increasing US power over an optimal power value were not observed [149]. In addition, RE increased with an increase in temperature [131, 160, 162], while RE decreased with an increase of the initial antibiotic concentration [76, 131, 140, 149, 162, 163]. However, the amount of antibiotics removed increased with increasing initial concentration. For example, 45.9, 88.9 and 121.9 mg/L TC were oxidized by sonication with $\text{Fe}_3\text{O}_4/\text{PS}$ when its initial concentrations were 50, 100 and 200 mg/L, respectively [149]. The effects of catalyst dosage, PS or PMS concentration, pH value, and other additives, on the degradation of antibiotics using sono/PS or PMS/ and catalyst are discussed below.

5.5.1 Effect of catalyst dosage

Ammar, *et al.* have investigated the effect of Fe^{2+} concentration on the degradation

of MTZ in a sono/Fenton/PS process [113]. The results revealed that the Fe^{2+} concentration was low enough to make the treated solution directly compatible with a safe environment, and the combination is an efficient method for the high elimination of MTZ [113].

Based on the sonocatalytic degradation of SMZ with pre-magnetized Fe^0/PS , Pan, *et al.* have demonstrated that the degradation rate of SMZ is mainly determined by the amount of Fe^{2+} produced from Fe^0 [161]. The SMZ removal at 60 min was 84.8%, 96.1%, 97.8%, 100% and 99.3% at 0.05, 0.1, 0.2, 0.4 and 0.8 mM Fe^0 , respectively. Thus, the removal of SMZ increased with increasing Fe^0 doses over the above range. Meanwhile, k_d value increased from 0.028 min^{-1} , at 0.05 mM Fe^0 , to 0.176 min^{-1} at 0.40 mM Fe^0 , but slightly decreased at 0.80 mM Fe^0 (0.143 min^{-1}) due to the consumption of SR by excess Fe^{2+} . Thus, 0.40 mM Fe^0 was noted to be the optimum dosage and the optimum ratio of Fe^0/PS was denoted as 2/5 [161].

Hou, *et al.* have concluded that initial degradation rates increase with various doses of Fe_3O_4 , in the range from 0 to 2.0 g/L, in the sonocatalytic degradation of TC with $\text{Fe}_3\text{O}_4/\text{PS}$ [149]. As an initiator, Fe_3O_4 activates PS to generate SR, and then accelerates the decomposition of TC. However, the final RE was similar, as a result of the same concentration of PS, since the SR yield is dependent on PS concentration [149]. In addition, the degradation rate of TC increases with increasing martite nanoparticle dosage, and the sonocatalytic RE of 100 mg/L TC reached 87% with 0.5 g/L martite (Fe_2O_3)/3 mM Oxone at pH 4 for 60 min [112].

5.5.2 Effect of PS or PMS concentration

In general, the degradation rate of antibiotics increases with increased initial PS concentration [149, 160]. During the sonocatalytic degradation of TC with $\text{Fe}_3\text{O}_4/\text{PS}$, the RE of TC increased with increasing PS concentration from 20 to 200 mM [149]. However, when the PS concentration was over 200 mM, the RE decreased as excessive amounts of PS produced sulfate anions rather than active SR. It is also speculated that

the SR formed could be scavenged by excess PS, thus inhibiting the generation of $\cdot\text{OH}$, meaning that it is sufficient to provide SR with 200 mM PS [149].

Soltani, *et al.* have demonstrated the similar effect of lower Oxone concentration on the sonocatalytic degradation of TC with martite nanoparticles and Oxone [112]. The results revealed that increasing the Oxone dosage from 1 to 7 mM increases the decomposition rate from 0.0282 to 0.0588 min^{-1} . Similarly, excessive amounts of Oxone (5 and 7 mM) led to insignificant improvements in the decomposition rate of TC. It was assumed that the excessive amounts of HSO_5^- react with SR to form $\text{SO}_5^{\cdot-}$, which has lower oxidation potential than $\text{SO}_4^{\cdot-}$, leading to poorer decomposition of TC. In addition, the reaction between sulfate radicals intensified when the Oxone concentration was excessive, leading to the generation of PS ions. Subsequently, the addition of extra amounts of Oxone not only causes the scavenging of SR, but also generates the less reactive species [112].

5.5.3 Effect of pH value

The pH value of a solution not only affects the leaching of metal and their oxides, but also influences the dissociation of antibiotics, and the adsorption of antibiotics onto the catalysts, thus manipulating the sonocatalytic degradation of antibiotics with PS or PMS.

5.5.3.1 RE decreased under alkaline conditions.

In homogeneous systems, antibiotics such as TC exist in the molecular form under acidic conditions, resulting in higher affinity to the cavitation bubbles where oxidation with higher concentration $\cdot\text{OH}$ and the pyrolysis of molecules can occur [34]. Thus, higher RE has been achieved under acidic conditions. For example, 90.5%-91.3% of 50 mg/L TC degradation and 25.7%-28.3% of TOC removal were achieved in 1 L solutions at pH 3 to pH 6 in 60 min under 20 kHz and 100 W sonication with 2 mM Fe^{2+} and 2 mM PS. However, the differences in the REs at the various pH values under acidic conditions are not significant. Therefore, it is not necessary to adjust the initial pH to a very low level, and an initial pH of 6 is an optimal pH condition [34]. Similarly, the

sonocatalytic degradation of 20 mg/L CAP has been carried out in 50 mL solutions by 22 kHz and 200 W sonication for 240 min with 5 mM PS and 0.1 mM Co^{2+} [145]. The results revealed that the RE of CAP decreases with increasing pH value, while k_I values are higher under acidic solutions (pH 1.0-3.3) than those obtained in neutral or basic solutions (pH 5.0-10.0) [145].

In heterogeneous systems, such as sono/ Fe^0 /PS, the efficient degradation of SDZ (95.7%–98.4%) has been achieved at a pH range of 3.0–7.0 [76], but the performance was greatly slowed (35.7%) at pH 10.0. Acidic conditions favour the corrosion of Fe^0 and produce more soluble Fe^{2+} , while alkaline conditions cause the precipitation of soluble iron ions and the passivation of the Fe^0 surface, resulting in a low production of oxidative radicals, both $\text{SO}_4^{\cdot-}$ and $\cdot\text{OH}$. Moreover, the $\text{SO}_4^{\cdot-}$ formed reacts with H_2O and OH^- under neutral or alkaline conditions, and also inhibits the reactivity of $\cdot\text{OH}$. [76].

Furthermore, a gradual decrease in solution pH was observed during the degradation of antibiotics at an initial pH 3.0–7.0; the formation of carboxyl acid products and the decomposition of PS led to this pH decrease. At an initial pH of 10.0, the pH value decreased to 6.5 by the end of degradation [76]. Pan *et al.* have found that pH value decreases faster with reaction time during the degradation of SMZ in a sono/premagnetized- Fe^0 /PS system than in other systems [161]. As pH dropped quickly, Fe^{2+} was produced faster, leading to the formation of more $\text{SO}_4^{\cdot-}$, a higher RE of SMZ, and better synergistic effects in the sono/premagnetized- Fe^0 /PS system [161].

5.5.3.2 Insignificant effect of pH value

Hou, *et al.* have found that the TC degradation rate increases with decreasing pH value in a system of Sono/ Fe_3O_4 /PS, but the REs were all similar after 1.5 h sonication [149]; the final REs were 89%, 86% and 85% at pH 3.7, 7.0 and 9.0, respectively. This indicates that pH value had an insignificant effect on the RE of TC.

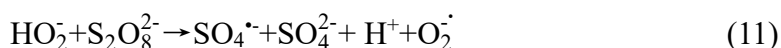
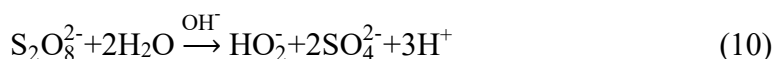
Carboxyl acids, such as acetic acid and sulfate acid, are produced during the reaction. Therefore, the final pH value decreased from initial pH values of 3.70, 7.00

and 9.00 to 2.66, 2.63 and 2.68 after 1.5 h reaction, respectively. This is probably the reason why similar REs were achieved by the end of the reactions at various initial pH values [149]. Similarly, the pH value decreased from 4.0 to 3.4, from 7.0 to 5.8 and from 10.0 to 7.3 during TC degradation via sono/PS in the absence of a buffer solution [160].

5.5.3.3 RE increased under alkaline conditions.

The TC degradation rate under sono/PS is highly dependent on the initial pH value. After 120 min of reaction, the TC degradation rates were 77.4%, 62.5% and 88.5% at pH 4, 7 and 10, without adding any buffer solution, respectively [160].

TC is an amphoteric molecule with pK_a values of 3.3, 7.7 and 9.7. TC molecules are predominantly neutral and positively charged at pH = 4 and negatively charged at pH = 9. The negatively charged TC molecules tend to attract reactive species such as $\cdot\text{OH}$ because of the high electrical density on ring system, which resulted in an acceleration in the degradation of TC [160, 165]. Moreover, alkaline-activated PS is primarily responsible for the production of $\text{SO}_4^{\cdot-}$, $\text{O}_2^{\cdot-}$ and $\cdot\text{OH}$ at pH ≥ 10 . Furthermore, SR can react with OH^- to generate $\cdot\text{OH}$ under alkaline conditions [160, 165]. Therefore, increasing pH enhances the decomposition of PS to form $\cdot\text{OH}$ and SR.



SR is the predominant species responsible for TC degradation at pH 4, whereas TC degradation was caused by both $\text{SO}_4^{\cdot-}$ and $\cdot\text{OH}$ at pH 7. Thus, the competing reactions between SR and $\cdot\text{OH}$, and TC reduce the TC degradation rate at pH 7 [160].

Similarly, TC degradation under a sono/martite/oxone process has been studied at initial pH values of 4, 7 and 9, and the k_I values were 0.0481, 0.0545 and 0.0641 min^{-1} , respectively [112]. On the one hand, the scavenging of SR and disintegration of the

active species by H^+ was thought to cause slight decreases in the TC degradation rate under acidic conditions. The increased degradation rate with increased initial pH can be explained by the conversion of $SO_4^{\bullet-}$ and $^{\bullet}OH$ in the presence of OH^- under alkaline conditions. On the other hand, the reaction between $^{\bullet}OH$ and SR leads to the production of HSO_4^- in the bulk solution, and then the dissociation of HSO_4^- into sulfate ions releases H^+ ions, decreasing the pH of the solution [166]. Therefore, an insignificant increase in the degradation rate was observed with increasing initial pH value [112].

5.5.4 Effect of temperature

Increasing temperature dramatically improved the cavitation activity and chemical effects, resulting in higher degradation rates of antibiotics under sono/ $S_2O_8^{2-}$ [131, 160] or Sono/Oxone [162] processes. PS activation can be performed by heat to produce SR, as shown in Eq. (13) [131, 160].



The k_{obs} of SDZ increased (3.56-27.39 h^{-1}) with increased bulk temperature (10-50 $^{\circ}C$) in the sono/ Fe^0 /PS system. The pseudo activation energy was 38.2 kJ/mol, demonstrating that higher temperature was beneficial to the removal of SDZ and verifying that thermal treatment can also be a persulfate activator. The activation energy obtained in sono/ Fe^0 /PS was approximately one order of magnitude lower than that obtained in the heat/PS system and Fe^0 /PS system, which indicates that the effective removal of SDZ can also be achieved by sono/ Fe^0 /PS processes even at a low bulk temperature (10 $^{\circ}C$) [76]. Upon increasing the temperature from 25 to 65 $^{\circ}C$, the degradation rate constant increased from 0.0229 to 0.1042 min^{-1} under the sono/ $S_2O_8^{2-}$ process [131]. Complete TC degradation occurs after 40, 60 and 75 min of reaction at 65, 55 and 45 $^{\circ}C$ respectively. The low activation energy (32.01 kJ/mol) indicates that the degradation of TC by sono/ $S_2O_8^{2-}$ is thermodynamically feasible [131]. Increasing temperature (25-65 $^{\circ}C$) enhanced the TC degradation rate constant (0.0175 to 0.1573 min^{-1}) during the sono/ $S_2O_8^{2-}$ process. TC was completely removed after 60, 90 and

120 min of reaction at 65, 55 and 45 °C respectively. An activation energy value of 42.66 kJ/mol was obtained [160]. Su *et al.* have observed an insignificant enhancement in COD removal in AMX solution by temperature (24 to 40 °C) during a sono/Co²⁺/Oxone process (the RE of COD reached more than 85% in 60 min at ambient temperature) [162].

5.5.5 Effect of other additives

5.5.5.1 Addition of H₂O₂.

H₂O₂ is a common oxidant and also the precursor to producing [•]OH, which is frequently used to accelerate the degradation of organic pollutants [113]. Under sonication, the formation of extra [•]OH, from H₂O₂ decomposition, enhanced MTZ removal [113]. In a homogenous Fe²⁺/PS (3 mM/1 mM) system, the RE of 500 mg/L MTZ in 200 mL solution reached 97% at pH 3 in 90 min of sonication with 20 kHz and the addition of 60 mM H₂O₂, as compared to an RE of 72% in the absence of PS [113]. In another homogenous Fe²⁺/PS (4 mM/1 mM) system, the RE of 261 mg/L FLU in 200 mL solution reached 98% at pH 4 after 80 min of sonication with 40 kHz and the addition of 20 mM H₂O₂, compared to an RE of 73% in sono/H₂O₂ [111].

In a heterogeneous martite/Oxone /(0.5 g/L/3 mM) system, the RE of 100 mg/L TC in 100 mL solution reached 87% at pH 4 in 60 min under 37 kHz and 320 W sonication with martite-nanoparticle-activated Oxone, compared to an RE of 78% in unmilled martite (sono/unmilled martite/Oxone) [112]. Only 6.5% of TC was removed by the adsorption process, while the decomposition of TC by Oxone alone was lower than 44%. As a result, when the H₂O₂ concentration rose from 10 to 40 mM, the *k_t* value increased from 0.0533 to 0.0907 min⁻¹. However, increasing H₂O₂ concentration up to 50 mM caused a substantial drop in the decomposition rate of TC [112].

5.5.5.2 Addition of scavengers.

The quenching effect of t-BuOH, EtOH and 1,4-benzoquinone is a signal for verifying the roles of [•]OH, O₂^{•-} and SO₄^{•-} in TC degradation by sono/Fe₃O₄/PS processes [149]. The results revealed that TC degradation is suppressed with the addition of 1.05

M EtOH. This indicates that $\text{SO}_4^{\bullet-}$ and $\cdot\text{OH}$ are the major radicals for the degradation of TC. In theory, EtOH is a scavenger of $\text{SO}_4^{\bullet-}$ and can also react with $\cdot\text{OH}$, and the reaction constants of EtOH with $\text{SO}_4^{\bullet-}$ and OH are $1.6\text{--}7.7\times 10^7$ and $1.2\text{--}2.8\times 10^9 \text{ M}^{-1}\text{S}^{-1}$, respectively [149].

In order to investigate the role of $\text{O}_2^{\bullet-}$, 1,4-benzoquinone was used as an $\text{O}_2^{\bullet-}$ quencher in a TC degradation via a sono/ Fe_3O_4 /PS process [149]. The addition of 0.021 M 1,4-benzoquinone did not significantly affect the TC degradation in the initial stages. However, the suppression became significant after 30 min, indicating the delayed formation of $\text{O}_2^{\bullet-}$ during the reaction [149].

t-BuOH is generally used as an OH scavenger and the reaction constant is $3.8\text{--}7.6\times 10^8 \text{ M}^{-1}\text{S}^{-1}$. Excess t-BuOH (1.05 M) was added to the solution to check the contribution percentage of $\cdot\text{OH}$ [149].

Zhou, *et al.* have demonstrated that SDZ degradation is inhibited by SO_4^{2-} , NO_3^- , $\text{HCO}_3^-/\text{CO}_3^{2-}$ and H_2PO_4^- to different extents in a sono/ Fe^0 /PS system [148]. Such inorganic anions would mainly react with $\text{SO}_4^{\bullet-}$ and/or $\cdot\text{OH}$ to form sub-radicals of less oxidative potential, which was also proven by the sonocatalytic degradation of SDZ in a sono/yolk-shell $\text{Fe}_3\text{O}_4@$ hollow@ mSiO_2 nanoparticle/PS system [164]. The inhibition effect was revealed to be probably due to the stronger metal ion complexation and radical scavenging in the hollow core of the yolk-shell nanoparticles [164]. Moreover, the presence of carbonate and even persulfate ions suppressed the sonocatalytic degradation of TC with martite nanoparticles and Oxone [112]. However, Cl^- enhanced the SDZ degradation with a low dose (5 mM), but inhibited it at a high dosage (100 mM) [148]. Moreover, the enhanced effects of chloride and carbon tetrachloride have also been demonstrated in the sonocatalytic degradation of TC [112].

At pH 3 and 5 with a buffer solution, the REs of SDZ reached 54.6% and 58.4%, respectively, which were lower than in the un-buffered systems. It was also speculated that the additional phosphate species (mainly HPO_4^{2-} and H_2PO_4^- at pH 3.0–5.0) play

the scavenging role for SR via complexation of the phosphate species. It also indicates that the soluble iron ions inhibit SDZ degradation. As the predominant oxidant under stable neutral or alkaline conditions, $\cdot\text{OH}$ was strongly scavenged by phosphate species, and significant inhibition of SDZ degradation was therefore found at pH 7 and 10 with a buffer solution [76].

Finally, the addition of humic acid in concentrations above 10 mg/L also reduced the degradation rate of TC in a sono/PS process, although the effect could be compensated using higher concentrations of PS [160]. The low RE of TOC is due to the generation of recalcitrant products during TC degradation [160]. Therefore, a longer exposure time is required for the efficient mineralization of antibiotics [112].

5.5.6 Stability of catalysts

In the heterogenous sonocatalytic system with martite nanoparticles and Oxone, the decomposition rate of TC dropped by only 10.8% after four consecutive experimental runs, indicating the appropriate reusability potential of martite nanoparticles [112]. In a sonocatalytic system with Fe_3O_4 and PS, the RE of TC reached 89% in 1.5 h in the primary experiment, and then the RE decreased to 73.5% after three repetitive experiments. A low dissolved iron concentration (<0.2 mM) was detected in the solution. It was speculated that Fe(III)-bearing iron oxides formed on the surface of the catalyst, which may be more soluble, less active and stable, and thus cause the RE decline. As for effect of sonication on the catalyst particle size distribution, the particle size distribution of the used catalysts is similar to that of the fresh catalysts, indicating that Fe_3O_4 is stable under sonication [149].

6 Degradation of antibiotics by sonophotocatalysis (sonication/photocatalysis)

6.1 Mechanism of sonophotocatalysis

Photocatalysis that are based on semiconductors provide favourable results,

compared to other AOPs, in the destruction of persistent organics. In recent years, conventional photocatalytic processes have exhibited some problems, such as difficulty in the separation and recovery of catalysts, the production of secondary pollution, and the high consumption of catalysts and energy, etc. [31]. Furthermore, the lack of efficient photoactivity under solar-light, the high recombination rate of photo-induced electron-hole ($e_{CB}^- - h_{VB}^+$) pairs, and low resistance to photo-corrosion has limited their practicality in environmental applications [84]. To overcome these obstacles, photocatalysis is usually combined with sonication, chemical oxidants or microwave techniques [31].

Sonophotocatalysis has attracted much attention because it is generally considered to be an applicable and environmentally friendly process [114]. The synergistic effect of sonocatalysis and photocatalysis generates a large number of ROS, and thus enhances the oxidation process to remove organic contaminants [84]. The cavitation effects induced by sonication eliminate the defects of photocatalysis, including the decrease in UV-available sites, mass transfer limitations and the blocking of the catalyst surface by contaminants [84]. The degradation mechanisms of TC by sonophotocatalysis are shown in Figure 5.

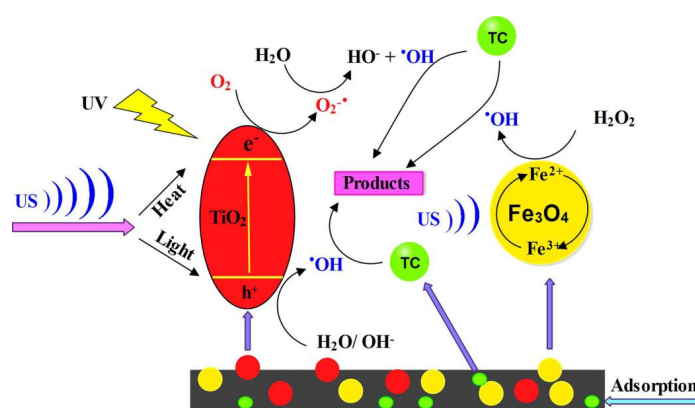


Figure 5 Degradation mechanisms of TC by sonophotocatalysis. Reprinted from ref. [31] Copyright (2019), with permission from Elsevier.

6.2 Application of sonophotocatalysis in antibiotic degradation

Vinesh, *et al.* have investigated the degradation of TC by sonophotocatalysis under simulated visible light with a reduced graphene-oxide (rGO) supported electron-deficient B-doped TiO₂ (Au/B-TiO₂/rGO) nanocomposite synthesized via the hydrothermal method [117]. The RE of TC under sonolysis, photocatalysis and sonophotocatalysis was found to be 25, 65 and 100%, respectively, when the reaction was performed in the presence of sonolysis and photocatalysis under 40 kHz, 600 W US, 300 W of visible light power with 0.25 g/L Au/B-TiO₂/rGO in 60 min (40 mL, 15 mg/L). The enhanced sonophotocatalytic activity (SF: ~1.3) observed was attributed to the generation of more ROS by the combination of sonication and photocatalysis [117]. According to trapping tests, holes, [•]OH and [•]O₂ contributed to the degradation process [31].

The application of sonophotocatalysis for the degradation of antibiotics has been summarized in Table 7.

Table 7 Degradation of antibiotics by sonophotocatalysis.

AB X	Catalysts	$\lambda_{UV/vis}/P_U$ V/vis (nm/W)	F _{US} /P _E (kHz/W)	t (min)	C ₀ /V (mg/L)/ mL	pH	RE _{Ph} oto (%)	RE _{Sono} (%)	RE _{Sono/} Photo (%)	SF	Refs.
OF X	1 g/L TiO ₂	350–400 /3.2 W/m ²	20/192*	120	10/300	6.0	85.0	15.0	~100.0	~1.0	[85]
TC	0.3 g/L TiO ₂ /MAC @T	254/6	20/40	60	30/<500	5.5	47.4	2.1	59.2	1.2	[31]
TC	0.25 g/L Au/B-TiO ₂	~300	40/600	60	15/40	-	65.0	25.0	100.0	1.3	[117]

	/rGO										
CL A	0.3 g/L ZnS QDs/SnO ₂	254/4	20/75	60	10/100	3.0	68.2	~8.0	86.7	1.7	[119]
RX M	0.3 g/L ZnS QDs/SnO ₂	254/4	20/75	60	10/100	3.0	72.6	~12.0	90.3	~1.1	[119]
AM X	1.0 g/L gC ₃ N ₄ - 20@Ni-Ti LDH	420- 470/400	20/200	150	~100	-	87.0	53.0	99.0	0.7	[39]
MO X	1 g/L NiFe- LDH/rGO	~10	36/150	60	20/100	8.0	62.7	8.2	90.4	1.3	[118]

Note: ABX: Antibiotics; $\lambda_{UV/vis}$: wavelength of light; P_{UV} : light power; W/m^2 : light power intensity; F_{us} : ultrasonic frequency; P_E : electrical power input; C_0 : initial antibiotic concentration ; V : the volume of antibiotic solution; RE : removal efficiency; synergy factors = $RE_{Sono/Photo}/(RE_{Sono}+RE_{Photo})$ [71, 81, 109]; Refs.: references.

As listed in Table 7, TiO₂ and its composites, as well as transition metal oxides, have usually been used as the catalysts for the degradation of antibiotics by sonophotocatalysis. The applications of sonophotocatalysts in the degradation of antibiotics are discussed below.

6.2.1 TiO₂ and its composites

TiO₂ is a common catalyst for promoting the photocatalytic degradation of organic contaminants. Hapeshi, *et al.* have investigated the degradation of OFX by sonophotocatalysis with TiO₂ (Conditions: 300 mL of 10 mg/L OFX, pH 6.0, 1.0 g/L catalysts, 20 kHz, 640 W/L US power, 350-400 nm UV, 3.2 W/m² UV power, 120 min treatment at 27 ± 2 °C) [85]. The working solution, containing 10 mg/L OFX, was prepared by spiking the appropriate mass of the compound in the secondary treated wastewater (collected from the urban wastewater treatment plant (UWTP) of Limassol, Cyprus) and then performing the necessary dilutions. The results revealed that the sonophotocatalytic degradation of OFX follows PFO kinetics. The k_I values were 0.1054, 0.0713, 0.0203 and 0.0131 min⁻¹ for sono/Photo/TiO₂, photo/TiO₂, sono/TiO₂ and sonication alone, respectively. The REs of OFX for 120 min reached 15, 62, 85 and

~100% for sonication, sono/TiO₂, photo/TiO₂ and sono/photo/TiO₂, respectively. Therefore, degradation by sonophotocatalysis was generally faster than all the individual processes, presumably due to the enhanced formation of reactive radicals. Additionally, the presence of the TiO₂ catalyst significantly increased the RE of OFX by sonication. It was assumed that the increase is attributed to the additional cavitation activity, which is used as an alternative energy source for TiO₂ to generate positive holes [85].

Kakavandi *et al.* have investigated the degradation of TC by sonophotocatalysis using TiO₂ that was decorated on magnetic activated carbon (MAC@T), where MAC was fabricated via the magnetization of AC using Fe₃O₄ nanoparticles [31]. The REs of TC for 60 min under various sonocatalytic and photocatalytic processes are listed in Table 8.

Table 8 REs of TC for 60 min under various sonication and photocatalytic processes (Conditions: <500 mL of 30 mg/L TC, pH 5.5, 0.3 g/L catalysts, 20 kHz, 40 W US power, 6 W UV power, 60 min treatment at 25 ± 2 °C,).

Process	Photo*	Sono*	Sono/Photo*	MAC@T	Sono/MAC@T	Photo/MAC@T	Photo/TiO ₂	Sono/Photo/MAC@T
RE(%)	2.1	4.0	7.4	36.8	38.5	47.4	44.9	59.2

* Without catalysts [31].

As listed in Table 8, it was assumed that the negligible REs of TC are caused by very low generation efficiencies of free radicals in photolysis or sonication alone. The increased RE value using the sono/photo process indicates the synergistic effect between sonication and photolysis [31]. 36.8% of RE obtained by MAC@T composite indicated the RE by adsorption onto the catalyst, while an RE of 47.4% by photo/MAC@T is comparable with that (44.9%) obtained by traditional photo/TiO₂ due to the synergistic effect of adsorption and photocatalytic degradation. The highest RE (59.2%) was obtained using the sonophotocatalysis process with MAC@T. This is because the catalyst played roles for adsorption, photocatalysis and sonocatalysis simultaneously. Furthermore, the synergistic effect is associated with a contribution by

sonication and the subsequent production of ROS in the system, while the surface of the catalyst was cleaned by sonication continuously to maintain the activity of catalyst [31].

6.2.2 Fenton and Fenton-like reactions

Zhou, *et al.* have compared the degradation kinetics and REs of SMZ using 5 different sonocatalytic and photocatalytic systems with Fe₃O₄ [116]. The SMZ degradation in the sono/photo/Fe₃O₄/OA system follows PFO kinetics under the conditions used - 25 mg/L SMZ, 0.4 g/L Fe₃O₄, 0.8 mM oxalic acid (OA), UV (365 nm, 9 W), US (20 kHz, 330 W), initial pH 3, 20 °C, and the k_1 value reached $3.5 \times 10^{-2} \text{ min}^{-1}$, which is about 10-times higher than that obtained in the sono/Fe₃O₄/OA system ($k_1 = 0.36 \times 10^{-2} \text{ min}^{-1}$). However, the degradation of SMZ in the photo/Fe₃O₄/OA system does not follow PFO kinetics, because there was an initial degradation lag period. Thus, sonication was used to reduce the initial lag period of SMZ degradation [116].

The high stability of the SMZ molecule meant that lower REs (ca. 10–20%) were observed after 60 min in the sono/Fe₃O₄, sono/photo/Fe₃O₄ and sono/Fe₃O₄/OA systems, but higher SMZ REs were achieved in the photo/Fe₃O₄/OA system and sono/photo/Fe₃O₄/OA system [116]. It was speculated that the rapid release of dissolved iron species in the initial reaction phases, induced by Fenton-like reactions, resulted in the efficient production of ROS. Moreover, in the sono/photo/OA and sono/Fe₃O₄/OA systems, oxalate mostly acts as a competitive reactant. By contrast, in the Photo/Fe₃O₄/OA and Sono/Photo/Fe₃O₄/OA systems OA acts as both a reactant and an ROS initiator [116]. The synergistic degradation of SMZ has also been demonstrated in a Sono/Photo/Goethite- Fe³⁺/OA system by integrating *in-situ* H₂O₂ generation under UV illumination and efficient Fe²⁺ species regeneration (Initial parameters: 25 mg/L SMZ , 0.5 g/L goethite, 0.8 mM OA, 330W US and pH 3, initial Fe³⁺ concentration of 250 μM) [115]. The cleavage of the S–N bond in the SMZ molecule was dominant under •OH attack. Meanwhile, organic mineralization and wastewater detoxification

were achieved.

Transition metal oxide (ZnO) or sulfide (ZnS and SnO₂) have been used to accelerate the degradation of antibiotics in sono/photo/Fenton-like processes [83, 119]. After pretreatment, the degradation of antibiotics becomes possible using biological treatment processes. The degradation of 10 mg/L RXM and CLA was studied in a sono/photo/Fenton-like system with ZnS quantum dots decorated onto SnO₂ nanosheets prepared using the hydrothermal method [119]. Without catalysts, REs were low using the Photo method alone, sonication alone, photo/H₂O₂, sono/H₂O₂ and sono/photo/H₂O₂, due to the insufficient formation of [•]OH. With 0.3 g/L catalyst and 6 mM H₂O₂, only 31.4% of 10 mg/L CLA and 36.4% of 10 mg/L RXM were removed from 100 mL aqueous solutions at pH 3 after 60 min. When sonication (20 kHz, 75 W) was used to enhance the degradation in the above system, the REs of CLA and RXM increased to 61.2% and 65.5%, while higher REs (68.2% and 72.6%) were obtained in the same system, but in the presence of UV (254 nm, 4 W). Surprisingly, The REs of CLA and RXM reached 86.7% and 90.3% in the sono/photo/Fenton process [119]. Consequently, the superior performance and synergistic effects of the sono/photo/catalyst process were attributed to the promotion of [•]OH generation [119].

6.2.3 Other nano-composites

Khataee, *et al.* have investigated the degradation of MOX by the sonophotocatalytic method using a NiFe-layered double hydroxide/reduced graphene oxide (NiFe-LDH/rGO) nanocomposite [118]. The RE of MOX (90.4%) by sonophotocatalysis under the used conditions - 100 mL of 20 mg/L MOX, pH 8.0, 1.0 g/L catalysts, 36 kHz, 150 W US power, 10 W UV power, 60 min treatment - was higher than the REs of sonocatalysis (72.4%) and photocatalysis (62.7%), but lower than their sum. The results revealed that [•]OH and [•]O₂⁻ radicals play the dominant role in MOX degradation.

Abazari, *et al.* have investigated the degradation of AMX by sonophotocatalysis

with nanocomposites of g-C₃N₄@Ni-Ti layered double hydroxides (g-C₃N₄@Ni-Ti LDH) synthesized using the hydrothermal method with NH₄F [39]. The conditions - 100 mL AMX, pH 8.0, 1.0 g/L catalysts, 20 kHz, 200 W US power, 420-470 nm, 400 W UV power and 150 min treatment – allowed the following RE order to be determined: sonocatalysis < photocatalysis < sonophotocatalysis. The formation of •OH on the surface of the g-C₃N₄-20@Ni-Ti LDH particles was approved using the terephthalic acid probe in photoluminescence spectroscopy [39]. Thus, the observed enhancement in the sonophotocatalytic activity of the nanocomposites can be related to their higher specific surface areas, the intimacy of the contact interfaces of their individual components, i.e., pristine g-C₃N₄ and Ni-Ti LDH, the synergistic effect between these components and restriction of electron-hole recombination.

Ghoreishian, *et al.* have investigated the degradation of TC by sonophotocatalysis with flower-like rGO/CdWO₄ hierarchical structures that were synthesized using a facile wet-chemistry method without any calcination [84]. rGO/CdWO₄ exhibited significant photoelectrochemical performance under the conditions used - 500 mL of 13.54 mg/L AMX, 0.432 g catalysts, 60 min treatment - and demonstrated superior sonophotocatalytic activity and mineralization efficiency compared with CdWO₄ [84]. Thus, the higher catalytic activity of rGO/CdWO₄ is attributable to rGO, which catches TC residuals from aqueous solution and acts as a charge acceptor to promote the separation of photo-generated carriers via its π - π conjugated structure.

6.3 Other concerning issues

6.3.1 Effective factors

Due to the emerging nature of sonophotocatalysis, little has been reported on the effects of critical factors. The performance of sonophotocatalytic systems is influenced by various parameters, such as US and UV conditions, catalyst dosage, pH value, initial antibiotic concentration, additives, etc. [31, 83-85]. In general, the RE of antibiotics increases with increasing US intensity, UV intensity [39] and catalyst dosage [20, 31,

85, 118, 119, 167], and acidic conditions favour degradation [20, 116]. For example, Tavasol, *et al.* have designed a photocatalyst of sea sediment/titanate to remove CPX from aqueous media in the presence of sono/photo/H₂O₂ [26]. Under the conditions - 150 mL of 100 mg/L CPX, pH 6.8, 40 kHz US, 15 W UV power, 100 min treatment - the removal of antibiotics was achieved with increasing titanium content loaded onto the sediments (1.5 g/L catalysts), due to higher surface area and higher photocatalytic activity that it provides [26].

In some cases, the ratio of catalyst and acid (e.g., Fe₃O₄/OA) is also an important factor for the degradation of antibiotics [116]. As discussed above, sonocatalysis or photocatalysis alone are not adequate to effectively remove antibiotics from aqueous solutions, but the addition of either H₂O₂ or PS significantly enhances the RE, while RE increases with increasing concentration of additives [20, 163]. For example, OFX degradation increases slightly upon increasing the H₂O₂ concentration, but with an optimum level of H₂O₂ concentration at 0.14 mM. [85]. Zeng, *et al.* have investigated the degradation of LEV by visible-light-driven sonophotocatalysis and PS activation over 3D urchin-like MoS₂/C nanoparticles [100]. The radical species $\cdot\text{OH}$ and $\text{SO}_4^{\cdot-}$ were accelerated, while $\cdot\text{O}_2^-$ was limited in this coupled system, which largely facilitates its excellent degradation performance with a synergistic effect [167].

By contrast, the addition of inhibitors decreases the degradation of antibiotics as a means to probe the role of $\cdot\text{OH}$ that is formed *in situ*. For example, the inhibitory effect of different inorganic salts on NOR degradation in a sono/nano-Cu⁰/H₂O₂ system followed the sequence: Na₂SO₄ > NaNO₃ > \approx no salt > NaCl > NaHCO₃ [20]. However, a contradictory result has been observed, in which a decreasing sequence of the inhibitory effect of anions towards TC degradation in a sono/photo/MAC@T process was observed to be: Cl⁻ > HCO₃⁻ > PO₄³⁻ > NO₃⁻ > SO₄²⁻ [31].

6.3.2 Mineralization and detoxification

Because of the significant synergy in the sonophotocatalysis of antibiotics, the

mineralization and detoxification of aqueous antibiotics solution have been improved [115, 116]. For example, under the conditions used - 40 mL of 15 mg/L TC, 0.25 g/L catalysts, 40 kHz, 600 W US power, 300 W UV power, 60 min treatment - 12.1, 45.7 and 73.6 % TOC removal have been achieved by sonolysis, photocatalysis and sonophotocatalysis, respectively [117].

The significant synergistic degradation of SMZ can be further evidenced by the results of mineralization and detoxification of treated water samples. 78% of TOC was removed in a sono/photo/Fe₃O₄/OA system after 1 h of reaction time, with an increase of the corresponding EC 50 from 17% (the raw sample) to 89%. The efficiencies of mineralization and detoxification were much higher than those achieved in the other six systems [116]. Montoya-Rodríguez *et al.* have observed 100% removal of AMP after 75 min of treatment with the sonochemical process. Moreover, the antimicrobial activity of AMP significantly decreased, which was related to attacks of [•]OH on the active nucleus [46]. In addition, the highest mineralization of the pollutant (40% of TOC removal) was achieved after 180 min of treatment with a sono/photo/Fenton process [46].

Toxicity depends on the chemical properties and concentration of not only the OFX that was initially present, but also of its transformation products (TPs). Interestingly, the by-products formed during the dissolved organic matter (DOM) oxidation seem to play a similar role with regards to the toxicity changes as that of the by-products formed during OFX degradation [85]. Antimicrobial activity (AA) has been assessed by the Kirby-Bauer method using *Staphylococcus aureus* as the indicator microorganism. As a result, 100% of AA was removed after 60 and 20 min for AMP and NAF by the sono/photo/Fenton process, respectively [69].

6.3.3 Stability and reusability of catalysts

The stability and reusability of catalysts used in sonophotocatalysis are critical to the promotion of the degradation of antibiotics. Evaluations have revealed that some

catalysts are robust. For example, insignificant loss was observed in the sonophotocatalytic activity of the nanocomposites of g-C₃N₄-20@Ni-Ti LDH even after five consecutive runs [39]. Both Fe leaching and loss of decontamination were slight after reuse, indicating that MAC@T has high stability and reusability [31]. The rapid degradation of SMZ and the decomposition of oxalate could still be achieved in the heterogeneous sonophotolytic Fenton-like system using goethite over five consecutive reaction cycles [115]. Besides, wastewater treatment is plausible using a reusable synthesized NiFe-LDH/rGO nanocomposite [118].

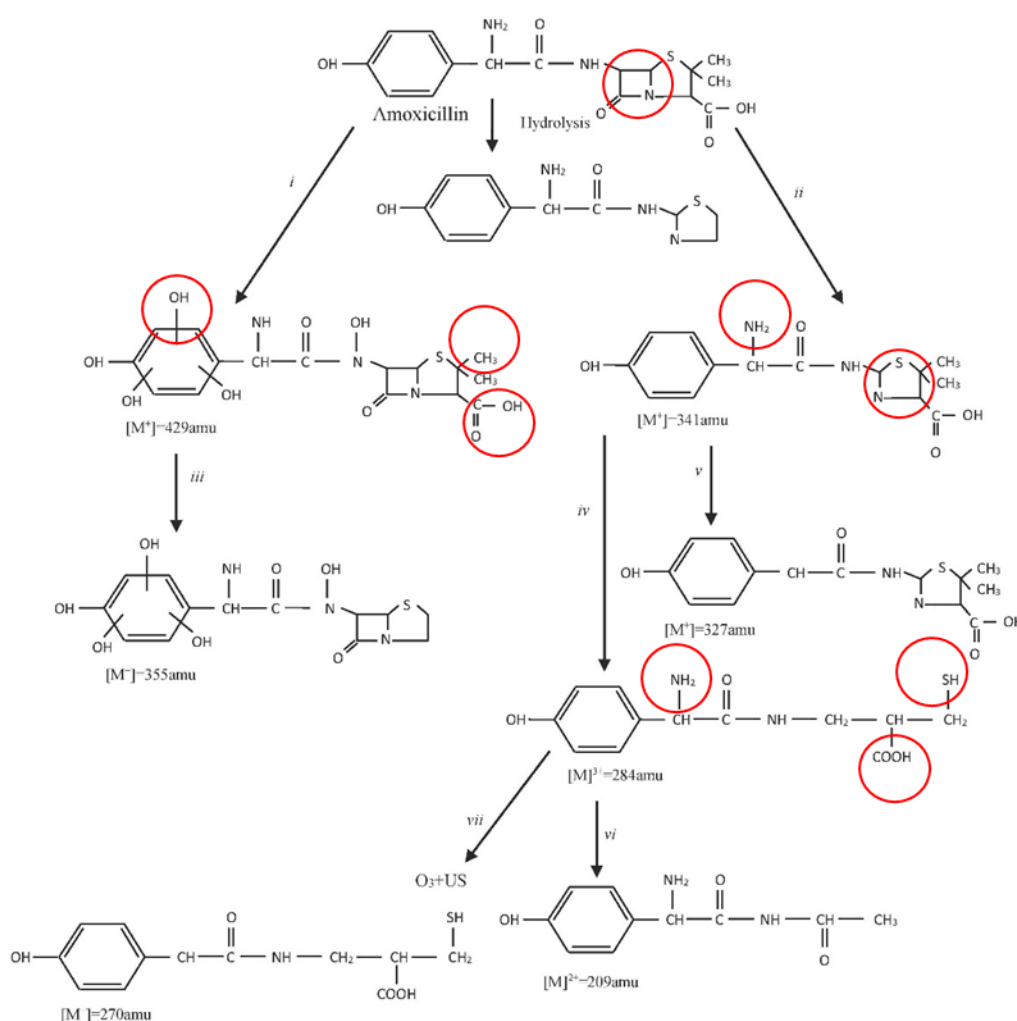
7 Degradation of antibiotics by sonozonation (Sonication/Ozonation)

7.1 Mechanisms of sonozonation

Ozone is a powerful oxidant that can directly react with contaminants or decompose into more powerful oxidants - free radicals. Ozonation has usually been used to remove refractory organics, including antibiotics, and improve biodegradability. However, high costs, poor gas-liquid mass transfer and selective oxidation have limited its use. Due to the cavitation effects, such as hotspots, microjets, shockwaves, turbulence, etc., sonication enables the mass transfer and [•]OH production to be improved, leading to significantly high degradation rates for antibiotics [78, 79, 80, 120, 121]. It was speculated that cavitation effects reduce the liquid-film thickness of gas bubbles containing O₃, and increase the gas/liquid specific surface area. Meanwhile, the diffusion of free radicals, generated in the vapour phase of cavitation bubbles and O₃/O₂ bubbles, into the bulk solution is enhanced under sonication to oxidize hydrophilic antibiotics [79].

For example, AMX cannot be efficiently oxidized through sonication alone, but can be removed efficiently using ozonation or sonozonation [78]. Moreover, the oxidative degradation efficiency of AMX using the above methods has been identified by intermediate analysis with GC-MS, mineralization analysis and the Microtox

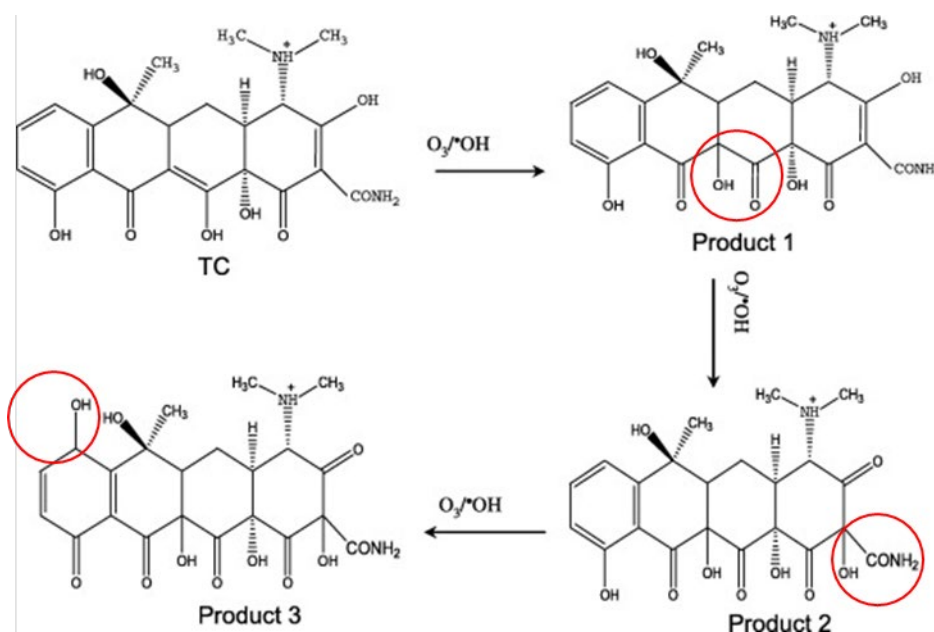
1579 toxicity test [78]. In ozonation processes, six products, formed via the hydroxylation of
 1580 AMX, demethylation, decarboxylation and the opening of beta-lactam and thiazolidine
 1581 rings with ROS, have been observed under alkaline conditions. The degradation
 1582 pathway of AMX by sonozonation is similar to that of ozonation. Scheme 6 shows the
 1583 pathway of intermediate formation during the degradation of AMX by the sonication,
 1584 ozonation and sonozonation processes. Meanwhile, the mineralization degrees reached
 1585 10% by sonication alone, 32% by ozonation alone and 45% by sonozonation under
 1586 optimized conditions.



1587
 1588 **Scheme 6.** Pathway of intermediate formation during the degradation of AMX by sonication alone, ozonation
 1589 alone and sonozonation at pH 10, 575 kHz, 75 W, 15 mg/L O₃(aq). Reprinted from ref. [78] Copyright (2012), with
 1590 permission from Elsevier.

1591 **Figure S4** shows the LC-APCI-MS of five major intermediates formed during the

degradation of TC by sonozonation, indicating the degradation pathway of TC (Scheme 6) [80]. As shown in Scheme 7, Product 1 was generated by an initial 1,3-dipolar cycloaddition towards the C_{11a}–C₁₂ double-bond and a rearrangement with the hydroxyl at position C₁₂. Subsequently, Product 2 was formed via the further oxidization of the double-bond C₂–C₃ in Product 1. Product 3 was finally synthesized by O₃ or [•]OH by successively attacking ring D (bearing hydroxyl group) of Product 2. Therefore, [•]OH dominates the degradation of TC in the sonozonation system [80].



Scheme 7. The degradation pathway of TC in the sonozonation system. Reprinted from ref. [80] Copyright (2012), with permission from Elsevier.

Recently, we have reported the mechanisms, reactors and effective factors of sonozonation for organic degradation [81]. In this review, the applications of sonozonation and the roles of effective factors on antibiotic degradation are discussed.

7.2 Application of sonozonation on antibiotic degradation

Kıdak *et al.* have investigated the degradation of AMX by sonozonation at 575 kHz US [78]. Under the optimized sonozonation conditions - 250 mL of 25 mg/L AMX solution, 0.13 mg/L O₃, 575 kHz, 75 W, pH 10, 90 min treatment - the highest degradation rate constant ($k_1 = 2.5 \text{ min}^{-1}$), highest mineralization (45% of TOC removal) and reduced toxicity ($\text{EC}_{50\%} = 67.5$) were achieved, compared with those obtained by

sonication alone ($k_1 = 0.04 \text{ min}^{-1}$ and 10% of TOC removal) and ozonation alone ($k_1=1.97 \text{ min}^{-1}$ and 32% of TOC removal and $\text{EC}_{50}\%= 13.6$) [78]. Based on the k_1 values obtained by the various processes, the synergistic factor of sonozonation for AMX degradation was calculated to be 1.24.

Naddeo *et al.* have investigated the degradation of SMX using sonozonation with 20 kHz and 370W/L US [120]. 61% of SMX was removed from 200 mL of a 10 mg/L SMX solution, with 3.3 g/h of O_3 dose, after 40 min in the sonozonation system, while 51% SMX was removed by ozonation alone [120]. The enhancement of SMX degradation by sonozonation can reduce the consumption of chemicals, which is particularly interesting for performing the scale-up of sonozonation process [120].

Guo *et al.* have also investigated the degradation of SMX by sonozonation with 20 kHz and 600W/L US [121]. A 100 mg/L (0.5 mM) SMX solution was treated in a 1.5 L-reactor with 3.0 g/h of O_3 dose, and about 95% of SMX was removed after 5 min treatment in the sonozonation system, while only 3% and about 85% SMX was removed by sonication alone and ozonation alone [121].

7.3 Role of effective factors

The RE of antibiotics by sonozonation is influenced by various parameters, including O_3 concentration/flow rate [79, 80, 120], pH value [78, 79, 80, 120, 121], initial antibiotic concentration [79, 80], US power/frequency [79, 80], and additives [78, 79, 80], as discussed below.

7.3.1 Effect of gaseous O_3 concentration, flowrate and dosage

In general, O_3 concentration in a gas increases with the yield or dosage of O_3 production under an identical gas flowrate. Naddeo *et al.* have noted that the degradation of SMX was enhanced by increasing ozone flows in the sonozonation system, which was attributed to improved O_3 mass transfer [120]. Guo *et al.* have found that the RE of SMX doubled as O_3 dosage increased from 2 to 5 g/h, because the increasing ozone concentration was able to improve the mass transfer of O_3 from the

gas to liquid phase [79]. In addition, the increasing O₃ concentration increase the amount of O₃ molecules and [•]OH that were available to react with antibiotics in solution [79].

Wang *et al.* have also demonstrated that the RE of TC increases with increasing gaseous O₃ concentration and gas flowrate in a sonozonation system [80]. On the one hand, k_l values were 0.42, 0.66, 0.85 and 1.34 min⁻¹ at 30, 35, 40 and 50 L/h of gas flowrate, respectively. The increasing gas flowrate increases the net surface area and improved O₃ mass transfer from the gas phase to aqueous phase, thus increasing the volumetric mass transfer coefficient of O₃ [80]. On the other hand, k_l values reached 0.66, 0.77, 0.84 and 1.04 min⁻¹ at 35.8, 44.5, 45.6 and 47 mg/L of gaseous O₃ concentration, respectively. This suggests that the increasing gaseous O₃ concentration increased the equilibrium O₃ concentration in the aqueous phase, according to Henry's law. The increasing equilibrium O₃ concentration also improved O₃ mass transfer from the gas phase to the liquid phase [80].

7.3.2 Effect of pH value

The pathways of ozonation generally include direct oxidation by O₃ molecules, which is more selective and predominant under acidic conditions, and the indirect oxidation by [•]OH that is formed *in situ*, which is non-selective and predominant under alkaline conditions [79, 80]. Therefore, the predominant reaction and reaction rate during ozonation can be controlled by adjusting pH value, which is also considered a critical factor for the efficiency of sonozonation [79]. The increase of reaction rate means that a shorter reaction time is required to complete the degradation of antibiotics, while O₃ consumption and operation costs are reduced [121].

Guo *et al.* have found that the degradation rate of SMX increases with increasing pH value. SMX has two pK_a values, of 1.6 and 5.7, resulting in protonated, non-protonated and deprotonated forms at different pH values. The amino groups are possible reaction centres that are most susceptible to O₃ electrophilic attack. The non-

protonated form is the predominant form at $\text{pH} < 7$, and is less susceptible to O_3 attack than the deprotonated form, leading to lower k_I values under acidic conditions (0.29 min^{-1} at $\text{pH} 3$; 0.30 min^{-1} at $\text{pH} 5$). At $\text{pH} 7$, SMX molecules were converted into the completely deprotonated form, which had a higher reactivity towards O_3 molecules. Under basic conditions, the oxidation of SMX was enhanced due to the generation of numerous $\cdot\text{OH}$ species (0.42 min^{-1} at $\text{pH} 7$; 0.50 min^{-1} at $\text{pH} 9$). Consequently, the degradation rate of SMX under basic conditions was higher than under acidic conditions [79].

Furthermore, the enhancement of sonication on SMX degradation by ozonation varied by 6–26% under different pH values, and the highest enhanced effect was observed at $\text{pH} 5$ [121]. This suggests that sonication promoted the diffusion of O_3 molecules in water under acidic conditions and increased the contact area between O_3 and SMX, resulting in increased RE of SMX by direct-oxidation with O_3 molecules. Under neutral and alkali conditions, sonication increased the degradation rates of SMX by only 6-7%. This indicates that sonication slightly enhanced O_3 decomposition and the yield of $\cdot\text{OH}$, which is responsible for the indirect-oxidation [121].

TC degradation rate has also increased as the pH value increased from 3 to 9 in a sonozonation process [80]. Similarly, there are four different species of TC molecule, TCH_3^+ , TCH_2 , TCH^- and TC^{2-} , in which the protonation-deprotonation reactions depend on pH value. The deprotonated TC with a positively charged group at higher pH values is more easily attacked by O_3 molecules and/or $\cdot\text{OH}$ than TC itself. Thus, the TC degradation rate increases with increasing pH [80]. Likewise, AMX is a hydrophilic and weak polyprotic acid with three pK_a values of 2.67, 7.11 and 9.55 at 37°C . At $\text{pH} 10$, dissolution is favoured for the more degradable forms of AMX when the amine is deprotonated and a pair of electrons is available for electrophilic attack, while the increased solubility of AMX at $\text{pH} 10$ leads to higher reaction rates in the presence of the readily abundant radicals formed in the 575 kHz US field [78].

7.3.3 Effect of initial antibiotic concentration

Since the concentrations of O_3 and $\cdot OH$ available are almost identical under the same operation conditions in a sonozonation system, and are independent of the initial antibiotic concentrations, the degradation rate decreases mostly with increasing antibiotic concentration. For example, the k_I value of SMX degradation decreased three-fold (from 0.37 to 0.09 min^{-1}) as SMX concentration increased from 50 to 400 mg/L in a sonozonation system. The additional reason for this is the fact that the competing reactions between SMX and its degradation products gradually turned predominant with the increasing initial SMX concentration. Such competing reactions reduced the reaction rates of SMX with O_3 and $\cdot OH$ [79]. Similarly, the TC degradation rate also decreased with increasing initial TC concentration in a sonozonation system, and the k_I value decreased from 0.92 to 0.59 min^{-1} when TC concentration increased from 200 to 800 mg/L [80].

7.3.4 Effect of power density of US

Increasing US power density can generally enhance the turbulence effect, resulting in increased antibiotic degradation rates, as the enhanced turbulence favours O_3 mass transfer from the gas to liquid phase [79]. It has been speculated that powerful sonication enhances mechanical mixing, making O_3 -containing bubbles smaller and reducing the thickness of liquid films [80]. In addition, more O_3 molecules can be decomposed to generate more ROS under more powerful sonication. For example, the k_I values of SMX degradation reached 0.25, 0.26 and 0.30 min^{-1} at 400, 600 and 800 W/L of power density in a sonozonation system, respectively [79]. Moreover, the TC degradation rate increased with increasing power density, and the k_I values of TC degradation reached 0.57, 0.71, 0.90, 1.04, 1.74 and 2.60 min^{-1} at 0, 85.3, 125.4, 142.8, 169.8 and 218.6 W/L of power density, respectively [80].

7.3.5 Other concerning issues

The chemical structures and hydrophobicity of antibiotics generally influence their

degradation kinetics and efficiency [120]. Little competitive oxidation of SMX, diclofenac and carbamazepine has been observed in a mixing solution under sonozonation, showing that the simultaneous presence of SMX, diclofenac and carbamazepine is not an obstacle for degradation via sonozonation [120].

This indicates that the oxidation of TC by $\cdot\text{OH}$ that are generated *in situ* dominates the degradation of TC by sonozonation. By contrast, the addition of the radical scavenger *t*-butanol can accelerate the SMX degradation rate [79], and it has been speculated that the direct oxidation of SMX by O_3 molecules is the dominant pathway in the sonozonation system. The presence of H_2O_2 improved the TC degradation rate when the H_2O_2 concentration did not exceeded 10 mM, while the presence of *t*-butanol inhibited the TC degradation rate to some extent [80].

Alkalinity and humic acid species reduced the RE (50% decrease) by sonication alone as radical reactions control the degradation of AMX [78]. However, the addition of alkalinity, humic acid and both did not significantly change the removal rate of AMX during both ozonation and sonozonation, since, in this case, the reaction of AMX with O_3 molecules controls the degradation [78].

Besides enhancing the degradation of antibiotics by ozonation, sonication can simultaneously promote the mineralization and detoxification of antibiotics in aqueous solutions. The Microtox toxicity test has been used to find the concentration value of the treated effluents that affects 50% of the microorganisms in a solution (EC50), and thus to assess the toxicity of solutions. The initial AMX solution shows high toxicity with a EC50 value of 14% [78]. Under sonozonation (250 mL of 25 mg/L AMX, 575 kHz, 75 W/L US power, 0.13 mg/L O_3 , pH 10.0, 90 min treatment), the EC50 value decreased to 10.87% and 13.59% after treatment with sonication and ozonation alone, respectively, showing that the intermediates with higher toxicity were formed during the degradation of AMX. By contrast, the EC50 value increased to 67.48% under sonozonation, indicating that fewer intermediates were formed with a higher mineralization degree [78]. For the degradation of 100 mg/L SMX by sonozonation,

with 20 kHz, 600 W/L US and 5.0 g/h O₃ at pH 7.0 for 30 min, the BOD₅/COD ratio increased from 0 to 0.54 after sonozonation treatment and the biological toxicity of the solution was reduced [79].

During the degradation of 400 mg/L TC by sonozonation with 20 kHz and 142.8 W/L of US at pH 7, Wang *et al.* found that the COD removal reached 91% after 90 min treatment, while very low COD removal was obtained by sonication alone, due to the lower production of free radicals by sonication at 20 kHz. 76% of COD removal was achieved by ozonation alone at a gas flow rate of 35 L/h, which contained 45.6 mg/L O₃ [80]. The initial TC solution resulted in 24% death of the crustaceans after 24 h of exposure. However, the acute toxicity reached its maximum after 10 min of sonozonation treatment, and the mortality was as high as 95%. The acute toxicity then gradually decreased to 80% in 70 min and 60% in 90 min of treatment [80].

Finally, it should be mentioned that most of the reported work, whether it used sonication alone or hybrid processes, made use of standard solutions and simulated wastewater to investigate the removal of antibiotics. Only a few studies have focused on the comparison of simulated and actual wastewater. Higher degradation rates (R_d) have been found for AMP in simulated urine than in distilled water ($\rho > 1$, $\rho = R_d$ in matrix/R_d in distilled water), which indicates that sonochemical processes are suitable for the removal of antibiotics in complex matrices [46]. OXA was difficult to mineralize (360 min) under sonication, while it can be completely mineralized using non-adapted microorganisms from a municipal wastewater treatment plant, which demonstrates that the sonication process transformed the antibiotic into substances that are bio-treatable using a typical aerobic biological system [128]. Furthermore, the highest (the most hydrophobic, i.e., CLX) and lowest (the most hydrophilic, i.e., CPD) R_d of antibiotics were observed in simulated hospital wastewater and seawater. A higher degradation rate for CLX was obtained in simulated hospital wastewater and seawater than in distilled water ($\rho > 1$), probably due to the salting-out effect exerted by matrix components. The moderate inhibition of CPD removal in hospital wastewater and seawater, compared to

distilled water, has been attributed to competition by $\cdot\text{OH}$ with the other substances in the matrices [129]. Compared with synthetic water, the RE of CIP for 15 min and mineralization for 60 min in real wastewater from a municipal wastewater treatment plant was decreased by 13.6 and 18.9% respectively, which illustrates that the treatment of CIP and TOC by the sono/ Fe^{2+} / H_2O_2 process is significantly hampered in a real matrix [32].

Another important factor to consider is the fact that almost all research on the removal of antibiotics by US involves processes that are performed on a bench scale, thus further pilot-scale investigations are recommended. Factors that should be considered when using pilot-scale systems include energy consumption by US, mass transfer, pH adjustment and application in real wastewater samples, temperature controls, *et al.*

Declaration of Competing Interest

The authors declare that they have no known competing financial interests or personal relationships that could have appeared to influence the work reported in this paper.

Acknowledgments

This research was supported by Fondazione CRT “*Sviluppo di tecnologie integrate per l'eliminazione dei residui di antibiotici dal latte vaccino*” and also by the China Scholarship Council. Pengyun Liu was supported by the China Scholarship Council (No. 201909505008).

8 References

- [1] S.A. Waksman, What is an antibiotic or an antibiotic substance?, *Mycologia*. 39 (1947) 565-569.
- [2] S. Suzuki, P.T.P. Hoa, Distribution of quinolones, sulfonamides, tetracyclines in aquatic environment and antibiotic resistance in Indochina, *Front. Microbiol.* 3 (2012) 67.
- [3] R. Gothwal, T. Shashidhar, Antibiotic pollution in the environment: a review, *Clean–Soil Air Water*. 43 (2015) 479-489.
- [4] K. Kümmerer, Antibiotics in the aquatic environment—a review—part I, *Chemosphere*. 75 (2009) 417-434.
- [5] V. Homem, L. Santos, Degradation and removal methods of antibiotics from aqueous matrices—a review, *J. Environ. Manage.* 92 (2011) 2304-2347.
- [6] S. Thiele-Bruhn, Pharmaceutical antibiotic compounds in soils—a review, *J. Plant. Nutr. Soil Sc.* 166 (2003) 145-167.
- [7] J. Wang, Z. Run, L. Chu, The occurrence, distribution and degradation of antibiotics by ionizing radiation: an overview, *Sci. Total Environ.* 646 (2019) 1385-1397.
- [8] D. Ghernaout, N. Elboughdiri, Antibiotics Resistance in Water Mediums: Background, Facts, and Trends, *Appl. Eng.* 4 (2020) 1.
- [9] X. Liu, G. Zhang, Y. Liu, S. Lu, P. Qin, X. Guo, B. Bi, L. Wang, B. Xi, F. Wu, W. Wang, T. Zhang, Occurrence and fate of antibiotics and antibiotic resistance genes in typical urban water of Beijing, China, *Environ. Pollut.* 246 (2019) 163-173.
- [10] P. Grenni, V. Ancona, A.B. Caracciolo, Ecological effects of antibiotics on natural ecosystems: A review, *Microchem. J.* 136 (2018) 25-39.
- [11] S. Li, W. Shi, M. You, R. Zhang, Y. Kuang, C. Dang, W. Sun, Y. Zhou, W. Wang, J. Ni, Antibiotics in water and sediments of Danjiangkou Reservoir, China: Spatiotemporal distribution and indicator screening, *Environ. pollut.* 246 (2019) 435-442.
- [12] K. Chen, J. Zhou, Occurrence and behavior of antibiotics in water and sediments from the Huangpu River, Shanghai, China, *Chemosphere*. 95 (2014) 604-612.
- [13] W. Li, Y. Shi, L. Gao, J. Liu, Y. Cai, Occurrence of antibiotics in water, sediments, aquatic plants, and animals from Baiyangdian Lake in North China, *Chemosphere*. 89 (2012) 1307-1315.
- [14] Y. Huang, Y. Liu, P. Du, L. Zeng, C. Mo, Y. Li, H. Lü, Q. Cai, Occurrence and distribution of antibiotics and antibiotic resistant genes in water and sediments of urban rivers with black-odor water in Guangzhou, South China, *Sci. total environ.* 670 (2019) 170-180.
- [15] L. Huang, Y. Mo, Z. Wu, S. Rad, X. Song, H. Zeng, S. Bashir, B. Kang, Z. Chen, Occurrence, distribution, and health risk assessment of quinolone antibiotics in water, sediment, and fish species of Qingshitan reservoir, South China, *Sci. Rep-UK*. 10 (2020) 1-18.
- [16] V. Yargeau, C. Leclair, Impact of operating conditions on decomposition of antibiotics during

1833 ozonation: a review, *Ozone-Sci. Eng.* 30 (2008) 175-188.

1834 [17] E.A. Serna-Galvis, J. Silva-Agredo, A.L. Giraldo, O.A. Flórez, R.A. Torres-Palma, Comparison
 1835 of route, mechanism and extent of treatment for the degradation of a β -lactam antibiotic by TiO_2
 1836 photocatalysis, sonochemistry, electrochemistry and the photo-Fenton system, *Chem. Eng. J.* 284
 1837 (2016) 953-962.

1838 [18] Z. Fang, J. Chen, X. Qiu, X. Qiu, W. Cheng, L. Zhu, Effective removal of antibiotic
 1839 metronidazole from water by nanoscale zero-valent iron particles, *Desalination*. 268 (2011) 60-67.

1840 [19] A.R. Rahmani, H. Rezaei-Vahidian, H. Almasi, F. Donyagard, Modeling and optimization of
 1841 ciprofloxacin degradation by hybridized potassium persulfate/zero valent-zinc/ultrasonic process,
 1842 *Environ. Processes*. 4 (2017) 563-572.

1843 [20] X. Ma, Y. Cheng, Y. Ge, H. Wu, Q. Li, N. Gao, J. Deng, Ultrasound-enhanced nanosized zero-
 1844 valent copper activation of hydrogen peroxide for the degradation of norfloxacin, *Ultrason.*
 1845 *Sonochem.* 40 (2018) 763-772.

1846 [21] M. Gholami, K. Rahmani, A. Rahmani, H. Rahmani, A. Esrafil, Oxidative degradation of
 1847 clindamycin in aqueous solution using nanoscale zero-valent iron/ H_2O_2 /US, *Desalin. Water Treat.*
 1848 57 (2016) 13878-13886.

1849 [22] H. Rahmani, M. Gholami, A.H. Mahvi, M. Ali-Mohammadi, K. Rahmani, Tinidazol antibiotic
 1850 degradation in aqueous solution by zero valent iron nanoparticles and hydrogen peroxide in the
 1851 presence of ultrasound radiation, *J. Water Chem. Technol.* 36 (2014) 317-324.

1852 [23] M. Magureanu, D. Piroi, N.B. Mandache, V. David, A. Medvedovici, C. Bradu, V.I. Parvulescu,
 1853 Degradation of antibiotics in water by non-thermal plasma treatment, *Water Res.* 45 (2011) 3407-
 1854 3416.

1855 [24] C. Adams, Y. Wang, K. Loftin, M. Meyer, Removal of antibiotics from surface and distilled
 1856 water in conventional water treatment processes, *J. Environ. Eng.* 128 (2002) 253-260.

1857 [25] O.A. Alsager, M.N. Alnajrani, H.A. Abuelizz, I.A. Aldaghmani, Removal of antibiotics from
 1858 water and waste milk by ozonation: kinetics, byproducts, and antimicrobial activity, *Ecotox.*
 1859 *Environ. Safe.* 158 (2018) 114-122.

1860 [26] F. Tavasol, T. Tabatabaie, B. Ramavandi, F. Amiri, Design a new photocatalyst of sea
 1861 sediment/titanate to remove cephalixin antibiotic from aqueous media in the presence of
 1862 sonication/ultraviolet/hydrogen peroxide: Pathway and mechanism for degradation, *Ultrason.*
 1863 *Sonochem.* (2020) 105062.

1864 [27] K.S. Suslick, D.A. Hammerton, R.E. Cline, Sonochemical hot spot, *J. Am. Chem. Soc.* 108
 1865 (1986) 5641-5642.

1866 [28] X. Ge, Z. Wu, M. Manzoli, Z. Wu, G. Cravotto, Feasibility and the Mechanism of Desorption
 1867 of Phenolic Compounds from Activated Carbons, *Ind. Eng. Chem. Res.* 59 (2020) 12223-12231.

1868 [29] X. Ge, Z. Wu, M. Manzoli, L. Jicsinszky, Z. Wu, A.E. Nosyrev, G. Cravotto, Adsorptive
 1869 Recovery of Iopamidol from Aqueous Solution and Parallel Reuse of Activated Carbon: Batch and
 1870 Flow Study, *Ind. Eng. Chem. Res.* 58 (2019) 7284-7295.

1871 [30] Z. Fang, J. Chen, X. Qiu, X. Qiu, W. Cheng, L. Zhu, Effective removal of antibiotic
 1872 metronidazole from water by nanoscale zero-valent iron particles, *Desalination*. 268 (2011) 60-67.

1873 [31] B. Kakavandi, N. Bahari, R.R. Kalantary, E.D. Fard, Enhanced sono-photocatalysis of
1874 tetracycline antibiotic using TiO₂ decorated on magnetic activated carbon (MAC@T) coupled with
1875 US and UV: A new hybrid system, *Ultrason. sonochem.* 55 (2019) 75-85.

1876 [32] K. González Labrada, D.R. Alcorta Cuello, I. Saborit Sánchez, M. García Batle, M.H. Manero,
1877 L. Barthe, U.J. Jáuregui-Haza, Optimization of ciprofloxacin degradation in wastewater by
1878 homogeneous sono-Fenton process at high frequency, *J. Environ. Sci. Heal. A.* 53 (2018) 1139-1148.

1879 [33] L. Hou, L. Wang, S. Royer, H. Zhang, Ultrasound-assisted heterogeneous Fenton-like
1880 degradation of tetracycline over a magnetite catalyst, *J. Hazard. Mater.* 302 (2016) 458-467.

1881 [34] C. Wang, J. Jian, Feasibility of tetracycline wastewater degradation by enhanced sonolysis, *J.*
1882 *Adv. Oxid. Technol.* 18 (2015) 39-46.

1883 [35] T. Zhou, X. Zou, X. Wu, J. Mao, J. Wang, Synergistic degradation of antibiotic norfloxacin in
1884 a novel heterogeneous sonochemical Fe⁰/tetrphosphate Fenton-like system, *Ultrason. Sonochem.*
1885 37 (2017) 320-327.

1886 [36] E. Hapeshi, A. Achilleos, A. Papaioannou, L. Valanidou, N.P. Xekoukoulotakis, D.
1887 Mantzavinos, D. Fatta-Kassinos, Sonochemical degradation of ofloxacin in aqueous solutions,
1888 *Water Sci. Technol.* 61 (2010) 3141-3146.

1889 [37] R.J. Wood, J. Lee, M.J. Bussemaker, A parametric review of sonochemistry: control and
1890 augmentation of sonochemical activity in aqueous solutions, *Ultrason. sonochem.* 38 (2017) 351-
1891 370.

1892 [38] E. De Bel, J. Dewulf, B. De Witte, H. Van Langenhove, C. Janssen, Influence of pH on the
1893 sonolysis of ciprofloxacin: biodegradability, ecotoxicity and antibiotic activity of its degradation
1894 products, *Chemosphere.* 77 (2009) 291-295.

1895 [39] R. Abazari, A.R. Mahjoub, S. Sanati, Z. Rezvani, Z. Hou, H. Dai, Ni-Ti layered double
1896 hydroxide@graphitic carbon nitride nanosheet: a novel nanocomposite with high and ultrafast
1897 sonophotocatalytic performance for degradation of antibiotics, *Inorg. Chem.* 58 (2019) 1834-1849.

1898 [40] Y.A.J. Al-Hamadani, C. Jung, J.K. Im, L.K. Boateng, J. R.V. Flora, M. Jang, J. Heo, C. Min
1899 Park, Y. Yoon, Sonocatalytic degradation coupled with single-walled carbon nanotubes for removal
1900 of ibuprofen and sulfamethoxazole, *Chem. Eng. Sci.* 162 (2017) 300-308.

1901 [41] Y. Gao, N. Gao, Y. Deng, J. Gu, Y. Gu, D. Zhang, Factors affecting sonolytic degradation of
1902 sulfamethazine in water, *Ultrason. Sonochem.* 20 (2013) 1401-1407.

1903 [42] W. Guo, Y. Shi, H. Wang, H. Yang, G. Zhang, Sonochemical decomposition of levofloxacin in
1904 aqueous solution, *Water Environ. Res.* 82 (2010) 696-700.

1905 [43] H. Wei, D. Hu, J. Su, K. Li, Intensification of levofloxacin sono-degradation in a US/H₂O₂
1906 system with Fe₃O₄ magnetic nanoparticles, *Chinese J. Chem. Eng.* 23 (2015) 296-302.

1907 [44] Y. Hu, G. Wang, M. Huang, K. Lin, Y. Yi, Z. Fang, P. Li, K. Wang, Enhanced degradation of
1908 metronidazole by heterogeneous sono-Fenton reaction coupled ultrasound using Fe₃O₄ magnetic
1909 nanoparticles, *Environ. Technol.* (2017) 1-22.

1910 [45] H.C. Yap, Y.L. Pang, S. Lim, A.Z. Abdullah, H.C. Ong, C.H. Wu, A comprehensive review on
1911 state-of-the-art photo-, sono-, and sonophotocatalytic treatments to degrade emerging contaminants,
1912 *Int. J. Environ. Sci. Te.* 16 (2019) 601-628.

1913 [46] D.M. Montoya-Rodríguez, E.A. Serna-Galvis, F. Ferraro, R.A. Torres-Palma, Degradation of
1914 the emerging concern pollutant ampicillin in aqueous media by sonochemical advanced oxidation

1915 processes-Parameters effect, removal of antimicrobial activity and pollutant treatment in hydrolyzed
 1916 urine, *J Environ. Manage.* 261 (2020) 110224.

1917 [47] S.G. Cetinkaya, M.H. Morcali, S. Akarsu, C.A. Ziba, M. Dolaz, Comparison of classic Fenton
 1918 with ultrasound Fenton processes on industrial textile wastewater, *Sustain. Environ. Res.* 28 (2018)
 1919 165-170.

1920 [48] E. Neyens, J. Baeyens, A review of classic Fenton's peroxidation as an advanced oxidation
 1921 technique, *J. Hazard. Mater.* 98 (2003) 33-50.

1922 [49] Z. Wu, M. Franke, B. Ondruschka, Y. Zhang, Y. Ren, P. Braeutigam, W. Wang, Enhanced effect
 1923 of suction-cavitation on the ozonation of phenol, *J. Hazard Mater.* 190 (2011) 375-380.

1924 [50] Z. Wu, H. Shen, B. Ondruschka, Y. Zhang, W. Wang, D.H. Bremner, Removal of blue-green
 1925 algae using the hybrid method of hydrodynamic cavitation and ozonation, *J. Hazard Mater.* 235
 1926 (2012) 152-158.

1927 [51] Y.G. Adewuyi, Sonochemistry: environmental science and engineering applications, *Ind. Eng.*
 1928 *Chem. Res.* 40 (2001) 4681-4715.

1929 [52] K.S. Suslick, Sonochemistry, *Science.* 247 (1990) 1439-1445.

1930 [53] L.H. Thompson, L.K. Doraiswamy, Sonochemistry: science and engineering, *Ind. Eng. Chem.*
 1931 *Res.* 38 (1999) 1215-1249.

1932 [54] C. Petrier, M.F. Lamy, A. Francony, A. Benahcene, B. David, V. Renaudin, N. Gondrexon,
 1933 Sonochemical degradation of phenol in dilute aqueous solutions: comparison of the reaction rates
 1934 at 20 and 487 kHz, *J. Phys. Chem. A.* 98 (1994) 10514-10520.

1935 [55] E.B. Flint, K.S. Suslick, The temperature of cavitation, *Science.* 253 (1991) 1397-1399.

1936 [56] K.S. Suslick, S.B. Choe, A.A. Cichowlas, M.W. Grinstaff, Sonochemical synthesis of
 1937 amorphous iron, *Nature.* 353 (1991) 414-416.

1938 [57] W.B. McNamara, Y.T. Didenko, K.S. Suslick, Sonoluminescence temperatures during multi-
 1939 bubble cavitation, *Nature.* 401 (1999) 772-775.

1940 [58] K.S. Suslick, E.B. Flint, Sonoluminescence from non-aqueous liquids, *Nature.* 330 (1987) 553-
 1941 555.

1942 [59] Y.T. Didenko, W.B. McNamara III, K.S. Suslick, Molecular emission from single-bubble
 1943 sonoluminescence, *Nature.* 407 (2000) 877-879.

1944 [60] N.C. Eddingsaas, K.S. Suslick, Light from sonication of crystal slurries, *Nature.* 444 (2006)
 1945 163-163.

1946 [61] S.J. Doktycz, K.S. Suslick, Interparticle collisions driven by ultrasound, *Science.* 247 (1990)
 1947 1067-1069.

1948 [62] P. Sathishkumar, R.V. Mangalaraja, S. Anandan, Review on the recent improvements in
 1949 sonochemical and combined sonochemical oxidation processes—A powerful tool for destruction of
 1950 environmental contaminants, *Renew. Sust. Energ. Rev.* 55 (2016) 426-454.

1951 [63] K. Kümmerer, Antibiotics in the aquatic environment—a review—part II, *Chemosphere.* 75 (2009)
 1952 435-441.

1953 [64] R. Daghrir, P. Drogui, Tetracycline antibiotics in the environment: a review, *Environ. Chem.*
 1954 *Lett.* 11 (2013) 209-227.

1955 [65] Z. Wu, B. Ondruschka, Roles of hydrophobicity and volatility of organic substrates on sonolytic
 1956 kinetics in aqueous solutions, *J. Phys. Chem. A.* 109 (2005) 6521-6526.

1957 [66] Z. Wu, B. Ondruschka, A. Stark, Ultrasonic cleavage of thioethers, *J. Phys. Chem. A.* 109 (2005)
1958 3762-3766.

1959 [67] Z. Wu, G. Cravotto, M. Adrians, B. Ondruschka, W. Li, Critical factors in sonochemical
1960 degradation of fumaric acid, *Ultrason. Sonochem.* 27 (2015) 148-152.

1961 [68] Z. Wu, J. Lifka, B. Ondruschka, Comparison of energy efficiency of various ultrasonic devices
1962 in aquasonochemical reactions, *Chem. Eng. Technol.* 29 (2006) 610-615.

1963 [69] D.M. Montoya-Rodríguez, Y. Ávila-Torres, E.A. Serna-Galvis, R.A. Torres-Palma, Data on
1964 treatment of nafcillin and ampicillin antibiotics in water by sonochemistry, *Data Br.* (2020) 105361.

1965 [70] R. Xiao, D. Diaz-Rivera, L.K. Weavers, Factors influencing pharmaceutical and personal care
1966 product degradation in aqueous solution using pulsed wave ultrasound, *Ind. Eng. Chem. Res.* 52
1967 (2013) 2824-2831.

1968 [71] Y.A.J. Al-Hamadani, K.H. Chu, J.R.V. Flora, D.H. Kim, M. Jang, J. Sohn, W. Joo, Y. Yoon,
1969 Sonocatalytical degradation enhancement for ibuprofen and sulfamethoxazole in the presence of
1970 glass beads and single-walled carbon nanotubes, *Ultrason. Sonochem.* 32 (2016) 440-448.

1971 [72] G. Wang, S. Li, X. Ma, J. Qiao, G. Li, H. Zhang, J. Wang, Y. Song, A novel Z-scheme
1972 sonocatalyst system, Er^{3+} : $\text{Y}_3\text{Al}_5\text{O}_{12}@\text{Ni}(\text{Fe}_{0.05}\text{Ga}_{0.95})_2\text{O}_4\text{-Au-BiVO}_4$, and application in
1973 sonocatalytic degradation of sulfanilamide, *Ultrason. Sonochem.* 45 (2018) 150-166.

1974 [73] A. Khataee, S. Fathinia, M. Fathinia, Production of pyrite nanoparticles using high energy
1975 planetary ball milling for sonocatalytic degradation of sulfasalazine, *Ultrason. Sonochem.* 34 (2017)
1976 904-915.

1977 [74] A. Seid-Mohammadi, G. Asgarai, Z. Ghorbanian, A. Dargahi, The removal of cephalexin
1978 antibiotic in aqueous solutions by ultrasonic waves/hydrogen peroxide/nickel oxide nanoparticles
1979 (US/H₂O₂/NiO) hybrid process, *Sep. Sci. Technol.* 55 (2020) 1558-1568.

1980 [75] K. Zhang, Z. Luo, T. Zhang, N. Gao, Y. Ma, Degradation effect of sulfa antibiotics by potassium
1981 ferrate combined with ultrasound (Fe(VI)-US), *Biomed Res. Int.* (2015).

1982 [76] X. Zou, T. Zhou, J. Mao, X. Wu, Synergistic degradation of antibiotic sulfadiazine in a
1983 heterogeneous ultrasound-enhanced Fe⁰/persulfate Fenton-like system, *Chem. Eng. J.* 257 (2014)
1984 36-44.

1985 [77] Z. Wu, F.J. Yuste-Córdoba, P. Cintas, Z. Wu, L. Boffa, S. Mantegna, G. Cravotto, Effects of
1986 ultrasonic and hydrodynamic cavitation on the treatment of cork wastewater by flocculation and
1987 Fenton processes, *Ultrason. Sonochem.* 40 (2018) 3-8.

1988 [78] R. Kıldak, Ş. Doğan, Medium-high frequency ultrasound and ozone based advanced oxidation
1989 for amoxicillin removal in water, *Ultrason. Sonochem.* 40 (2018) 131-139.

1990 [79] W. Guo, R. Yin, X. Zhou, H. Cao, J. Chang, N. Ren, Ultrasonic-assisted ozone oxidation
1991 process for sulfamethoxazole removal: impact factors and degradation process, *Desalin. Water Treat.*
1992 57 (2016) 21015-21022.

1993 [80] Y. Wang, H. Zhang, L. Chen, S. Wang, D. Zhang, Ozonation combined with ultrasound for the
1994 degradation of tetracycline in a rectangular air-lift reactor, *Sep. Purif. Technol.* 84 (2012) 138-146.

1995 [81] Z. Wu, A. Abramova, R. Nikonov, G. Cravotto, Sonozonation (sonication/ozonation) for the
1996 degradation of organic contaminants-a review, *Ultrason. Sonochem.* (2020) 105195.

1997 [82] R. Yin, W. Guo, H. Wang, J. Du, X. Zhou, Q. Wu, H. Zheng, J. Chang, N. Ren, Enhanced
1998 peroxymonosulfate activation for sulfamethazine degradation by ultrasound irradiation:
1999 performances and mechanisms, *Chem. Eng. J.* 335 (2018) 145-153.

2000 [83] A. Almasi, M. Mohammadi, F. Baniamerian, F. Baniamerian, Z. Berizi, M.H. Almasi, Z. Pariz,
2001 Modeling of antibiotic degradation in sonophotocatalytic process, increasing biodegradability and
2002 process optimization by response surface methodology (RSM), *Int. J. Environ. Sci. Te.* 16 (2019)
2003 8437-8448.

2004 [84] S.M. Ghoreishian, G.S.R. Raju, E. Pavitra, C.H. Kwak, Y.K. Han, Y.S. Huh, Ultrasound-
2005 assisted heterogeneous degradation of tetracycline over flower-like rGO/CdWO₄ hierarchical
2006 structures as robust solar-light-responsive photocatalysts: Optimization, kinetics, and mechanism,
2007 *Appl. Surf. Sci.* 489 (2019) 110-122.

2008 [85] E. Hapeshi, I. Fotiou, D. Fatta-Kassinos, Sonophotocatalytic treatment of ofloxacin in
2009 secondary treated effluent and elucidation of its transformation products, *Chem. Eng. J.* 224 (2013)
2010 96-105.

2011 [86] R.D.C. Soltani, M. Mashayekhi, A. Khataee, M.J. Ghanadzadeh, M. Sillanpää, Hybrid
2012 sonocatalysis/electrolysis process for intensified decomposition of amoxicillin in aqueous solution
2013 in the presence of magnesium oxide nanocatalyst, *J. Ind. Eng. Chem.* 64 (2018) 373-382.

2014 [87] Y. Ren, Z. Wu, M. Franke, P. Braeutigam, B. Ondruschka, D.J. Comeskey, P.M. King,
2015 Sonochemical degradation of phenol in aqueous solutions, *Ultrason. Sonochem.* 20 (2013)
2016 715-721.

2017 [88] Y. Ren, Z. Wu, B. Ondruschka, P. Braeutigam, M. Franke, H. Nehring, U. Hampel,
2018 Oxidation of Phenol by Microbubble - Assisted Microelectrolysis, *Chem. Eng. Technol.* 34 (2011)
2019 699-706.

2020 [89] Z. Wu, , B. Ondruschka, G. Cravotto, Degradation of phenol under combined irradiation of
2021 microwaves and ultrasound, *Environ. Sci. Technol.* 42 (2008) 8083-8087.

2022 [90] Franke, Marcus, *et al.*, Enhancement of chloroform degradation by the combination of
2023 hydrodynamic and acoustic cavitation, *Ultrason. Sonochem.* 18 (2011) 888-894.

2024 [91] R.S. Sutar, V.K. Rathod, Ultrasound assisted Laccase catalyzed degradation of Ciprofloxacin
2025 hydrochloride, *J. Ind. Eng. Chem.* 31 (2015) 276-282.

2026 [92] A.K. Subramani, P. Rani, P.H. Wang, B.Y. Chen, S. Mohan, C.T. Chang, Performance
2027 assessment of the combined treatment for oxytetracycline antibiotics removal by sonocatalysis and
2028 degradation using *Pseudomonas aeruginosa*, *J. Environ. Chem. Eng.* 7 (2019) 103215.

2029 [93] R. Pulicharla, R.K. Das, S.K. Brar, P. Drogui, R.Y. Surampalli, Degradation kinetics of
2030 chlortetracycline in wastewater using ultrasonication assisted laccase, *Chem. Eng. J.* 347 (2018)
2031 828-835.

2032 [94] W. Yan, Y. Xiao, W. Yan, R. Ding, S. Wang, F. Zhao, The effect of bioelectrochemical systems
2033 on antibiotics removal and antibiotic resistance genes: a review, *Chem. Eng. J.* 358 (2019) 1421-
2034 1437.

2035 [95] M.S. Saghafeini, S.M. Emadian, M. Vossoughi, Performances evaluation of Photo-Fenton
2036 process and sonolysis for the treatment of Penicillin G formulation effluent, *Procedia Environ. Sci.*
2037 8 (2011) 202-208.

2038 [96] P. Villegas-Guzman, J. Silva-Agredo, A.L. Giraldo-Aguirre, O. Flórez-Acosta, C. Petrier, R.A.
2039 Torres-Palma, Enhancement and inhibition effects of water matrices during the sonochemical
2040 degradation of the antibiotic dicloxacillin, *Ultrason. Sonochem.* 22 (2015) 211-219.

2041 [97] A.M. Lastre-Acosta, G. Cruz-González, L. Nuevas-Paz, U.J. Jáuregui-Haza, A.C.S.C. Teixeira,
 2042 Ultrasonic degradation of sulfadiazine in aqueous solutions, *Environ. Sci. Pollut. R.* 22 (2015) 918-
 2043 925.

2044 [98] X. Yang, H. Wei, K. Li, Q. He, J. Xie, J. Zhang, Iodine-enhanced ultrasound degradation of
 2045 sulfamethazine in water, *Ultrason. Sonochem.* 42 (2018) 759-767.

2046 [99] X. Wang, Y. Wang, D. Li, Degradation of tetracycline in water by ultrasonic irradiation, *Water*
 2047 *Sci. Technol.* 67 (2013) 715-721.

2048 [100] H. Rahmani, M. Gholami, A.H. Mahvi, M. Alimohammadi, G. Azarian, A. Esrafil, K.
 2049 Rahmani, M. Farzadkia, Tinidazole removal from aqueous solution by sonolysis in the presence of
 2050 hydrogen peroxide, *B. Environ. Contam. Tox.* 92 (2014) 341-346.

2051 [101] A. Mirzaei, F. Haghighat, Z. Chen, L. Yerushalmi, Sonocatalytic removal of ampicillin by
 2052 Zn(OH)F: Effect of operating parameters, toxicological evaluation and by-products identification,
 2053 *J. Hazard Mater.* 375 (2019) 86-95.

2054 [102] P. Gholami, L. Dinpazhoh, A. Khataee, A. Hassani, A. Bhatnagar, Facile hydrothermal
 2055 synthesis of novel Fe-Cu layered double hydroxide/biochar nanocomposite with enhanced
 2056 sonocatalytic activity for degradation of cefazolin sodium, *J. Hazard Mater.* 381 (2020) 120742.

2057 [103] P. Gholami, L. Dinpazhoh, A. Khataee, Y. Orooji, Sonocatalytic activity of biochar-supported
 2058 ZnO nanorods in degradation of gemifloxacin: synergy study, effect of parameters and phytotoxicity
 2059 evaluation, *Ultrason. Sonochem.* 55 (2019) 44-56.

2060 [104] R.D.C. Soltani, M. Mashayekhi, M. Naderi, G. Boczkaj, S. Jorfi, M. Safari, Sonocatalytic
 2061 degradation of tetracycline antibiotic using zinc oxide nanostructures loaded on nano-cellulose from
 2062 waste straw as nanosonocatalyst, *Ultrason. Sonochem.* 55 (2019) 117-124.

2063 [105] M. Hoseini, G.H. Safari, H. Kamani, J. Jaafari, M. Ghanbarain, A.H. Mahvi, Sonocatalytic
 2064 degradation of tetracycline antibiotic in aqueous solution by sonocatalysis, *Toxicol. Environ. Chem.*
 2065 95 (2013) 1680-1689.

2066 [106] A. Khataee, R. Hassandoost, S.R. Pouran, Cerium-substituted magnetite: Fabrication,
 2067 characterization and sonocatalytic activity assessment, *Ultrason. Sonochem.* 41 (2018) 626-640.

2068 [107] Li, Siyi, *et al.*, Sonocatalytic degradation of norfloxacin in aqueous solution caused by a novel
 2069 Z-scheme sonocatalyst, mMBIP-MWCNT-In₂O₃ composite, *J. Mol. Liq.* 254 (2018) 166-176.

2070 [108] Y. He, Z. Ma, L.B. Junior, Distinctive binary g-C₃N₄/MoS₂ heterojunctions with highly
 2071 efficient ultrasonic catalytic degradation for levofloxacin and methylene blue, *Ceram. Int.* (2020).

2072 [109] A. Khataee, P. Gholami, B. Kayan, D. Kalderis, L. Dinpazhoh, S. Akay, Synthesis of ZrO₂
 2073 nanoparticles on pumice and tuff for sonocatalytic degradation of rifampin, *Ultrason. Sonochem.*
 2074 48 (2018) 349-361.

2075 [110] J. Qiao, M. Lv, Z. Qu, M. Zhang, X. Cui, D. Wang, C. Piao, Z. Liu, J. Wang, Y. Song,
 2076 Preparation of a novel Z-scheme KTaO₃/FeVO₄/Bi₂O₃ nanocomposite for efficient sonocatalytic
 2077 degradation of ceftriaxone sodium, *Sci. Total Environ.* 689 (2019) 178-192.

2078 [111] M. Harrabi, H.B. Ammar, K. Mbarki, I. Naifar, C. Yaiche, F. Aloulou, B. Elleuch, Ultrasonic
 2079 power improvement of flumequine degradation effectiveness in aqueous solution via direct and
 2080 indirect action of mechanical acoustic wave, *Ultrason. Sonochem.* 48 (2018) 517-522.

2081 [112] R.D.C. Soltani, M. Mashayekhi, S. Jorfi, A. Khataee, M.J. Ghanadzadeh, M. Sillanpää,
 2082 Implementation of martite nanoparticles prepared through planetary ball milling as a heterogeneous

2083 activator of oxone for degradation of tetracycline antibiotic: Ultrasound and peroxy-enhancement,
 2084 Chemosphere. 210 (2018) 699-708.

2085 [113] Ammar, Hafedh Belhadj, Sono-Fenton process for metronidazole degradation in aqueous
 2086 solution: effect of acoustic cavitation and peroxydisulfate anion, Ultrason. Sonochem. 33 (2016)
 2087 164-169.

2088 [114] A. Almasi, A. Dargahi, M. Mohamadi, H. Biglari, F. Amirian, M. Raei, Removal of Penicillin
 2089 G by combination of sonolysis and Photocatalytic (sonophotocatalytic) process from aqueous
 2090 solution: process optimization using RSM (Response Surface Methodology), Electron. Physician. 8
 2091 (2016) 2878.

2092 [115] T. Zhou, X. Wu, Y. Zhang, J. Li, T.T. Lim, Synergistic catalytic degradation of antibiotic
 2093 sulfamethazine in a heterogeneous sonophotolytic goethite/oxalate Fenton-like system, Appl. Catal.
 2094 B Environ. 136 (2013) 294-301.

2095 [116] T. Zhou, X. Wu, J. Mao, Y. Zhang, T.T. Lim, Rapid degradation of sulfonamides in a novel
 2096 heterogeneous sonophotochemical magnetite-catalyzed Fenton-like (US/UV/Fe₃O₄/oxalate) system,
 2097 Appl. Catal. B Environ. 160 (2014) 325-334.

2098 [117] V. Vinesh, A.R.M. Shaheer, B. Neppolian, Reduced graphene oxide (rGO) supported electron
 2099 deficient B-doped TiO₂ (Au/B-TiO₂/rGO) nanocomposite: an efficient visible light
 2100 sonophotocatalyst for the degradation of Tetracycline (TC), Ultrason. Sonochem. 50 (2019) 302-
 2101 310.

2102 [118] A. Khataee, T.S. Rad, S. Nikzat, A. Hassani, M.H. Aslan, M. Kobya, E. Demirbaş, Fabrication
 2103 of NiFe layered double hydroxide/reduced graphene oxide (NiFe-LDH/rGO) nanocomposite with
 2104 enhanced sonophotocatalytic activity for the degradation of moxifloxacin, Chem. Eng. J. 375 (2019)
 2105 122102.

2106 [119] M. Hosseini, M.R.R. Kakhkha, A. Fakhri, S. Tahami, M.J. Lariche, Degradation of macrolide
 2107 antibiotics via sono or photo coupled with Fenton methods in the presence of ZnS quantum dots
 2108 decorated SnO₂ nanosheets, J. Photochem. Photobio. B Biol. 185 (2018) 24-31.

2109 [120] V. Naddeo, C.S. Uyguner-Demirel, M. Prado, A. Cesaro, V. Belgiorno, F. Ballesteros,
 2110 Enhanced ozonation of selected pharmaceutical compounds by sonolysis, Environ. Technol. (United
 2111 Kingdom). 36 (2015) 1876-1883.

2112 [121] W. Guo, R. Yin, X. Zhou, J. Du, H. Cao, S. Yang, N. Ren, Sulfamethoxazole degradation by
 2113 ultrasound/ozone oxidation process in water: kinetics, mechanisms, and pathways, Ultrason.
 2114 Sonochem. 22 (2015) 182-187.

2115 [122] Y.H. Huang, H.T. Su, L.W. Lin, Degradation of furfural in aqueous solution using activated
 2116 persulfate and peroxymonosulfate by ultrasound irradiation, J. Environ. Sci. 266 (2020) 110616.

2117 [123] H. Zhang, L. Duan, D. Zhang, Decolorization of methyl orange by ozonation in combination
 2118 with ultrasonic irradiation, J. Hazard Mater. 138 (2006) 53-59.

2119 [124] R. Xiao, Z. He, D. Diaz-Rivera, G.Y. Pee, L.K. Weavers, Sonochemical degradation of
 2120 ciprofloxacin and ibuprofen in the presence of matrix organic compounds, Ultrason. Sonochem. 21
 2121 (2014) 428-435.

2122 [125] E. De Bel, C. Janssen, S. De Smet, H. Van Langenhove, J. Dewulf, Sonolysis of ciprofloxacin
 2123 in aqueous solution: Influence of operational parameters, Ultrason. Sonochem. 18 (2011) 184-189.

2124 [126] K.S. Suslick, J.J. Gawienowski, P.F. Schubert, H.H. Wang, Alkane sonochemistry, J. Phys.
 2125 Chem. 87 (1983) 2299-2301.

2126 [127] W. Guo, H. Wang, Y. Shi, G. Zhang, Sonochemical degradation of the antibiotic cephalixin
 2127 in aqueous solution, *Water SA*. 36 (2010).

2128 [128] E.A. Serna-Galvis, J. Silva-Agredo, A.L. Giraldo-Aguirre, O.A. Flórez-Acosta, R.A. Torres-
 2129 Palma, High frequency ultrasound as a selective advanced oxidation process to remove penicillinic
 2130 antibiotics and eliminate its antimicrobial activity from water, *Ultrason. Sonochem.* 31 (2016) 276-
 2131 283.

2132 [129] E.A. Serna-Galvis, D. Montoya-Rodríguez, L. Isaza-Pineda, M. Ibáñez, F. Hernández, A.
 2133 Moncayo-Lasso, R.A. Torres-Palma, Sonochemical degradation of antibiotics from representative
 2134 classes-Considerations on structural effects, initial transformation products, antimicrobial activity
 2135 and matrix, *Ultrason. Sonochem.* 50 (2019) 157-165.

2136 [130] P. Villegas-Guzman, J. Silva-Agredo, O. Florez, A.L. Giraldo-Aguirre, C. Pulgarin, R.A.
 2137 Torres-Palma, Selecting the best AOP for isoxazolyl penicillins degradation as a function of water
 2138 characteristics: Effects of pH, chemical nature of additives and pollutant concentration, *J. Environ.*
 2139 *Manage.* 190 (2017) 72-79.

2140 [131] G.H. Safari, S. Nasser, A.H. Mahvi, K. Yaghmaeian, R. Nabizadeh, M. Alimohammadi,
 2141 Optimization of sonochemical degradation of tetracycline in aqueous solution using sono-activated
 2142 persulfate process, *J. Environ. Health Sci. Eng.* 13 (2015) 76.

2143 [132] M. Matouq, T. Tagawa, S. Nii, High frequency ultrasound waves for degradation of
 2144 amoxicillin in the presence of hydrogen peroxides for industrial pharmaceutical wastewater
 2145 treatment, *Glob. NEST J.* 16 (2014) 805-813.

2146 [133] W. Guo, Y. Shi, H. Wang, H. Yang, G. Zhang, Intensification of sonochemical degradation of
 2147 antibiotics levofloxacin using carbon tetrachloride, *Ultrason. Sonochem.* 17 (2010) 680-684.

2148 [134] S. Dehghan, B. Kakavandi, R.R. Kalantary, Heterogeneous sonocatalytic degradation of
 2149 amoxicillin using ZnO@Fe₃O₄ magnetic nanocomposite: influential factors, reusability and
 2150 mechanisms, *J. Mol. Liq.* 264 (2018) 98-109.

2151 [135] A. Hassani, A. Khataee, S. Karaca, C. Karaca, P. Gholami, Sonocatalytic degradation of
 2152 ciprofloxacin using synthesized TiO₂ nanoparticles on montmorillonite, *Ultrason. Sonochem.* 35
 2153 (2017) 251-262.

2154 [136] J. Qiao, H. Zhang, G. Li, S. Li, Z. Qu, M. Zhang, J. Wang, Y. Song, Fabrication of a novel Z-
 2155 scheme SrTiO₃/Ag₂S/CoWO₄ composite and its application in sonocatalytic degradation of
 2156 tetracyclines, *Sep. Purif. Technol.* 211 (2019) 843-856.

2157 [137] A.A. Pradhan, P.R. Gogate, Degradation of p-nitrophenol using acoustic cavitation and Fenton
 2158 chemistry, *J. Hazard Mater.* 173 (2010) 517-522.

2159 [138] D.H. Bremner, S. Di Carlo, A.G. Chakinala, G. Cravotto, Mineralisation of 2, 4-
 2160 dichlorophenoxyacetic acid by acoustic or hydrodynamic cavitation in conjunction with the
 2161 advanced Fenton process, *Ultrason. Sonochem.* 15 (2008) 416-419.

2162 [139] Y. Guo, X. Mi, G. Li, X. Chen, Sonocatalytic degradation of antibiotics tetracycline by Mn-
 2163 modified diatomite, *J. Chem.* (2017).

2164 [140] S. Hu, L. Li, M. Luo, Y. Yun, C. Chang, Aqueous norfloxacin sonocatalytic degradation with
 2165 multilayer flower-like ZnO in the presence of peroxydisulfate, *Ultrason. Sonochem.* 38 (2017) 446-
 2166 454.

2167 [141] S. Rahdar, C.A. Igwegbe, A. Rahdar, S. Ahmadi, Efficiency of sono-nano-catalytic process of
 2168 magnesium oxide nano particle in removal of penicillin G from aqueous solution, *Desalin. Water*
 2169 *Treat.* 106 (2018) 330-335.

2170 [142] A. Yazdani, M.H. Sayadi, Sonochemical degradation of azithromycin in aqueous solution,
 2171 *Environ. Health. Eng. Manag. J.* 5 (2018) 85-92.

2172 [143] Y. Deng, C.M. Ezyske, Sulfate radical-advanced oxidation process (SR-AOP) for
 2173 simultaneous removal of refractory organic contaminants and ammonia in landfill leachate, *Water*
 2174 *Res.* 45 (2011) 6189-6194.

2175 [144] N. Yousef Tizhoosh, A. Khataee, R. Hassandoost, R. Darvishi Cheshmeh Soltani, E.
 2176 Doustkhah, Ultrasound-engineered synthesis of WS₂@CeO₂ heterostructure for sonocatalytic
 2177 degradation of tylosin, *Ultrason. Sonochem.* (2020) 105114.

2178 [145] X. Meng, Y. Chu, Enhancement of chloramphenicol sonochemical degradation by sodium
 2179 peroxydisulfate, *Adv. Mater. Res.* (2013) 33-36

2180 [146] J. Wang, S. Wang, Activation of persulfate (PS) and peroxymonosulfate (PMS) and
 2181 application for the degradation of emerging contaminants, *Chem. Eng. J.* 334 (2018) 1502-1517.

2182 [147] J.K. Crandall, Y. Shi, C.P. Burke, Potassium monoperoxysulfate, in: *Encyclopedia of Reagents*
 2183 *for Organic Synthesis*, John Wiley & Sons, Ltd. (2001).

2184 [148] T. Zhou, X. Zou, J. Mao, X. Wu, Decomposition of sulfadiazine in a sonochemical Fe⁰-
 2185 catalyzed persulfate system: parameters optimizing and interferences of wastewater matrix, *Appl.*
 2186 *Catal. B: Environ.* 185 (2016) 31-41.

2187 [149] L. Hou, H. Zhang, X. Xue, Ultrasound enhanced heterogeneous activation of peroxydisulfate
 2188 by magnetite catalyst for the degradation of tetracycline in water, *Sep. Purif. Technol.* 84 (2012)
 2189 147-152.

2190 [150] A. Eslami, A. Asadi, M. Meserghani, H. Bahrami, Optimization of sonochemical degradation
 2191 of amoxicillin by sulfate radicals in aqueous solution using response surface methodology (RSM),
 2192 *J. Mol. Liq.* 222 (2016) 739-744.

2193 [151] S. Wang, J. Wang, Carbamazepine degradation by gamma irradiation coupled to biological
 2194 treatment, *J. Hazard. Mater.* 321 (2017) 639-646.

2195 [152] A. Ghauch, A.M. Tuqan, Oxidation of bisoprolol in heated persulfate/H₂O systems: kinetics
 2196 and products, *Chem. Eng. J.* 183 (2012) 162-171.

2197 [153] S. Yang, P. Wang, X. Yang, L. Shan, W. Zhang, X. Shao, R. Niu, Degradation efficiencies of
 2198 azo dye Acid Orange 7 by the interaction of heat, UV and anions with common oxidants: persulfate,
 2199 peroxymonosulfate and hydrogen peroxide, *J. Hazard. Mater.* 179 (2010) 552-558.

2200 [154] N. Gao, Q. Wang, P. Rao, G. Li, L. Dong, X. Zhang, Y. Shao, W. Chu, B. Xu, N. An, J. Deng,
 2201 Degradation of imidacloprid by UV-activated persulfate and peroxymonosulfate processes: Kinetics,
 2202 impact of key factors and degradation pathway, *Ecotox. Environ. Safe.* 187 (2020) 109779.

2203 [155] M. Kermani, M. Farzadkia, M. Morovati, M. Taghavi, S. Fallahizadeh, R. Khaksefidi, S.
 2204 Norzaee, Degradation of furfural in aqueous solution using activated persulfate and
 2205 peroxymonosulfate by ultrasound irradiation, *J. Environ. Manag.* 266 (2020) 110616.

2206 [156] X. Ao, W. Liu, Degradation of sulfamethoxazole by medium pressure UV and oxidants:
 2207 peroxymonosulfate, persulfate, and hydrogen peroxide, *Chem. Eng. J.* 313 (2017) 629-637.

2208 [157] M. Ahmadi, F. Ghanbari, M. Moradi, Photocatalysis assisted by peroxymonosulfate and
 2209 persulfate for benzotriazole degradation: effect of pH on sulfate and hydroxyl radicals, *Water Sci.*
 2210 *Technol.* 72 (2015) 2095-2102.

2211 [158] A. Rastogi, S.R. Al-Abed, D.D. Dionysiou, Sulfate radical-based ferrous–peroxymonosulfate
 2212 oxidative system for PCBs degradation in aqueous and sediment systems, *Appl. Catal. B.* 85 (2009)
 2213 171-179.

2214 [159] W. Guo, S. Su, C. Yi, Z. Ma, Degradation of antibiotics amoxicillin by Co_3O_4 -catalyzed
 2215 peroxymonosulfate system, *Environ. Prog. Sustain. Energy.* 32 (2013) 193-197.

2216 [160] S. Nasser, A.H. Mahvi, M. Seyedsalehi, K. Yaghmaeian, R. Nabizadeh, M. Alimohammadi,
 2217 G.H. Safari, Degradation kinetics of tetracycline in aqueous solutions using peroxydisulfate
 2218 activated by ultrasound irradiation: effect of radical scavenger and water matrix, *J. Mol. Liq.* 241
 2219 (2017) 704-714.

2220 [161] Y. Pan, Y. Zhang, M. Zhou, J. Cai, X. Li, Y. Tian, Synergistic degradation of antibiotic
 2221 sulfamethazine by novel pre-magnetized Fe^0/PS process enhanced by ultrasound, *Chem. Eng. J.* 354
 2222 (2018) 777-789.

2223 [162] S. Su, W. Guo, C. Yi, Y. Leng, Z. Ma, Degradation of amoxicillin in aqueous solution using
 2224 sulphate radicals under ultrasound irradiation, *Ultrason. Sonochem.* 19 (2012) 469-474.

2225 [163] M. Malakotian, S.N. Asadzadeh, M. Khatami, M. Ahmadian, M.R. Heidari, P. Karimi, N.
 2226 Firouzeh, S.V. Rajender, Protocol encompassing ultrasound/ Fe_3O_4 nanoparticles/persulfate for the
 2227 removal of tetracycline antibiotics from aqueous environments, *Clean Techn. Environ. Policy.* 21
 2228 (2019) 1665-1674.

2229 [164] K. Roy, C. Agarkoti, R.S. Malani, B. Thokchom, V.S. Moholkar, Mechanistic study of
 2230 sulfadiazine degradation by ultrasound-assisted Fenton-persulfate system using yolk-shell
 2231 $\text{Fe}_3\text{O}_4@hollow@m\text{SiO}_2$ nanoparticles, *Chem. Eng. Sci.* 217 (2020) 115522.

2232 [165] S. Jiao, S. Zheng, D. Yin, L. Wang, L. Chen, Aqueous photolysis of tetracycline and toxicity
 2233 of photolytic products to luminescent bacteria, *Chemosphere.* 73 (2008) 377-382.

2234 [166] Wikipedia, the free encyclopedia n.d., Beta-lactam core structures. Available from:
 2235 https://en.wikipedia.org/wiki/File:Beta-lactam_core_structures.svg. 25 February 2021.

2236 [167] Wikipedia, the free encyclopedia n.d., Tetracycline. Available from:
 2237 <https://de.wikipedia.org/wiki/Tetracycline>. 25 February 2021.

2238 [168] T.D. Pham, Z.M. Ziora, M.A. Blaskovich, Quinolone antibiotics, *MedchemComm.* 10 (2019)
 2239 1719-1739.

2240 [169] M.I. Andersson, A.P. MacGowan, Development of the quinolones, *J. Antimicrob. Chemoth.*
 2241 51 (2003) 1-11.

2242 [170] B. Schnyder, W.J. Pichler, Allergy to sulphonamides, *J. allergy clin. immun.* 131 (2013) 256-
 2243 257.

2244 [171] S. Mutak, Azalides from azithromycin to new azalide derivatives, *J. antibiot.* 60 (2007) 85-
 2245 122.